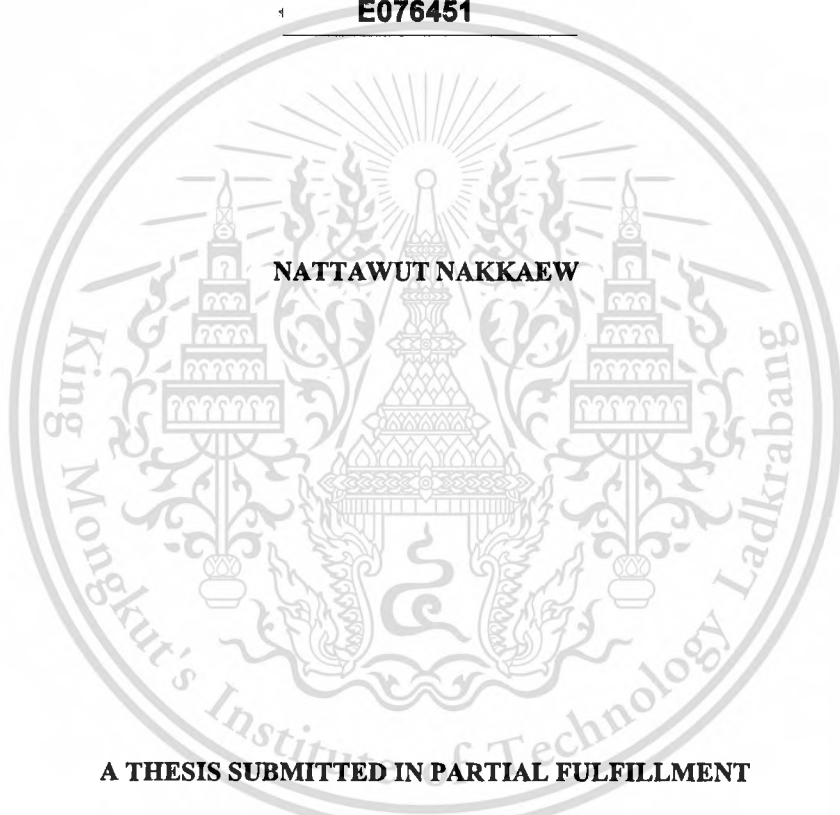


MODEL OF AIR/FUEL RATIO FOR SI ENGINE



E076451



NATTAWUT NAKKAEW

A THESIS SUBMITTED IN PARTIAL FULFILLMENT
OF THE REQUIREMENT FOR THE DEGREE OF
MASTER OF ENGINEERING IN AUTOMOTIVE ENGINEERING

(INTERNATIONAL PROGRAM)

INTERNATIONAL COLLEGE

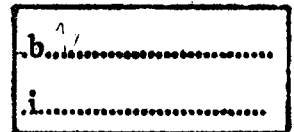
KING MONGKUT'S INSTITUTE OF TECHNOLOGY LADKRABANG

2012

เลขหมู่.....
เลขทะเบียน.....
วัน,เดือน,ปี.....

76451

KMITL-2011-IC-M-004-012





COPYRIGHT 2012

INTERNATIONAL COLLEGE

KING MONGKUT'S INSTITUTE OF TECHNOLOGY LADKRABANG

This material is reserved for educational use only, not allowed for commercial use.

Forbidden to modify the content, and cite the document when use.

Thesis Title	Model of Air/Fuel Ratio for SI Engine
Student	Mr. Nattawut Nakkaew
Student ID.	50061908
Degree	Master of Engineering
Program	Automotive Engineering (International Program)
Year	2012
Thesis Advisor	Assoc. Prof. Dr. Pitikhate Sooraksa
Thesis Co-Advisor	Asst. Prof. Dr. Chinda Charoenphonphanich
Thesis Co-Advisor	Prof. Dr. Masaki Yamakita
Thesis Co-Advisor	Dr. Teera Phatrapronnant

ABSTRACT

Understanding behavior of spark ignition engine, for example air fuel ratio or lambda value and performance helps in designing and developing flex-fuel engine control system to achieve maximum power under standard emission. This thesis presents the development of observation data engine model by using engine mapping. The empirical study was done on eddy current dynamometer in order to explore torques and air/fuel ratios of a spark ignition engine which ran on gasoline and gasoline-ethanol blends, E-10, E-20 and E-85 with two experimental methods: steady state test and sweep test. The experiment data was captured while the fuel injection durations and engine speed were controlled to obtain the air/fuel ratio in the ranges of between 0.7 and 1.3, whereas the required engine speeds were in between 1,000 and 4,000 rpm. The spark ignition timing was calibrated according to the optimum condition for the gasoline fuel and throttle was set at the wide open throttle position (WOT) only.

The comparisons between both data-capturing methods are described as the following: The average injection duration has increased in accordance with quantity of mixed ethanol. The difference of injection duration between gasoline and gasoline-ethanol blend E-10 is small (approximately to 12 ms). The average injection durations of E-20 and E-85 are equal to 12.43 ms and 15.37 ms and are different from gasoline 3.5% and 28% respectively. The average torque of steady state test and sweep test methods are roughly equal (80.26 N.m and 80.33 N.m). Torques varied according to fuel types. The average torque of gasoline-ethanol blend E-10 is equal to 79 N.m, average torque of gasoline-ethanol blend E-20 is equal to 67 N.m and average torque of gasoline-ethanol blend E-85 is equal to 56.71 N.m. The difference of torque between gasoline and gasoline-ethanol blend E-10 is small (less than 0.9%). The average torques is decreased due to the increasing in ethanol percentage. The average torques of gasoline-ethanol E-20 and gasoline-ethanol E-85 are approximately to 16% and 29% less than gasoline. The average air mass flow of steady state experiment is equal to 37.95 g/s and for the sweep test experiment are approximately to 27 g/s. In case of the sweep test, the air mass flows are approximately 27% less than the steady state test condition and do not depend on fuel types.

The “eMapnMod” program, based on MATLAB, has been developed as a tool for engine identification which employs recursive least square (RLS) to filter noise and vibration on captured data. To adjust the RLS, the forgetting factor has been applied for signal processing.

With RLS forgetting factor 0.9 and polynomial regression, the simulation results of torque given by the eMapnMod were significantly closed to the experimental results. The maximum average error of torques between the experiment and estimation is 0.92% (gasoline sweep test) and the maximum error between the estimation and validation result is 1.07% (gasoline-ethanol blend E-10).

ACKNOWLEDGMENTS

Many people and institutions have been a great inspiration and help me. Full scholarship opportunity in master of engineering program in automotive engineering from Thailand Advanced Institute of Science and Technology and Tokyo Institute of Technology (TAIST-Tokyo Tech).

First, I would like to thank my KMITL advisors Assoc.Prof.Dr.Pitikhate Sooraksa and Asst.Prof.Dr.Chinda Charoenphonphanich for guiding me through my research, Assoc.Prof.Dr. Masaki Yamakita from Tokyo Institute of Technology (Tokyo-Tech) has also suggested and Dr. Teera Phatrapornnant (NECTEC researcher) for providing suggestion and work place for my research.

In addition, I would also like to thanks Mr. Jaturawit Janpaiboon has always been available to answer my questions. Mr. Montri Chatpoj, Mr.Patin Pongkacha, Mr.Suradech Dongpumaet, Mr. Panithi Sira-uksorn and all of research assistants of EST- Lab have also assisted and supported me in my research.

Finally, I especially thank King Mongkut's Institute of Technology Ladkrabang (KMITL), KMITL International College, Automotive Engineering Program, The National Electronic and Computer Technology Center (NECTEC) and National Science and Technology Development Agency (NSTDA).

Nattawut Nakkaew

CONTENTS

	Page
ABSTRACT.....	I
ACKNOWLEDGMENTS	III
CONTENTS.....	IV
LIST OF TABLES	IX
LIST OF FIGURES	X
CHAPTER 1 INTRODUCTION	1
1.1 Background and Problem.....	1
1.2 Literature Reviews	2
1.3 Objectives.....	4
1.4 Scopes and Limitations	4
1.5 Research Methodology.....	5
1.6 Research Overview	5
CHAPTER 2 BACKGROUND THEORY	6
2.1 Internal Combustion Engine.....	6
2.2 Spark Ignition (SI) Engine	7
2.3 Engine Operation Parameters.....	8
2.3.1 Air Fuel Mixture.....	8
2.3.2 Stoichiometric Air Fuel Ratio	9
2.3.3 Ethanol Property.....	11

CONTENTS (CONT.)

	Page
2.3.4 Fuel Delivery	12
2.3.5 Ignition Timing.....	12
2.3.6 Volumetric efficiency	14
2.3.7 Torque.....	14
2.4 Engine Mapping	15
2.5 Observation Data Model	16
2.6 Adaptive Filter Algorithm.....	17
2.6.1 Recursive Least-Square	18
2.6.2 Summary of RLS Algorithm	21
2.6.3 Model Validation.....	22
2.7 Engine Control Systems	22
2.7.1 Injection Control System.....	24
2.7.2 Ignition Control System.....	24
CHAPTER 3 EXPERIMENTAL PROCEDURES.....	26
3.1 Experimental Setup	26
3.1.1 Spark Ignition (SI) Engine.....	28
3.1.2 Engine Dynamometer	29
3.1.3 Strain-Gauge Load Cell.....	31
3.1.4 Oxygen Sensor and Oxygen Meter.....	32

CONTENTS (CONT.)

	Page
3.1.5 Air Mass Flow Sensor	33
3.2 Engine Control Systems	34
3.2.1 Crankshaft Pulse Generator	36
3.2.2 Fuel Injection Controller	37
3.2.3 Spark Ignition Control	39
3.2.4 Throttle Position Control	41
3.3 Data Acquisition	42
3.4 eMapnMod Program	44
3.5 Experimentations	46
3.5.1 Steady State	46
3.5.2 Sweep Test	47
CHAPTER 4 RESULTS AND DISSCUSSIONS	48
4.1 Steady State	48
4.1.1 Sampling Cycle Experiment “Steady State”	48
4.2 Sweep Test	49
4.2.1 Sampling Cycle Experiment “Sweep Test”	49
4.3 Experiment	51
4.4 Estimation	51
4.4.1 eMapnMod Estimation Process	51

CONTENTS (CONT.)

	Page
4.4.2 Forgetting Factor Identification.....	51
4.4.3 Steady State	54
4.4.4 Sweep Test.....	54
4.5 Experimental Results.....	55
4.5.1 Steady State (Gasoline)	55
4.5.2 Sweep Test (Gasoline).....	60
4.5.3 Sweep Test (Gasoline-Ethanol Blend E-10).....	64
4.5.4 Sweep Test (Gasoline-Ethanol Blend E-20).....	68
4.5.5 Sweep Test (Gasoline-Ethanol Blend E-85).....	72
4.6 Simulation Results.....	76
4.6.1 Steady State (Gasoline)	76
4.6.2 Sweep Test (Gasoline).....	78
4.6.3 Sweep Test (Gasoline-Ethanol Blend E-10).....	79
4.6.4 Sweep Test (Gasoline-Ethanol Blend E-20).....	81
4.6.5 Sweep Test (Gasoline-Ethanol Blend E-85).....	83
4.7 Validation Results	85
4.7.1 Steady State (Gasoline)	85
4.7.2 Sweep Test (Gasoline).....	87
4.7.3 Sweep Test (Gasoline-Ethanol Blend E-10).....	89
4.7.4 Sweep Test (Gasoline-Ethanol Blend E-20).....	91

CONTENTS (CONT.)

	Page
4.7.5 Sweep Test (Gasoline-Ethanol Blend E-85).....	93
4.8 Summary	95
CHAPTER 5 CONCLUSIONS AND SUGGESTIONS	98
5.1 Conclusion.....	98
5.2 Suggestion	99
REFERENCES	101
APPENDICES	104
APPENDIX A Gasoline-Ethanol Blends (Gasohol).....	105
APPENDIX B Engine Test Stand Drawing	108
BIOGRAPHY	109

LIST OF TABLES

Table	Page
2-1 Specifications of Standard Gasoline, Gasoline-Ethanol Blend and Ethanol.....	11
3-1 Experimental Components	26
A-1 Specifications of Standard Gasoline, Ethanol and Gasohol.....	105



LIST OF FIGURES

Figure	Page
2.1 Four-stroke cycle.....	6
2.2 Cylinder gas pressure between gasoline and gasoline-ethanol blend	13
2.3 Engine mapping.....	15
2.4 Observation data engine model block diagram	16
2.5 The system identification	17
2.6 Recursive least-square algorithm block diagram	18
2.7 Spark ignition engine structure	23
2.8 Timing diagram.....	25
3.1 Engine test stand drawing	27
3.2 Engine test stand.....	27
3.3 Engine test stand computer controller.....	28
3.4 Mazda BP-ZE gasoline engine.....	28
3.5 Engine dynamometer control diagram	29
3.6 Eddy current retarder “Telma”.....	30
3.7 Dynamometer controller	30
3.8 Dynamometer control program.....	31
3.9 Strain-gauge load cell “S-beam type tension and compression”.....	32
3.10 Wide-band oxygen sensor “Innovate LM-1”	32
3.11 Air mass flow sensor “Hot wire”	33
3.12 Air mass flow sensor	33
3.13 Air mass flow sensor signal voltage.....	34
3.14 Engine control system diagram	35
3.15 Engine control device.....	35
3.16 34x Reluctor wheel.....	36

LIST OF FIGURES (CONT.)

Figure	Page
3.17 Crankshaft pulse generator	37
3.18 Fuel injection system diagram.....	37
3.19 Fuel injection control module “FC163”	38
3.20 Injection control program “FC-163”	39
3.21 Ignition control system diagram.....	39
3.22 Ignition control module	40
3.23 Ignition control program	40
3.24 Throttle with servo motor.....	41
3.25 wCK programmer.....	42
3.26 Data acquisition diagram (DAQ)	42
3.27 Data acquisition module “MyOS01”	43
3.28 Engine parameter logger program.....	44
3.29 eMapnMod program.....	44
3.30 eMapnMod flow chart.....	45
3.31 Steady state experiment flow chart	46
3.32 Sweep test experiment flow chart	47
4.1 Air mass flow measurement at engine speed 3,000 rpm	48
4.2 Torque measurement at engine speed 3,000 rpm	49
4.3 Engine speed at fuel injection duration 11 ms	49
4.4 Air mass flow at fuel injection duration 11 ms	50
4.5 Torque measurement at fuel injection duration 11 ms	50
4.6 Lambda value at fuel injection duration 11 ms	50
4.7 Power spectral density of experiment data (Torque)	52
4.8 Torque estimation when change forgetting factor.....	53

LIST OF FIGURES (CONT.)

Figure	Page
4.9 Torque measurement vs torque estimation at 3,000 rpm	54
4.10 Torque measurement vs torque estimation at injection duration 11 ms.....	54
4.11 Air mass flow measurement (g/s).....	55
4.12 Average air mass flow (g/s)	56
4.13 Fuel mass flow (g/s)	57
4.14 Average fuel mass flow (g/s)	57
4.15 Torque measurement (Nm)	58
4.16 Average torque vs. maximum torque (AFR = 14)	59
4.17 Volumetric efficiency.....	59
4.18 Average volumetric efficiency	59
4.19 Air mass flow measurement (g/s).....	60
4.20 Average air mass flow (g/s)	61
4.21 Injection duration (ms).....	61
4.22 Torque measurement (N.m)	62
4.23 Average torque vs. maximum torque ($\lambda = 0.9$)	63
4.24 Volumetric efficiency.....	63
4.25 Average volumetric efficiency	63
4.26 Air mass flow measurement (g/s).....	64
4.27 Average air mass flow (g/s)	64
4.28 Injection duration (ms).....	65
4.29 Torque measurement (N.m)	65
4.30 Average torque vs. maximum torque ($\lambda = 0.9$)	66
4.31 Volumetric efficiency.....	67
4.32 Average volumetric efficiency	67

LIST OF FIGURES (CONT.)

Figure	Page
4.33 Air mass flow measurement (g/s).....	68
4.34 Average air mass flow (g/s)	68
4.35 Injection duration (ms).....	69
4.36 Torque measurement (N.m)	69
4.37 Average torque vs. maximum torque ($\lambda = 0.9$)	70
4.38 Volumetric efficiency.....	71
4.39 Average volumetric efficiency	71
4.40 Air mass flow measurement (g/s).....	72
4.41 Average air mass flow (g/s)	72
4.42 Injection duration (ms).....	73
4.43 Torque measurement (N.m).....	73
4.44 Average torque vs. maximum torque ($\lambda = 0.9$)	74
4.45 Volumetric efficiency.....	75
4.46 Average volumetric efficiency	75
4.47 Torque estimation (N.m).....	76
4.48 Average torque estimation vs. maximum torque estimation (AFR = 14).....	77
4.49 Average torque measurement vs. average torque estimation.....	77
4.50 Torque estimation (N.m).....	78
4.51 Average torque estimation vs. maximum torque estimation ($\lambda = 0.9$).....	78
4.52 Average torque measurement vs. average torque estimation.....	79
4.53 Torque estimation (N.m).....	80
4.54 Average torque estimate vs. maximum torque ($\lambda = 0.9$)	80
4.55 Average torque measurement vs. average torque estimation.....	81
4.56 Torque estimation (N.m).....	81

LIST OF FIGURES (CONT.)

Figure	Page
4.57 Average torque estimation vs. maximum torque ($\lambda = 0.9$).....	82
4.58 Average torque measurement vs. average torque estimation.....	82
4.59 Torque estimation (N.m).....	83
4.60 Average torque estimation vs. maximum torque ($\lambda = 0.9$).....	84
4.61 Average torque measurement vs. average torque estimation.....	84
4.62 Torque validation (N.m).....	85
4.63 Average torque validation vs. maximum torque validation (AFR = 14)	86
4.64 The measurement, estimated and validated torque	86
4.65 Torque validation (N.m).....	87
4.66 Average torque validation vs. maximum torque validation ($\lambda = 0.9$)	88
4.67 Average measurement, estimate and validate torque	88
4.68 Torque validation (N.m).....	89
4.69 Average torque validation vs. maximum torque validation ($\lambda = 0.9$)	90
4.70 Average measure, estimated and validated of torque.....	90
4.71 Torque validation (N.m).....	91
4.72 Average torque validation vs. maximum torque ($\lambda = 0.9$)	92
4.73 Average measure, estimated and validated torque	92
4.74 Torque validation (N.m).....	93
4.75 Average torque validation vs. maximum torque validation ($\lambda = 0.9$)	94
4.76 Average measure, estimated and validated of torque.....	94
4.77 Average air mass flow (g/s)	95
4.78 Average injection duration (ms).....	96
4.79 Average torque (N.m)	96

CHAPTER 1

INTRODUCTION

1.1 Background and Problem

Understanding in air fuel ratio and performance of conventional spark ignition engine helps in designing and developing engine control system to achieve maximum power under standard emission. The development of air fuel ratio control should be designed control system to work precisely to make maximum power with under standard emission and also need specific design, analysis and engine control algorithm test.

Especially, Engine control algorithm must be test with actual engine because the experimental conditions and results will be similar to actual vehicle. Generally, the engine should be tested on an engine dynamometer or chassis dynamometer. It can assign many conditions for engine testing without vehicle running (non-road).

The problems of engine test on the dynamometer will spend too long time, and high cost for designing, developing, assembling of engine test stand devices and sensors on engine test stand and also including the energy consumption, energy cost and engine running time during engine control algorithm test.

The observation engine modeling can solve this problem which can be used to simulate the engine condition on computer. This engine modeling is required experimental data (engine mapping) from actual engine operating conditions and simulation in computer. This can reduce time, methods and cost in developing engine control algorithm.

The experiment methods for investigation engine behavior are divided into two methods, steady state test and sweep test. During steady state engine mapping a dwell period is required at each test point to allow instrumentation. This method is an accurate but a very time intensive procedure. Sweep test is not dwelling period. It ramps the engine between two operating point while data is logged continuously which much reduced time.

1.2 Literature Review

There are two methods for identify engine modeling, Theoretical method and experiment method. The theoretical method such as mean value engine model (MVEM) [24,25], Neural Networks [26], Nonlinear Dynamics [27], Mathematical Modeling [30,31], State-space model [7,32] and these methods are derived from mathematical sub-model. The experiment method is observation data from measurement such as engine mapping method [2,6,28] are methods for identity engine modeling from experiment data.

The purpose of the engine mapping is the observation behaviors of the engine [31] such as engine speed, air fuel ratio, torque, etc. Timothy Holliday and Anthony J.Lawrance [6] presented the engine mapping is “table” which heart of the engine controller. The table is indexed by the speed (engine speed: RPM) and amount of air entering the combustion chamber on each intake stroke (LOAD). The cell of the table contains the values of the three calibration parameters; air fuel ratio, EGR (exhaust gas recirculation) and SPK ignition timing. The engine controller measures RPM and LOAD and set values of the calibration parameter.

Ward M.C. et al [28] examined a core of engine mapping termed “spark sweep” with 1.8 liter turbocharge Volkswagen engine on dynamometer. During a spark sweep engine speed, lambda and designated relative load (RL) are controlled to constant values with the only variable being ignition angle then data processing, statistical and optimization on I-CAM software which based on MATLAB/SIMULINK.

In case of experiment method, Steady state mapping is fundamental to optimizing internal combustion engine operation for more accurate but time in experiment consuming. Ward M.C. et al [31] presented comparison of accuracy and repeatability of the sweep approach under experimental conditions, with that of steady state testing for reduce mapping time. The sweep test is ramps the engine between two operating point, while data is logged continuously. The starting point is concentrates on the application of engine torque as the variable. In sweep test, the mechanical and thermal inertias in the engine exhibit an initial lag, this mean that data from the beginning of the ramp could be discarded.

The gasoline-ethanol blend has been used to fuel in standard gasoline engine to compare with gasoline. Most of researches presented, the same air quantity, higher gasoline-ethanol blend or ethanol quantity are required to produce stoichiometric air fuel ratio when comparison with gasoline. Due to lower heating value of ethanol, octane is higher than gasoline. Ethanol can use

with higher compression ratio and then the performance of engine has been improve. Owen and Coley [8] presented, the improvement of performance to 16% with single-cylinder, ethanol-fueled engine when increase the compression ratio from 8.0 to 18. The output power and fuel consumption are improved. Kremer and Fachetti [14] presented, the increasing ethanol content in gasoline from 22% to 24% did not have significant effects on engine calibration, emission and fuel consumption. But when increase ethanol above 26%, power loss, drivability problem and fuel consumption increases are expected.

Dai et al. [15] developed a simulation model for an engine fuelled by ethanol and gasoline-ethanol blends E-22 and E-85. The model was validated by experimental data. The E-85 increases engine thermal efficiency, BMEP and reduces exhaust hydrocarbons and carbon monoxide at varying mixture equivalence ratio, in comparison with E-22. Using retard ignition timing, the oxides of nitrogen emissions were also reduce in E-85.

Li et al. [16] presented, modified a motorcycle gasoline-fuelled spark ignition engine to operate with ethanol. The effects of nozzle orifice size, fuel injection duration, spark timing and the excess air/ fuel ratio on engine power output, fuel and energy consumptions and engine exhaust emission levels are studied on an engine test stand. The maximum engine power output is increased by 5.4% and the maximum torque output is increased by 1.9% with the ethanol fuel in comparison with the baseline.

Muharrem et al [36] studied the effects of ethanol-gasoline (E-5, E-10) and methanol-gasoline (M-5, M-10) fuel blends compare with gasoline on the performance and combustion characteristics of a SI engine. The experiment, a vehicle 4 cylinders 4 strokes, multi-point injection system on chassis dynamometer while running the vehicle at two speeds (80 km/h and 100 km/h), and 4 difference wheel power (5, 10, 15 and 20 kW). The results, BSFC increased, cylinder gas pressure started to rise later than gasoline and higher peak heat release rate than gasoline.

1.3 Objectives

1.3.1 To identify engine mapping of torque and lambda value (λ) with spark ignition engine fueled for; gasoline and gasoline-ethanol blend (gasohol) E-10, E-20 and E-85 which aims to control fuel quantity, by adjusting fuel injection duration.

1.3.2 Create an observation engine model from experimental data (engine mapping) with recursive least square algorithm on MATLAB software.

1.4 Scopes and Limitations

1.4.1 The working methods are design and development engine test stand using eddy current dynamometer.

1.4.2 The parameters collection are fuel types, air fuel ratio or lambda (λ), torque, engine speed and the fuel injection duration of spark ignition engine (MAZDA BP-ZE) running on engine dynamometer test stand.

1.4.3 The test procedure has been separated into 2 methods; steady state test and sweep test. Both of test procedures are evaluated under wide open throttle (WOT) conditions and the experiments were started up from fully warmed-up of engine temperature.

1.4.4 The excepted conditions for example, cold start, idle speed and a compensation of natural atmosphere (air temperature and humidity of engine test room), The term of emission, fuel consumption, and spark ignition timing do not focuses in this work.

1.5 Research Methodology

This thesis focuses on identifying observation data model of standard spark ignition engine when fuel types and fuel quantity have been changed. This research aims to measure engine parameters when adjusting the fuel injection duration and creating an observation data model from experimental data.

This research is divided into 4 procedures. First is a design, develop and setup engine test stand. Second step is setup the SI engine on engine test stand and also including a sensor and actuators. The next step is collecting the engine behaviors by adjusting fuel quantity when fueled gasoline and gasoline-ethanol blend (E-10, E-20 and E-85). Finally, the filter algorithm is used to reduce noise and vibration from experiment data.

1.6 Research Overview

This thesis is divided into five chapters; Chapter 1 is introducing the research topic and explains on the objectives, scopes and limitations of the research and the project methodology.

The following Chapter 2 will explain about the spark ignition engine. In addition will focus on theoretical explanation on air fuel ratio, engine mapping, filter algorithm (RLS) and engine control system are introduced.

In Chapter 3 will explain about method to measure the engine performances, engine test stand setting, experimental apparatus which including type of sensors, engine control device and data acquisition. Then explain engine control program and eMapnMod program.

Next, Experimental method and results will be shown and discussed in Chapter 4. Finally, the conclusion will be made in Chapter 5 by concluding the overall results obtained as well as the knowledge learned from the research.

CHAPTER 2

BACKGROUND THEORY

2.1 Internal Combustion Engine

The purpose of internal combustion engine is the production of mechanical power from the chemical energy contained in the fuel. In the internal combustion engine, energy is released by burning or oxidizing the fuel inside the engine [1].

The internal combustion engine is generated drive torque by combusting an air fuel mixture. More specifically, air is drawn into an intake manifold through a throttle. The air is distributed to cylinder and is mixed with fuel. The air fuel mixture is compressed within a cylinder by a reciprocally driven piston. The compressed air fuel mixture is combusted and the resultant combustion driver a piston within the cylinder, which rotatable drives a crankshaft [2].

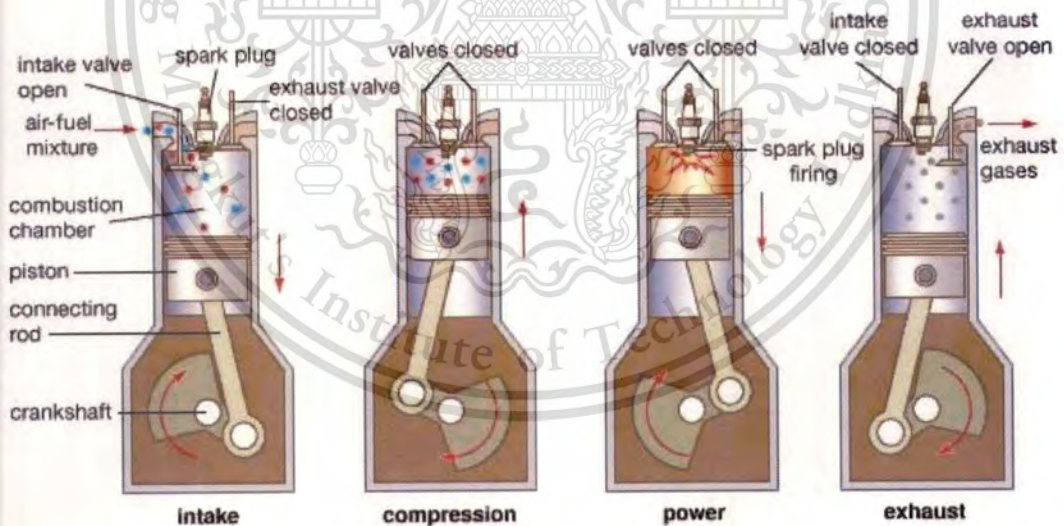


Figure 2.1 Four-stroke cycle [3]

The movement of a piston up and down inside the cylinder is called “stroke”. The torque can be generated by crankshaft which is connected to a piston by the connecting rod. The linear motion of a piston is converted into rotation movement. Commonly, the spark ignition engine use

a four stroke cycle because the piston has to travel up and down twice to complete a full power cycle turning a crankshaft through 720 degree. Both SI and CI engines used this cycle which comprises;

2.1.1.1 An intake stroke, which starts the piston at top dead center (TDC) and ends with the piston at bottom dead center (BDC) which draws fresh mixture into the cylinder. To increase the mass inducted, the inlet valve opens shortly before the stroke starts and closes after it ends.

2.1.1.2 A compression stroke, when both valves are closed and the mixture inside the cylinder is compressed to a small fraction of its initial volume. Toward the end of the compression stroke, combustion is initiated and the cylinder pressure rises more rapidly.

2.1.1.3 A power stroke, or expansion stroke, which starts with the piston at TDC and ends at BDC as the high-temperature, high-pressure, gases push the piston down and force the crank to rotate. About five times as much work is done on the piston during the power stroke as the piston had to do during compression. As the piston approaches BDC the exhaust valve opens to initiate the exhaust process and drop the cylinder pressure to close to the exhaust pressure.

2.1.1.4 An exhaust stroke, where the remaining burned gases exit the cylinder: first, because the cylinder pressure may be substantially higher than the exhaust pressure: then as they are swept out by the piston as it moves toward TDC. As the piston approaches TDC the inlet valve opens, just after TDC the exhaust valve closes and the cycle starts again.

2.2 Spark Ignition (SI) Engine

In SI engine, the air and fuel usually mixed in the intake system prior to the entry to the cylinder using a fuel injection system. Most of modern SI engines are equipped with port fuel injectors (PFI) and spark plugs. An SI engine starts the combustion process in each cycle by use of a spark plug. The spark plug gives a high-voltage electrical discharge between two electrodes which ignites the air fuel mixture in the combustion chamber surrounding the spark plug. Amount of air fuel mixture and spark ignition angle are important parameters for fuel consumption, efficiency and emission.

2.3 Engine Operation Parameters

The engine parameters are used to characterize engine behaviors. In this work, the engine parameters for identifying engine mapping are described as the following;

2.3.1 Air Fuel Mixture

The efficiency of spark ignition engine is depends on amount of air fuel mixture is call air fuel ratio. If the combustion process is complete, all of the hydrocarbon (HC) will be completely with the available oxygen (O_2). The ratio of air fuel mixture that accomplishes is stoichiometric or lambda $\lambda = 1$ or ideal ratio. The stoichiometric of gasoline is approximated 14.7 parts of air per 1 part of gasoline by weight. It good compromise between power output and exhaust emission is achieved. The air fuel ratio has air more than ideal ratio, called "lean mixture" ($\lambda > 1$). Lean mixture is providing fuel economy but high emission of NO_x [4]. The air fuel ratio is below an ideal ratio, called "rich mixture" ($\lambda < 1$). Rich mixture is providing maximum power output [5]. The air fuel ratio AFR_{act} and lambda value λ are given by equation (2-1) and (2-2).

$$AFR_{act} = \frac{\dot{m}_{ac}}{\dot{m}_{fc}} \quad (2-1)$$

$$\lambda = \frac{AFR_{act}}{AFR_{stoich}} \quad (2-2)$$

Equation (2-1) \dot{m}_{ac} is actual air mass flow rate in to the engine and \dot{m}_{fc} is actual fuel mass flow rate into the engine. Equation (2-2) AFR_{stoich} is stoichiometric air fuel ratio.

The limited ranges of air fuel mixtures are;

- Too rich mixture ($\lambda \ll 1$), typical maximum ratio about 10:1 are waste fuel, pollutants, reduce performance and more fuel consumption.
- Too lean mixture ($\lambda \gg 1$), normal minimum ratio about 18:1 are miss-firing, overheat of the cooling system due to longer period of flame and overheat of exhaust valve due to the combustion continue after exhaust valve open.

2.3.2 Stoichiometric Air Fuel Ratio

The spark ignition engine takes the air from the atmosphere and fuel, and then process of combustion releases the chemical energy from fuel. The stoichiometric or theoretical combustion is the ideal process where fuel is burned completely. The stoichiometric in each fuel is depends on the property of fuel and chemical composition. The main of fuel composition is a hydrocarbon, and their burning will obviously result in the release of hydrogen and carbon as residuals, along with heat and pressure.

The ignition of engine is release chemical energy from air fuel mixture as thermal energy which increases cylinder pressure and temperature. The ideal reaction of hydrocarbon gives the results in only CO_2 and H_2O . The combustion process to occur energy released from Q_{LV} of the fuel, heat release rate and timing are directly effect to engine performance.

The stoichiometric can be calculated by chemical equation. Most spark ignition engines obtain their energy from the combustion of a hydrocarbon fuel with air, which converts chemical energy of the fuel to internal energy in the gases within the combustion chamber. The maximum amount of chemical energy that can be released from the fuel, when the fuel is reacts with a stoichiometric amount of oxygen. The oxygen is just enough to convert all carbon in the fuel to CO_2 and all hydrogen to H_2O , with no oxygen left over.



Equations (2-3) shows the stoichiometric reaction of ethanol, Oxygen balance give; $a = 3$, Carbon balance give; $b = 2$, Hydrogen balance give; $c = 3$, then reaction equation becomes equation (2-4), means the reaction of oxygen 3 moles with fuel ethanol 1 mole can produce carbon dioxide 2 moles and 3 moles of water.

In balancing a chemical condition, the molecules react with molecules not mass quantity. But the energy released by the reaction will thus have unit of energy per kmole of fuel.

$$m = NM \quad (2-5)$$

The one kmole of a substance has kilogram of mass equal to number of molecular mass of substance as shown in equation (2-5), m is mass in kilogram, N is mole number (kmole) and M is molecular mass (kg/kmole). The molar mass of oxygen, hydrogen and carbon are 32, 1.008 and 12.01 respectively. Then, the molecular mass of C_2H_6O (ethanol) is 46.068 Kg and $3O_2$ is 96 Kg.

The molecular mass, the stoichiometric of ethanol is 96:46 or 2:1. However, the air not only oxygen but also nitrogen and argon are essentially. Generally, the air has 21% oxygen and 79% as nitrogen by volume or 23.16 and 76.84 by mass. Then, the stoichiometric of ethanol is (2.08/0.231) : 1 or 9 : 1.

Generally, The stoichiometric air fuel ratio of gasoline is 14.7 : 1. Then, the stoichiometric of gasoline-ethanol blend E-10, E-20 and E-85 can be calculated by equation (2-6) [29].

$$EFF_{stoich} = \frac{E_{ethanol}}{100} \times E100_{Stoich} + \frac{G_{Gasoline}}{100} \times G_{Stoich} \quad (2-6)$$

Where;

EFF_{stoich}	=	Stoichiometric of gasoline-ethanol blend
$E_{ethanol}$	=	Ethanol percentage
$E100_{Stoich}$	=	Stoichiometric of ethanol
$G_{Gasoline}$	=	Gasoline percentage
G_{Stoich}	=	Stoichiometric of gasoline

In this study, the gasoline-ethanol blends (gasohol) have been used to experimental on actual engine. The stoichiometric air fuel ratio and low heating value of gasoline, gasoline-ethanol blend (gasohol) and ethanol as shown in Table 2-1.

Table 2-1 Specifications of standard gasoline, gasoline-ethanol blend (gasohol) and ethanol

Fuel	%Ethanol	Low Heating Value (MJ/kg)	Stoichiometric AFR
Gasoline	0	44.4	14.7
Gasohol E10	10	43.47	14.13
Gasohol E20	20	41.38	13.29
Gasohol E85	85	33.1	9.86
Ethanol[34]	99.50	26.9	9.00

2.3.3 Ethanol Property

The main advantage of ethanol is anti-knock performance, allowing its use in higher compression ratio engine, due to higher octane number and lower heating value (Q_{LV}). When blended gasoline with ethanol can effectively operate at higher compression ratios, with subsequent improvement in power output and efficiency when compare with gasoline. In case of fuel consumption, for the same air quantity, the spark ignition engine is required to higher amount of the ethanol or gasoline-ethanol blend to produce a stoichiometric air fuel mixture to compare with gasoline.

In standard gasoline engine, when fuelled ethanol or gasoline-ethanol blend. It may be impractical to raise the compression ratio and increasing the fuel injection duration. An advancing the spark timing may offer improvements in performance similar to those obtained with a small increase in compression ratio. In flex-fuel engine, due to anti-knock performance of ethanol the compression ratio is higher than gasoline operation. Engine knock is occurring when fuelled gasoline. The retarded ignition timing can be helped to reduce engine knock condition.

2.3.4 Fuel Delivery

There are two dynamic delays in the fuel delivery system. First the delay due to the control action of the injection control unit and response of injector. Second the delay due to the wall wetting. Because the port-injection system, a two phased fuel liquid and vapor phase are occurs in the intake manifold. The fuel vapor phase directly into cylinder and liquid phase is fuel film deposits on the intake manifold wall (puddle), in the same time, fuel film can evaporate and directly fuel vapor phase enter into cylinder together [9]. In this experiment, the both of dynamic delays are *negligible*. The fuel flow entering \dot{m}_{fc} can be calculated by using the air mass flow rate measured from air flow sensor and measurement of air fuel ratio from wide band oxygen sensor *without* transport delay and a time lag associated with engine/sensor process.

$$\dot{m}_{fc} = \frac{\dot{m}_{ac}}{\lambda \cdot AFR_{stoich}} \quad (2-7)$$

Equation (2-7) shows the injecting fuel flow out of injector \dot{m}_{fi} can be obtained by commanded injection signal and assuming the injectors open without dead time. Then, \dot{m}_{fi} can be calculated by using injectors open time t_{inj} and injector flow rate \dot{m}_{inj} .

$$\dot{m}_{fi} = t_{inj} \dot{m}_{inj} \quad (2-8)$$

2.3.5 Ignition Timing

The performance of spark ignition engine is due to the pressure from the air fuel mixture combustion in cylinder. The maximum pressure must have occurred when the piston is just a little past top dead center (TDC). If the air fuel mixture ignites too late from TDC (during the piston moving down), the power stroke is operated on less compression ratio, the peak of cylinder pressure is reduced and decreasing work transfer from gas to piston. Then the power (pressure) on top of piston has been reduced.

If the air fuel mixture ignites too early before piston coming past TDC, the power stroke is operated on compression stroke (the piston moving up) the power on top of piston has been loss. This condition is known as pre-ignition or engine knock and can be damaged the engine components. Thus, the air fuel mixture must be igniting before the piston is in the optimum position.

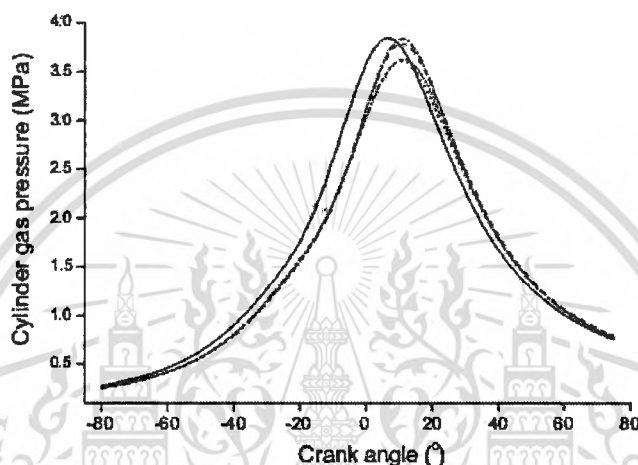


Figure 2.2 Cylinder gas pressure between gasoline and gasoline-ethanol blend [37]

The spark timing effects to peak cylinder pressure. Figure 2.2 shows the comparison of cylinder gas pressure between gasoline and gasoline-ethanol blend. The cylinder gas pressure of gasoline (blue line) started to raise early than gasoline-ethanol blend (E-5 and E-10) at same ignition timing and engine speed conditions. The maximum cylinder pressure of gasoline has been occurred early and closer to top dead center (TDC). In case of gasoline-ethanol blend (E-5 and E-10), the maximum cylinder pressure has been occurred later than gasoline and after piston moving down [36]. This may be explained, when quantity of ethanol is increased, the cylinder pressure and temperature are decreased at the beginning of combustion [37]. Then the gasoline-ethanol blend must be early igniting air fuel mixture than the gasoline.

2.3.6 Volumetric efficiency

The volumetric efficiency: η_v is used to measure the effectiveness of an engine's induction process. Because the engine cannot get fully charged due to the dynamic loss in the intake manifold, intake port and valve [7]. The intake airflow rate varies according to engine capacity, engine speed and air density. It can be defined by equation (2-9), which \dot{m}_{act} is air mass flow rate measured from air flow sensor.

$$\eta_v = \frac{2\dot{m}_{act}}{\rho_i V_d N} \quad (2-9)$$

The air density can be calculated using the ideal gas law, expressed as a function of temperature and pressure.

$$\rho_i = \frac{p}{RT} \quad (2-10)$$

2.3.7 Torque

The combustion process in the cylinder produces engine torque. The amount of engine torque is influenced by air fuel mixture, spark ignition timing and combustion efficiency. In this experiment, the spark ignition timing is negligible and assumes the engine torque is a function of engine speed, air charge per stroke, amount of fuel and effective efficiency η_e . The torque can be calculated by equation (2-11).

$$T_e = \eta_e \frac{\dot{m}_{fc} Q_{LV}}{2\pi N} \quad (2-11)$$

Where	T_e	=	Effective torque (measured on the engine shaft)
	η_e	=	Effective efficiency
	Q_{LV}	=	Heating value of fuel

2.4 Engine Mapping

Engine mappings are based on measurement system to comprise of the equipment used to sense engine experimental behaviors into a recordable form, and recording parameters. Formally, the elements of a measurement system are including the sensor, the transducer, the signal conditioner, and the signal processor.

The main purpose of measurement system is produced an accurate numerical value of the measured. Ideally, the recorded value should be the exact value of the physical variable sensed by the measurement system. In practice, the perfect measurement system neither exists nor is needed; a result needs to have only a certain accuracy that is achieved using the simplest equipment and measurement strategy. This can be accomplished provided there is a good understanding of the system's response characteristics.

A method of engine mapping is included testing the engine over a plurality of actual engine operating and gathering actual engine data corresponding to the actual engine operating conditions [2].

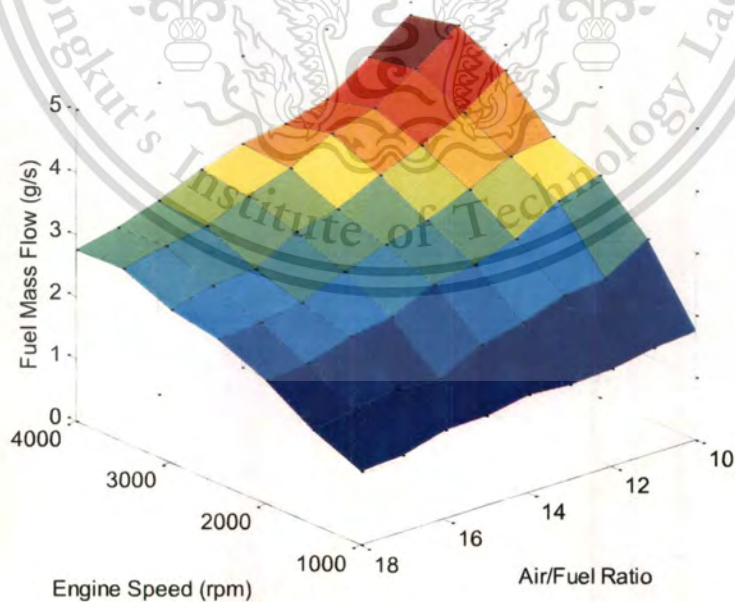


Figure 2.3 Engine mapping

Figure 2.3 shows the engine mapping is like a map that describes the engine behavior. Normally, engine speed (RPM) must be selected to compare with other parameters such as air entering the combustion chamber (LOAD), lambda value (λ) and throttle position (TPS). Therefore adjusting some parameters has affected to the engine. The significance of finding engine mapping is in initiate process for design and development of engine control units (ECUs). The purpose of the engine mapping as a function of adjustable engine parameters such as RPM, LOAD, AFR, and output are power or torque, exhaust emission, exhaust temperature [6].

2.5 Observation Data Model

Observation is way of gathering data by watching behavior, events and physical characteristics. The observation can be divided into 2 methods; direct and indirect observations. Direct observation is when we observe interactions, processes or behaviors as occur. Indirect observation is when we watch the results of interactions, processes or behaviors.

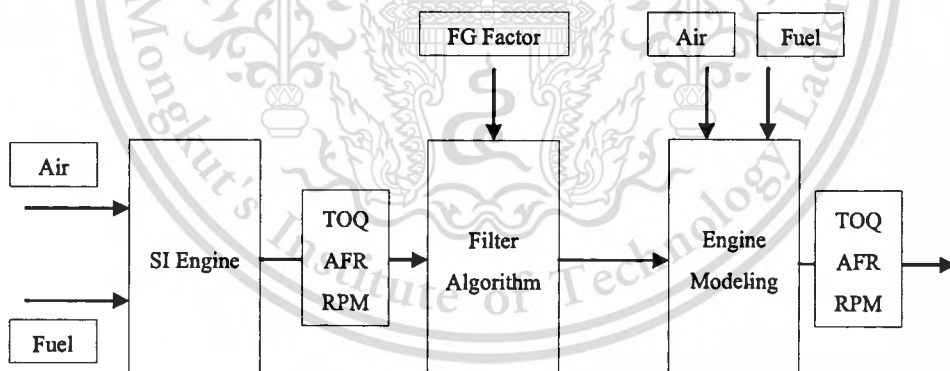


Figure 2.4 Observation data engine model block diagram

Figure 2.4 shows the observation engine model from actual engine. In this work, the observe engine parameters are input and output. Input parameters are air mass flow and fuel mass flow (injection duration). Output parameters are break torque, air fuel ratio and engine speed. The adaptive algorithm used to estimate data from experimental data (engine-mapping).

2.6 Adaptive Filter Algorithm

The adaptive algorithm is widely used in signal processing today. For unwanted signals filter, noise cancellation, reduce the bit rate in signal transmission, etc. The methods of adaptive filter are change some parameters or coefficients of filter according to kind of algorithm, the signal characteristics, unwanted signal or influence on the compensate signal. It can adjust to unknown environment and tracking signal of system characteristics varying with time.

The purposes of adaptive filter are system identification and inverse filtering. In system identification the adaptive filter is used to approximate and unknown system. Both the unknown system and the adaptive filter are driven by the same input signal and the adaptive filter coefficients are adjusted in a way, that the output signal resembles the output of the unknown system as shown in Figure 2.5.

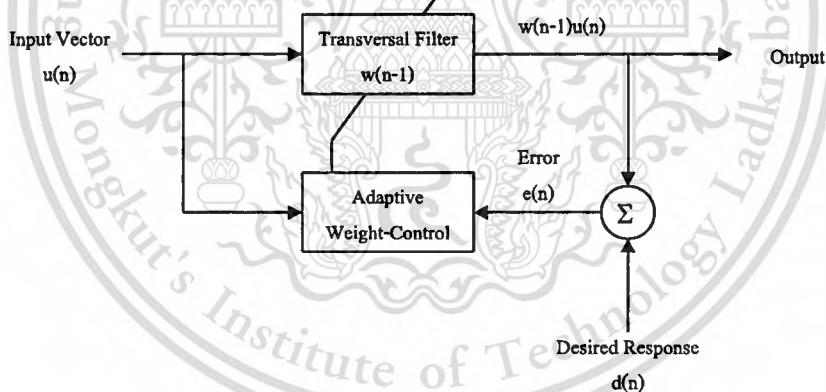


Figure 2.5 The system identification

For inverse modeling or equalization the adaptive filter is used in series with the unknown system and the learning algorithm tries to compensate the influence of the unknown system on the test signal $u(n)$ by minimizing the difference between the adaptive filter output and the delay test signal.

Adaptive algorithms are very important role in many diverse applications such as communication, acoustics, speech, radar, seismology and biomedical engineering [10].

2.6.1 Recursive Least-Square

The recursive least square (RLS) algorithm is one of the most popular adaptive algorithms. It is easy and exactly derived from the normal equation for determining the coefficients of an adaptive filter. The RLS algorithm uses information from all past input samples not only from the current tap-input samples to estimate the autocorrelation matrix of the input vector. To decrease the influence of input sample from the far past, a weighting factor for influence of each sample is used [11].

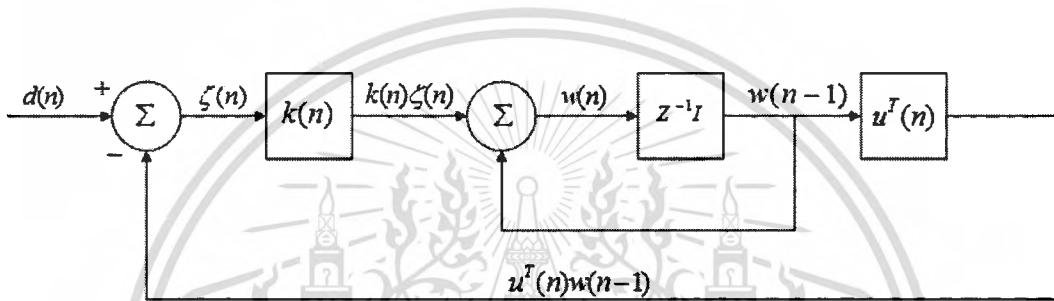


Figure 2.6 Recursive least-square algorithm block diagram

There are many RLS algorithms in the literatures, e.g., classical recursive least square (RLS), RLS with vary quickly with time [12], RLS with combining tracking and regularization to prevent the algorithm gain from tending to zero [13], RLS with forgetting factor [17], Fast Transversal RLS this algorithm is designed to provide similar performance to the standard RLS algorithm while reducing the computation order [18].

$$\varepsilon(n) = \sum_{i=1}^n \lambda^{n-i} - |e(n)|^2 \quad (2-12)$$

The general recursive least-square (RLS) algorithm can define cost function $\varepsilon(n)$ at time n in equation (2-12); λ^{n-i} is forgetting factor or weighting factor and $e(n)$ is error signal.

The forgetting factor or weighting reduces the influence of old data usually taking in the form $0 < \lambda < 1$. When error signal $e(n)$ is;

$$e(n) = d(n) - y(n) \quad (2-13)$$

$$y(n) = w^T(n)u(n) \quad (2-14)$$

Equations (2-13) and (2-14); $d(n)$ is experiment data vector; $y(n)$ is estimated data vector; $u(n)$ is input data set and $w(n)$ is time update for the tap-weight vector.

$$z(n) = \Phi^{-1}(n)\hat{w}(n) \quad (2-15)$$

When $z(n)$ is vector correlation and Φ^{-1} is inverse correlation matrix

$$\Phi(n) = \sum_{i=1}^n \lambda^{n-i} u(i)u^T(i) \quad (2-16)$$

$$z(n) = \sum_{i=1}^n \lambda^{n-i} u(i)d(i) \quad (2-17)$$

$$\Phi(n) = \lambda\Phi(n-1) + u(n)u^T(n) \quad (2-18)$$

$$z(n) = \lambda z(n-1) + u(n)d(n) \quad (2-19)$$

However, using a matrix inversion lemma for compute the inverse matrix $\Phi^{-1}(n)$ as shown in equation (2-20);

$$\Phi^{-1}(n) = \lambda^{-1}\Phi^{-1}(n-1) - \frac{\lambda^{-2}\Phi^{-1}(n-1)u(n)u^T(n)\Phi^{-1}(n-1)}{1 + \lambda^{-1}u^T(n)\Phi^{-1}(n-1)u(n)} \quad (2-20)$$

For calculation easily can be given $P(n) = \Phi^{-1}(n)$ and the gain vector $k(n)$ can be updated with equation (2-21);

$$k(n) = \frac{\lambda^{-1}P(n-1)u(n)}{1 + \lambda^{-1}u^T(n)P(n-1)u(n)} \quad (2-21)$$

Then; substitute $P(n) = \Phi^{-1}(n)$ and equation (2-21) into (2-20) and we have

$$P(n) = \lambda^{-1}P(n-1) - \lambda^{-1}u^T(n)P(n-1) \quad (2-22)$$

And we can rewrite equation (2-21) as;

$$\begin{aligned} k(n)[1 + \lambda^{-1}u^T(n)P(n-1)u(n)] &= \lambda^{-1}P(n-1)u(n) \\ k(n) + \lambda^{-1}k(n)u^T(n)P(n-1)u(n) &= \lambda^{-1}P(n-1)u(n) \\ k(n) &= \lambda^{-1}P(n-1)u(n) - \lambda^{-1}k(n)u^T(n)P(n-1)u(n) \\ k(n) &= [\lambda^{-1}P(n-1) - \lambda^{-1}k(n)u^T(n)P(n-1)]u(n) \end{aligned} \quad (2-23)$$

We obtain gain vector $k(n)$;

$$k(n) = P(n)u(n) = \Phi^{-1}(n)u(n) \quad (2-24)$$

Equation (2-24), we are now able to explain the gain vector $k(n)$ is equal to input samples set $u(n)$ multiply by inverse correlation matrix $\Phi^{-1}(n)$. The time-update for weight vector equation, that of $w(n)$ from equations (2-15), (2-19) and $P(n) = \Phi^{-1}(n)$.

$$w(n) = \lambda P(n)z(n-1) + P(n)u(n)d(n) \quad (2-25)$$

Equation (2-26) priori estimation error $\zeta(n)$ is;

$$\zeta(n) = d(n) - w^T(n-1)u(n) \quad (2-26)$$

Substituting equations (2-22), (2-24) and (2-26) into (2-25).

$$w(n) = w(n-1) + k(n)\zeta(n) \quad (2-27)$$

Initialization of RLS algorithm for these variables in order to start the recursions the time update for the weight vector $w(n) = 0$ and Inverse conversion matrix $P(0)$ approximate unitization is commonly used: $P(0) = \delta I$ which $\delta > 100\sigma_u^2$. For large data length, the initial values assigned at $n = 0$ are not important, since they are forgotten due to exponential forgetting factor (λ).

2.6.2 Summary of RLS Algorithm

1. Initialization of RLS Algorithm;

$$w(n) = 0 \quad P(0) = \delta I$$

2. Inverse matrix (2-22);

$$P(n) = \lambda^{-1}P(n-1) - \lambda^{-1}u^T(n)P(n-1)$$

3. Gain vector (2-24);

$$k(n) = P(n)u(n) = \Phi^{-1}(n)u(n)$$

4. Priors estimation error (2-26);

$$\zeta(n) = d(n) - w^T(n-1)u(n)$$

5. Weight vector (2-27);

$$w(n) = w(n-1) + k(n)\zeta(n)$$

6. Estimate model output (2-14);

$$y(n) = w^T(n)u(n)$$

2.6.3 Model Validation

The validation is tested by comparison of the measurement data and estimation data (Estimate data). The acceptable estimation data should be track the measurement data. However, mostly data come with measurement noise. There are not possible to exactly fit the measurement data.

In addition, the data set are the other part of training data. The data set is split into 70 percent part that used for identification and the 30 percent part used for validation. Moreover, the experimental data were preprocessed by normalization. However, there are several tools can be used for verification. In this case, the ordinarily famous methods: the root mean square error. They are determined by equation below.

$$MSE(n) = \sqrt{\frac{(d(n) - y(n))^2}{n}} \quad (2-28)$$

Root mean square error is estimator for quantity the difference between estimator value and the true value.

2.7 Engine Control Systems

Engine control systems for spark ignition engine (SI-engine) are including two parts; fuel delivery system and ignition system. First time, these system help to fuel delivery into an engine and ignited the air fuel mixture in the combustion chamber. Now, engine controls systems have been developed for reduce the fuel consumption, exhaust emission, an increase safety, an improve the drivability and comfort of conventional engines.

The engine control systems become more complex and powerful; electric and electronic devices are replacing an ever-increasing number of mechanical functions. The engine control system structure as shown in Figure 2.7.

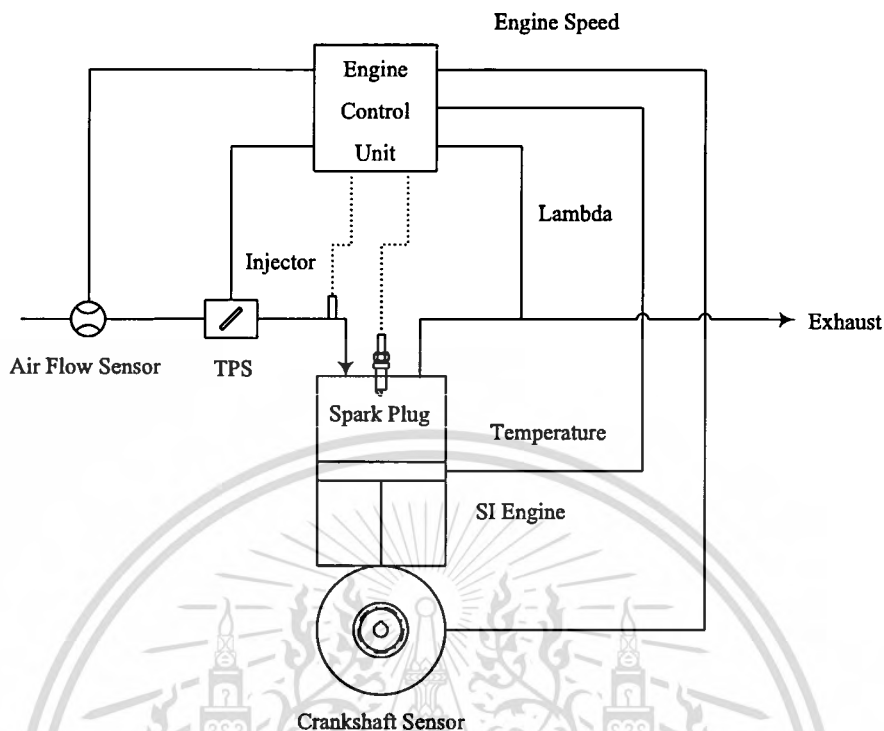


Figure 2.7 Spark ignition engine structure

Figure 2.7 shows the various actuators and sensors of a SI engine control systems. The engine control units (ECUs) must set all actuator commands according to driver demands and available sensor signals, taking into account constraints imposed by engine safety considerations and pollutant emission limitations. The crankshaft sensor allows the synchronization of the ECUs with the engine's reciprocating behavior or engine speed. The throttle position sensor to measure throttle plate angle. Airflow sensor or MAP sensor to measure air mass flow rate or manifold absolute pressure and temperature of air entering into the intake manifold.

The power or work of spark ignition engine has been controlled by the quantity of air fuel mixture in the cylinder during each stroke and ignition timing advance. Typically, this fuel quantity is varies by changing with the throttle plate angle, pressure, temperature and density of air into the intake manifold. Now, the throttle plate has controls by electronic which offer improved fuel economy and pollutant emission [19].

2.7.1 Injection Control System

Fuel delivery systems of SI engine are carburetor and injection system. The carburetor is most common device for control the fuel flow into the intake manifold. It works on pressure difference principle of air through the venture device without electronic control. Fuel injection systems have in-cylinder injection (direct injection) and manifold injection.

In-cylinder injection, the fuel is directly injected into combustion chamber. The advantage is the engine can higher compression ratio than manifold injection at stoichiometric operation.

The manifold injection, the fuel is injected into the intake manifold. The advantage is the creation of homogeneous fuel distribution in the cylinder at stoichiometric operation and air fuel mixture temperature into intake port is lower than in-cylinder injection by evaporating fuel.

The fuel injection is only part of the engine's combustion cycle. The fuel mass needs air mass flow rate or manifold absolute pressure to provides the necessary information to calculate the amount of fuel required. The mass of air entering the cylinder must be calculated using a physical model of the intake system and then sends an electric signal to the fuel injector. This signal determines the amount of time injector open and sprays fuel this method is known as the pulse width modulation (PWM).

The injection timing can be derived from equation (2-8). The lift curves of the intake valves and the exhaust valves of an engine are assumed to be constant (not variable-valve timing). The injection has been injected the fuel between intake valves closed.

2.7.2 Ignition Control System

The ignition system is used to create a spark, or current flow across each pair of spark plug electrodes at the proper instant under all engine-operating conditions. The purpose of the ignition control system has three main jobs. First, generate an electrical spark that has enough heat to ignite the air fuel mixture in the combustion chamber. Second, maintain that spark long enough to allow for the combustion of air fuel mixture in the cylinder. Last, deliver the spark to

each cylinder so combustion can begin at the right time during the compression stroke of each cylinder [5]. The timing diagram of injection, ignition and intake valve open as shown in Figure 2.8.

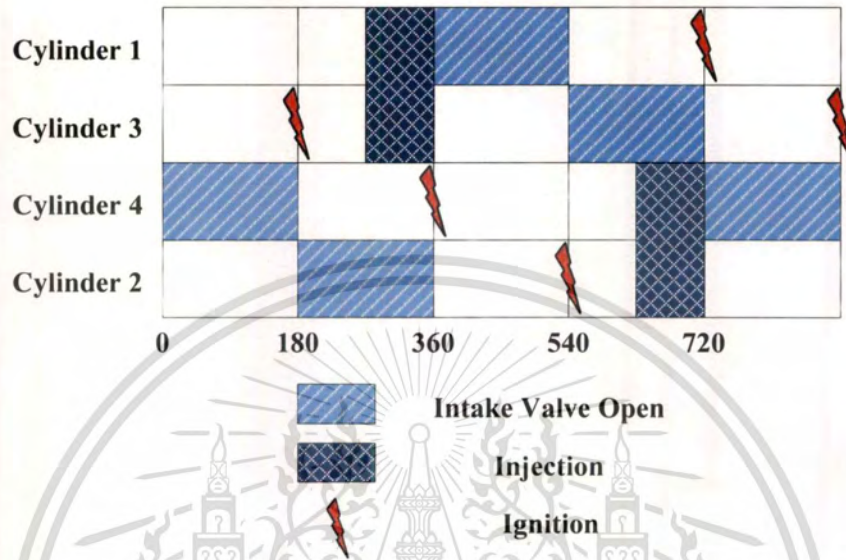


Figure 2.8 Timing diagram

CHAPTER 3

EXPERIMENTAL PROCEDURES

This research, the observation engine model of air fuel ratio is needed engine mapping from experiment data for example; air mass flow rate, air fuel ratio, fuel mass flow rate or fuel injection duration, engine speed, torque and other parameters. The method for measuring engine performances is required engine test stand and experimental devices for collects the data.

3.1 Experimental Setup

Engine test stand is important devices for development and optimization of engine and engine control units (ECUs). In this work, engine test stand is used to identify engine mapping which the initial step for spark ignition engine model identification.

The engine test stands including SI engine, dynamometer, fuel supply system, ignition system, engine cooling system, engine control systems and sensors for measuring and monitoring engine parameters as shown in Table 3-1, Figure 3.1, Figure 3.2 and Figure 3.3.

Table 3-1 Experimental Components

No.	Components	No.	Components
1	Engine	9	Wide-Band Oxygen Sensor
2	Dynamometer	10	Wide-Band Oxygen Meter
3	Fuel Supply Pump	11	Radiator
4	Air Flow Sensor	12	Exhaust Muffler
5	Throttle	13	Ignition Control Unit
6	Fuel Rail & Injectors	14	Injection Control Unit
7	Ignition Coils	15	Data Acquisition Module
8	Crank Shaft Sensor	16	Dynamometer Controller

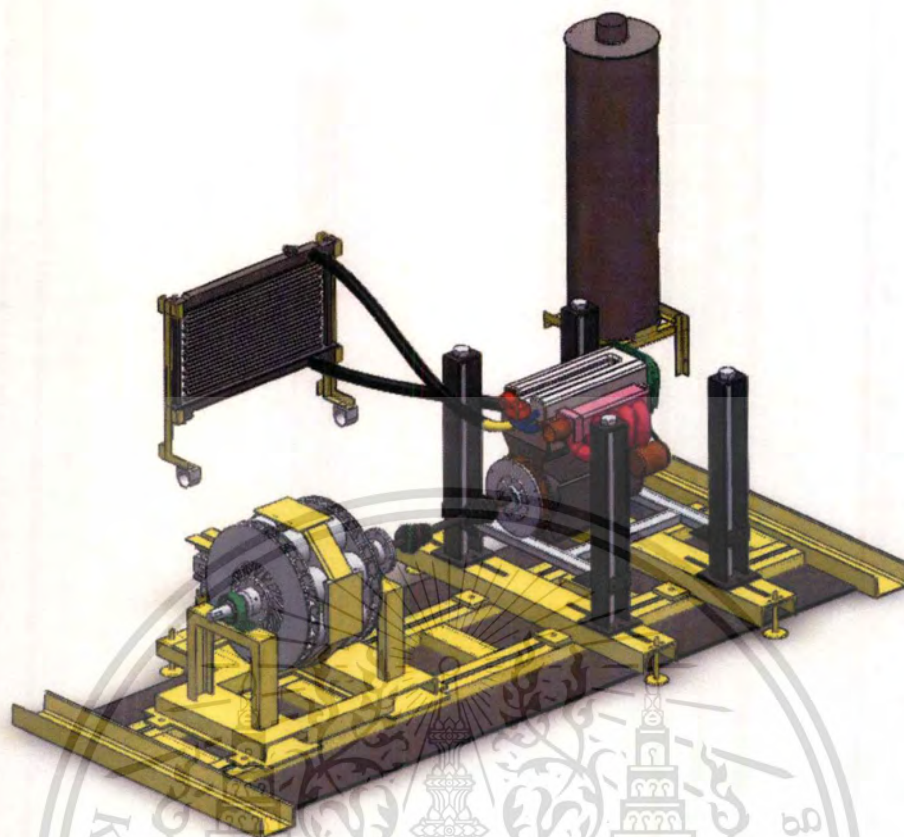


Figure 3.1 Engine test stand drawing



Figure 3.2 Engine test stand

This material is reserved for educational use only, not allowed for commercial use.

Forbidden to modify the content, and cite the document when use.



Figure 3.3 Engine test stand computer controller

3.1.1 Spark Ignition (SI) Engine



Figure 3.4 Mazda BP-ZE gasoline engine

This material is reserved for educational use only, not allowed for commercial use.

Forbidden to modify the content, and cite the document when use.

Figure 3.4 shows the Mazda BP-ZE 1.8 liters standard gasoline engine DOHC four-stroke 16 valves with water-cooling, four-cylinder engine has specifications as a cylinder diameter 83 mm, a stroke of 85 mm, compression ratio of 9.8, red line of 7,200 rpm and fuel injection flow rate equal to 250 ml/min has been considered. In addition, the distributor has been replaced by ignition coil for more precise control of ignition spark timing.

3.1.2 Engine Dynamometer

Engine dynamometer is used to performance test and characterizes the engine. This experiment “Telma” CC135 electric retarder air cooled has been considered. The principle of electric retarder is based on the creation eddy current in metal disc rotating between two electromagnets, it make opposing the rotation of the metal disc. The energy has been absorbed and transfer to heating of the metal disc. The electronic retarder has been controlled by dynamometer controller with engine speed close loop control module as shown in Figure 3.5, Figure 3.6 and Figure 3.7.

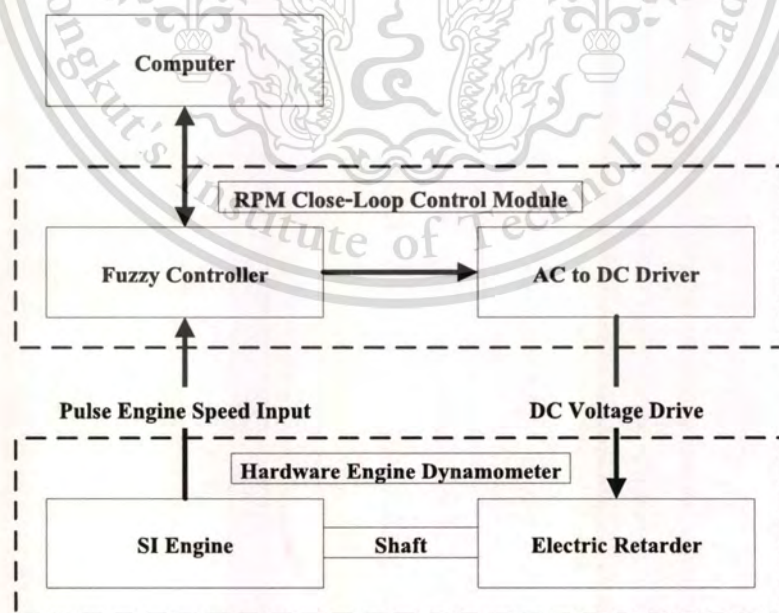


Figure 3.5 Engine dynamometer control diagram [21]

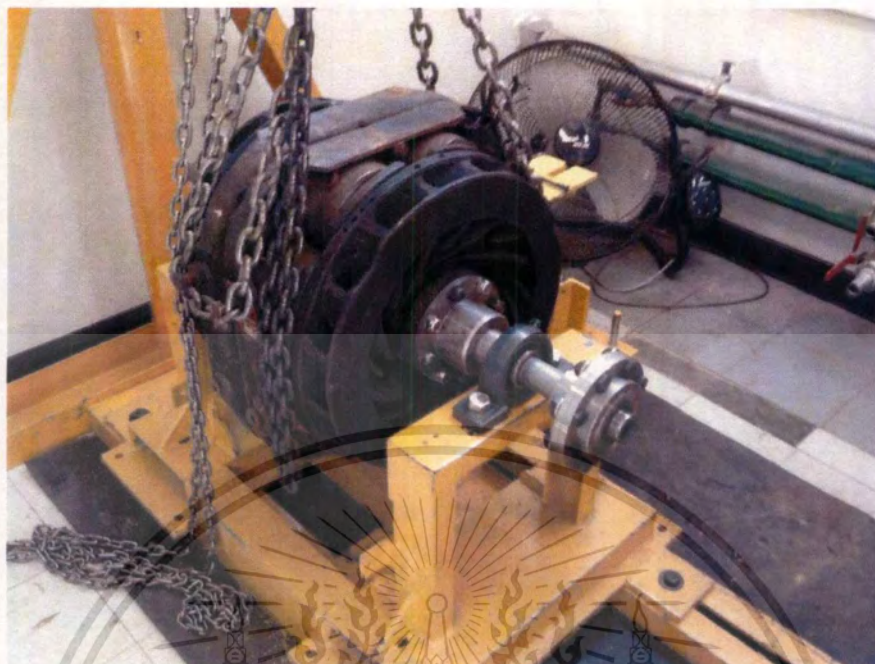


Figure 3.6 Eddy current retarder "Telma"

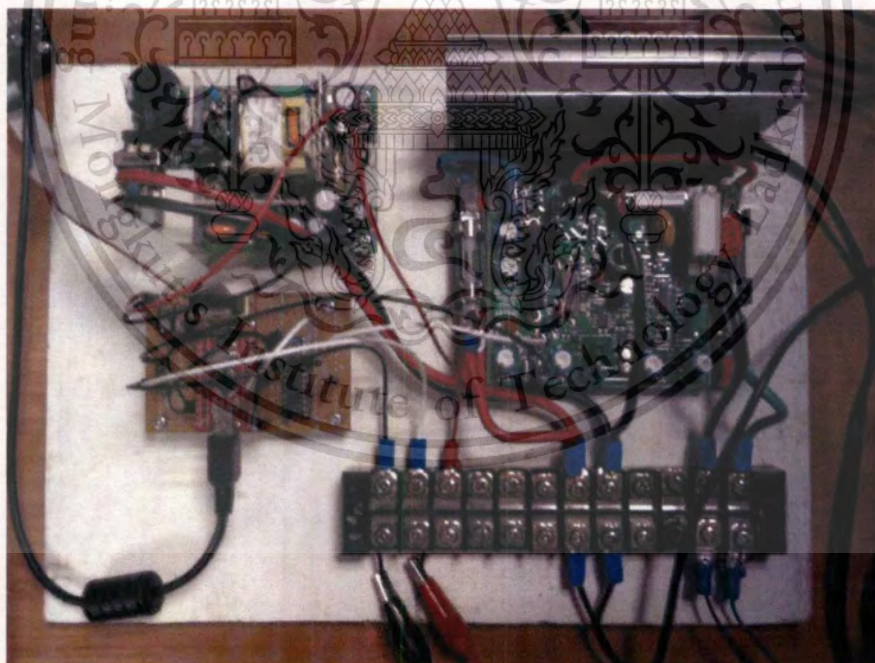


Figure 3.7 Dynamometer controller

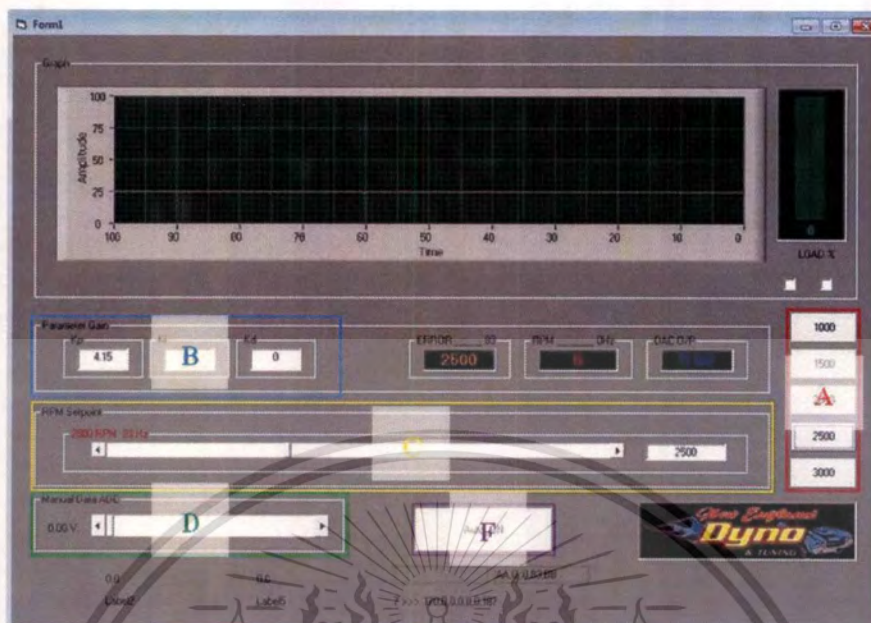


Figure 3.8 Dynamometer control program

Figure 3.8 shows the dynamometer control program has been developed by the embedded system technology (EST) NECTEC. “A” section is used to select the set point of engine speed. “B” section is used to adjust parameters gain. “C” section is used to adjust engine speed bar and also display engine speed. “D” section is used to adjust drive voltage and also display the drive voltage. “F” section is used for automatic engine speed close-loop control.

3.1.3 Strain-Gauge Load Cell

It is devices for producing an electrical output which changes in magnitude when a force or weight is applied and which may be displayed on a readout instrument or used in a control device. The heart of the load cell is the bonded-foil strain gauge which is an extremely sensitive device, whose electrical resistance changes in direct proportion to the applied force [23]. The “Tedea Huntleigh model 614” S-beam type tension and compression capacities 50-300 Kg has been considered in this engine test stand as shown in Figure 3.9.

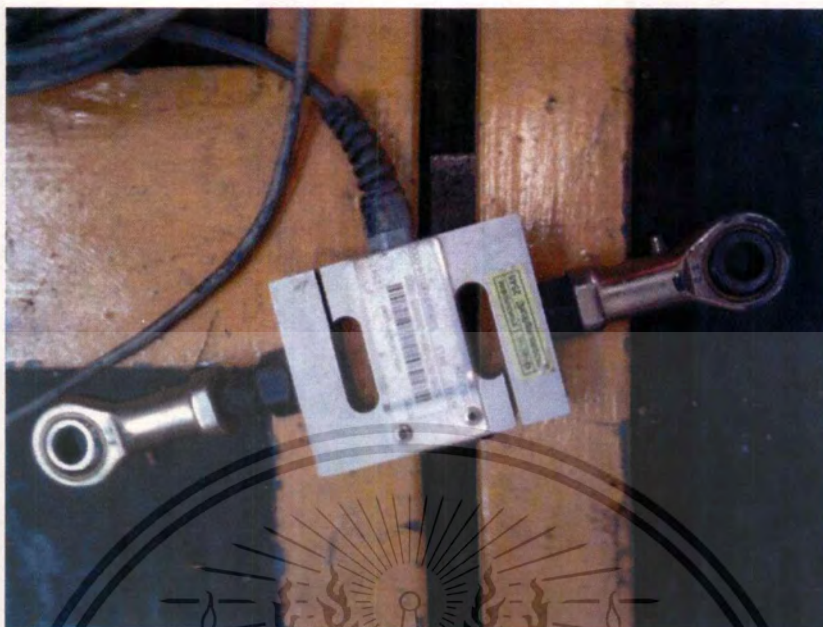


Figure 3.9 Strain-gauge load cell "S-beam type tension and compression"

3.1.4 Oxygen Sensor and Oxygen Meter



Figure 3.10 Wide-band oxygen sensor "Innovate LM-1"

This material is reserved for educational use only, not allowed for commercial use.

Forbidden to modify the content, and cite the document when use.

An oxygen sensor or lambda sensor is an electronic device that measures the proportion of oxygen (O_2) in the exhaust gas. If the air fuel ratio exiting a gas-combustion engine is rich (with un-burn fuel vapor) or lean (with excess oxygen). In this experiment the “Innovate LM-1” wide band oxygen sensor has been considered. The voltage output 1.0 V. for an AFR equal to 10 and 2.0 V for an AFR equal to 20 (gasoline) [22].

3.1.5 Air Mass Flow Sensor

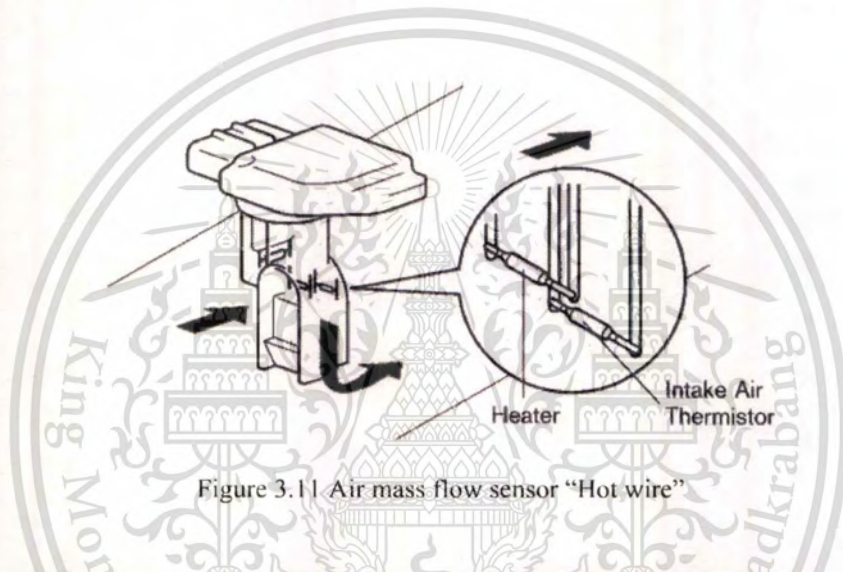


Figure 3.11 Air mass flow sensor “Hot wire”



Figure 3.12 Air mass flow sensor

The air mass flow sensor (Figure 3.11 and Figure 3.12) is converts the amount of air through the throttle into a voltage signal. Normally, the ECUs need to know intake air volume to calculate engine load, it necessary to determine quantity of fuel and ignition timing.

The air mass flow sensor hot wire type. This type included thermistor, hot wire and electronic control circuit.

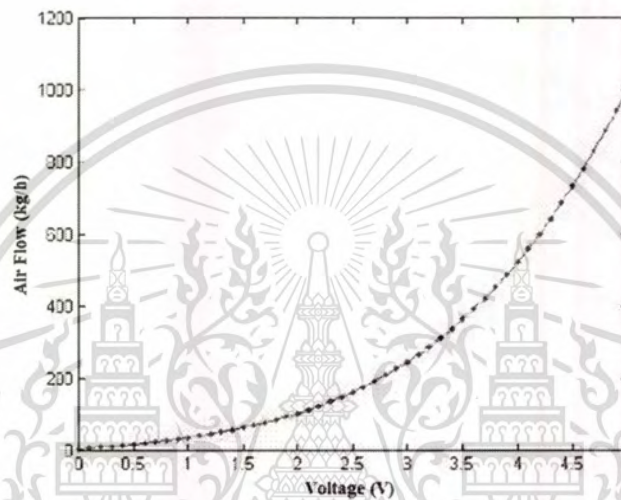


Figure 3.13 Air mass flow sensor signal voltage

Equation (3-1) shows, the air mass flow value can be estimated by function “polyfit” degree 4 in MATLAB program.

$$\dot{m}_{act} = 0.608V^4 + 3.356V^3 + 2.943V^2 + 25.37V + 2.178 \quad (3-1)$$

3.2 Engine Control Systems

An engine control system is used to controls various aspects of an SI engine operation. The engine control systems include the control quantity of fuel injected into cylinder per engine cycle, control the advance ignition timing and also data logger or data acquisition as shown in Figure 3.14.

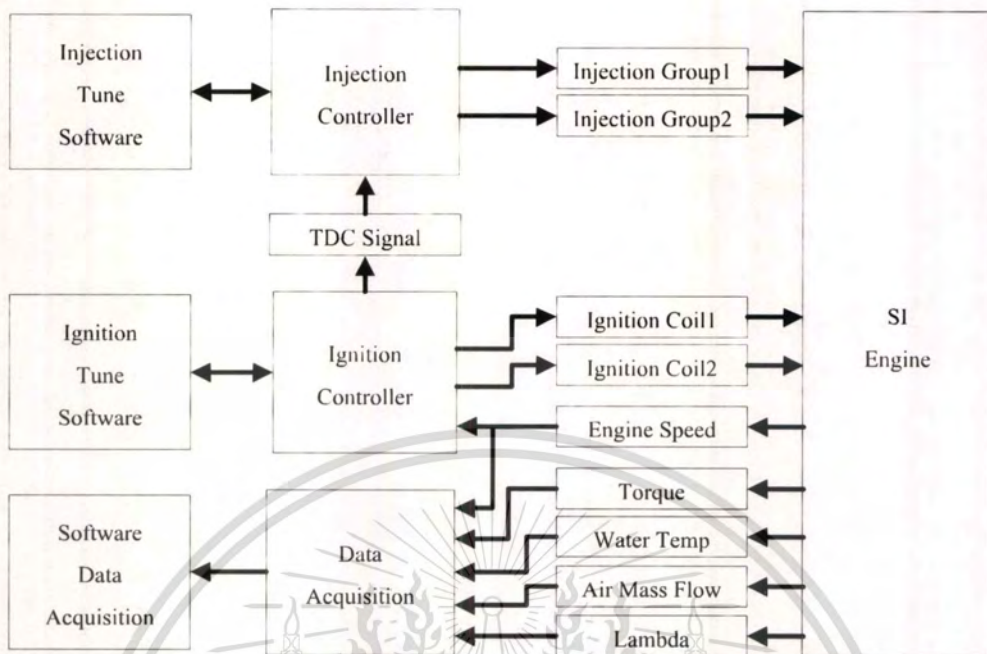


Figure 3.14 Engine control system diagram

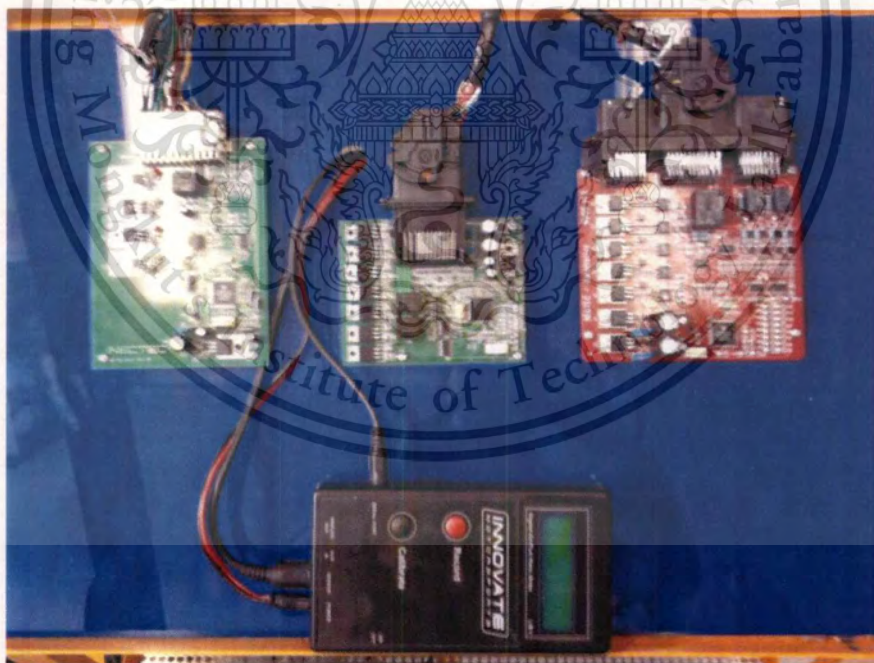


Figure 3.15 Engine control device

3.2.1 Crankshaft Pulse Generator

The crankshaft pulse generator consists of a metal disk or reluctor wheel positioned on the crankshaft and a detector that covers a magnetic coil. The reluctor wheel movement past the coil causes a disturbance in the magnetic field, creating the electric pulses that the computer uses to determine the speed and position of the crankshaft. But the sensor does not produce direct crankshaft location and speed; it sends the electric signal to the engine control system, which then calculates the desired values.



Figure 3.16 34x Reluctor wheel

The crankshaft pulse generator has been attached to the crank shaft pulley. The crankshaft pulse generator included the reluctor wheel and crankshaft position sensor. The reluctor wheel are spaced (pulse interval) 10 degree according to crankshaft angle. The number of gear teeth has 36 teeth but 2 teeth are missing, there are a total of 34 teeth [21] as shown in Figure 3.17.

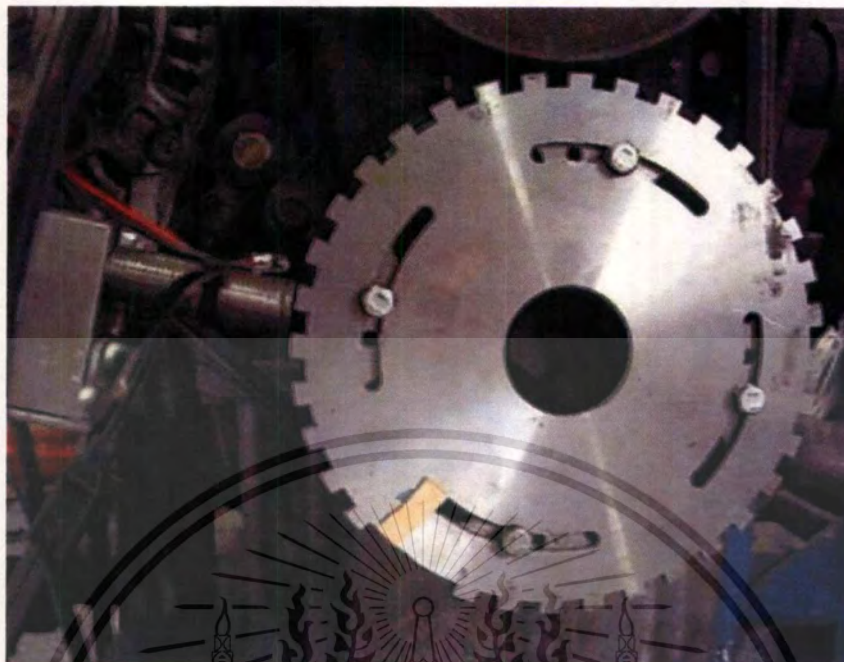


Figure 3.17 Crankshaft pulse generator

3.2.2 Fuel Injection Controller

The control of fuel quantity is based on the opening of the injectors. Generally, the ECUs determines the fuel quantity by changing the pulse duration (pulse width), which represents the amount of time till the injectors remain open.

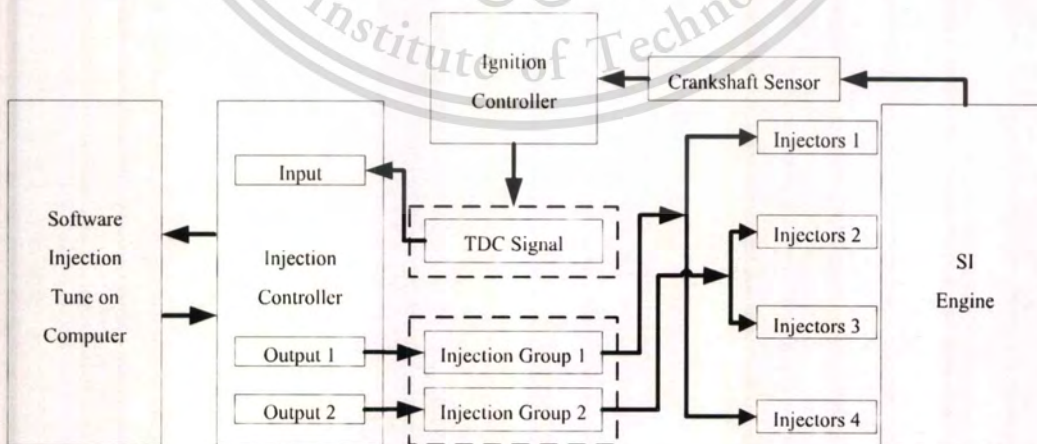


Figure 3.18 Fuel injection system diagram

Figure 3.18 shows the multi-point fuel injection (MPFI) has been considered. This system requires one injector per cylinder. Fuel is injected twice per engine operation cycle; each injection delivery half of fuel quantity. The injectors are divided into groups (group 1 has injectors 1 and 4 and group has 2 injectors 2 and 3) each group being same injection signal. The injection pulse is relative to the top dead center signal (TDCs) in each cycle. The performance (torque) and air fuel have been change from the timing of injector open or injection duration in unit millisecond (ms) with injection control software on computer.



Figure 3.19 Fuel injection control module "FC163"

Figure 3.19 shows the FC163 natural gas injection control system ECUs has been applied to be injection controller. The microcontroller is dsPIC co-processor from Microchip that has 16 bits 60 MHz, connecting with computer via RS-232 to USB port.

The FC163 fuel controller software has been used for control fuel injection into intake manifold. In the "A" table x-axis show throttle position sensor: TPS (%) and y-axis show engine speed (RPM). "B" section displays the analog engine speed and digital engine speed. "C", "D" and "E" section displays injection duration (ms), throttle position sensor (%) and manifold absolute pressure (MAP) respectively as shown in Figure 3.20

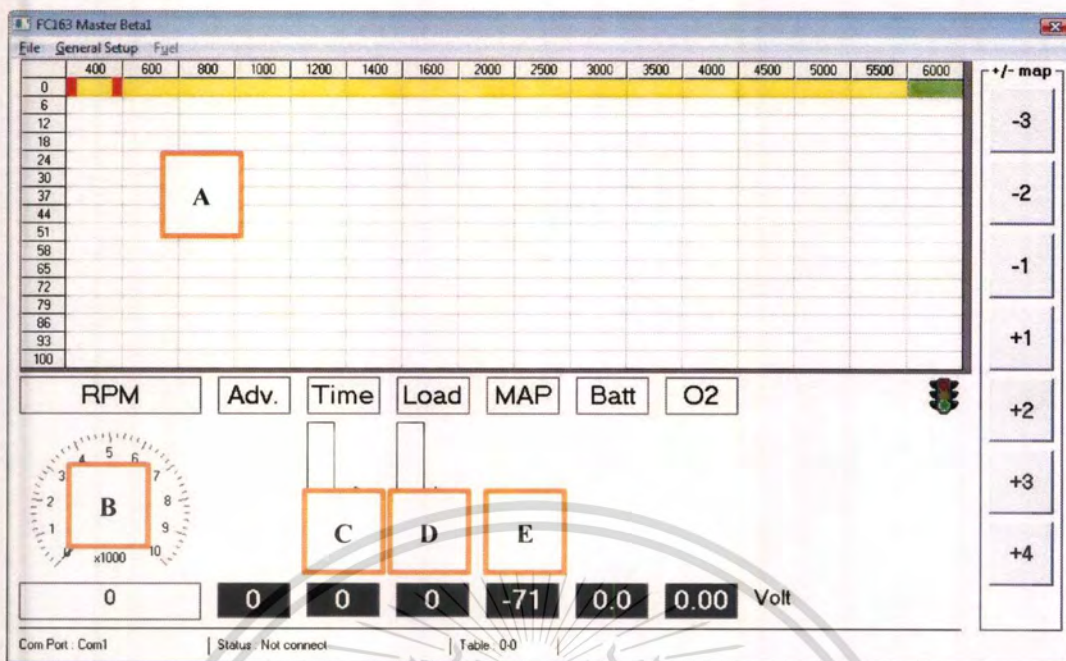


Figure 3.20 Injection control program “FC-163”

3.2.3 Spark Ignition Control

A spark ignition engine requires a spark to initiate combustion in the combustion chamber. ECUs can adjust the exact timing of the spark (called ignition timing) to provide better power and economy.

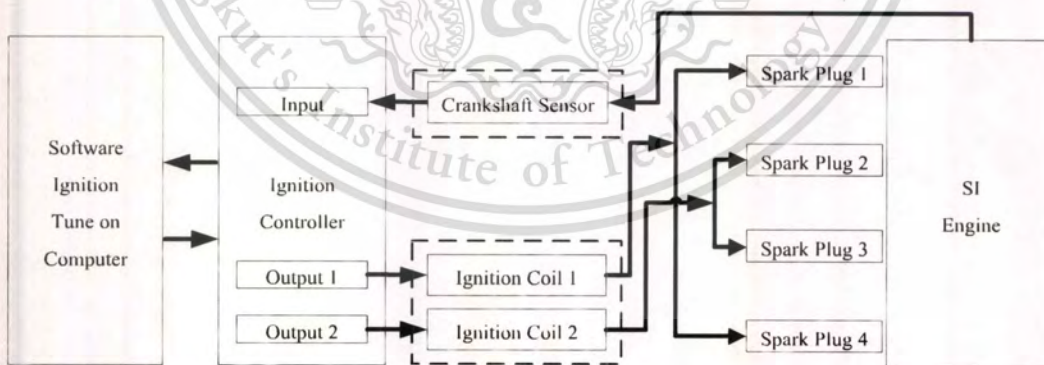


Figure 3.21 Ignition control system diagram

Figure 3.21 shows the ignition control system, the dual spark ignition system has been considered. This system requires two ignition coils. The spark plugs are divided into ignition coils

(ignition coil 1 spark plugs 1 and 4 and ignition coil 2 spark plug 2 and 3) each ignition coil being same ignition signal. The ignition pulse has relative to the crankshaft signal. The change advance ignition timing has influence for engine performance of engine with ignition control software on computer.



Figure 3.22 Ignition control module

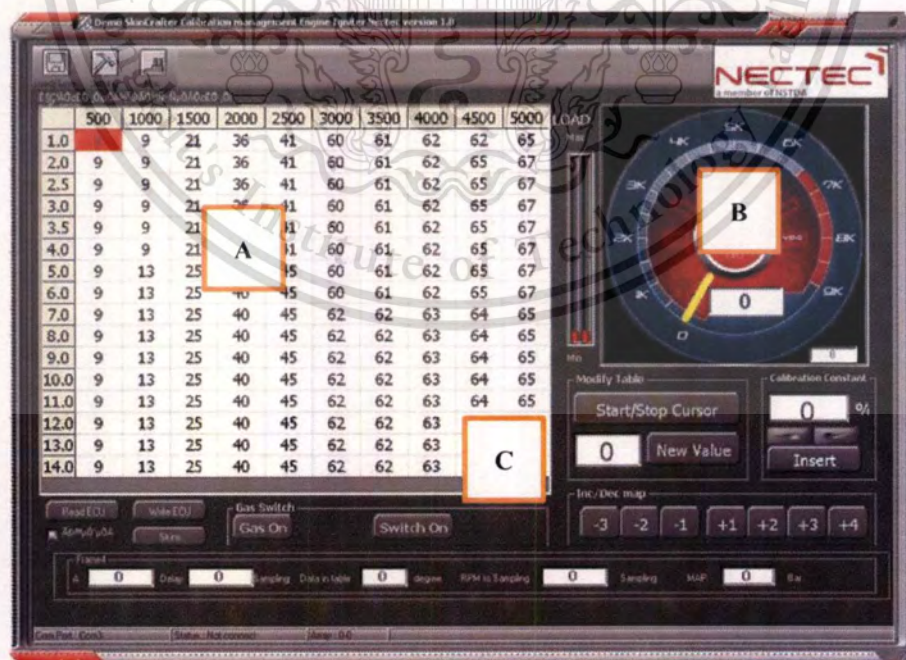


Figure 3.23 Ignition control program

This material is reserved for educational use only, not allowed for commercial use.

Forbidden to modify the content, and cite the document when use.

Figure 3.22 shows the ignition control module has been developed by NECTEC. It has applied to be ignition controller. The microcontroller is dsPIC processor from Microchip that has 16 bits 30 MIPS connecting with computer via MX232. The crankshaft sensor is digital input signal and TPS is analog input for select ignition timing value in ignition timing table.

Figure 3.23 shows NECTEC ignition control program has been used for control ignition timing. In the “A” table, x-axis show throttle position sensor: TPS (%) and y-axis show engine speed (RPM). “B” Section is used to displays analog engine speed and digital engine speed and “C” Section uses for adjusts ignition timing value in the table.

3.2.4 Throttle Position Control

The throttle position controls of SI engine have a direct physical mechanism linkage or flexible cable between an accelerator pedal and the throttle body so that the throttle plate is pulled open by the accelerator cable as the driver presses the pedal. However, in this experiment the engine operation room and control room are separated then the flexible cable is difficult to control and position throttle plate position.



Figure 3.24 Throttle with servo motor

Figure 3.24 shows the electronic servo motor has been installed for control the throttle plate via wCK programmer program software. Which, the close throttle position is 170 and wide open throttle position is 248 as shown in Figure 3.25.

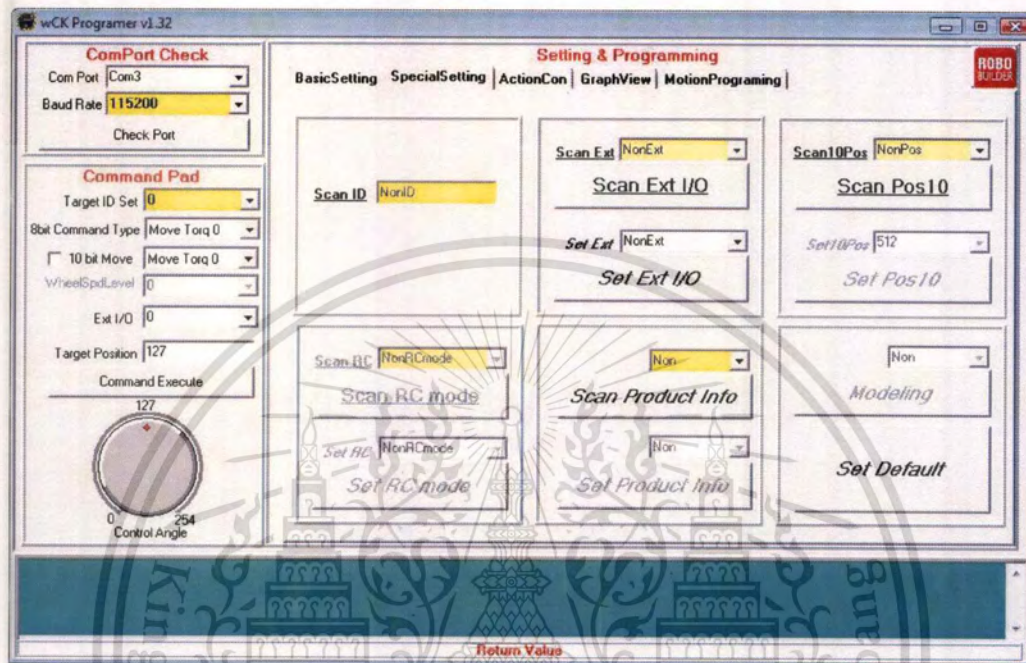


Figure 3.25 wCK programmer

3.3 Data Acquisition

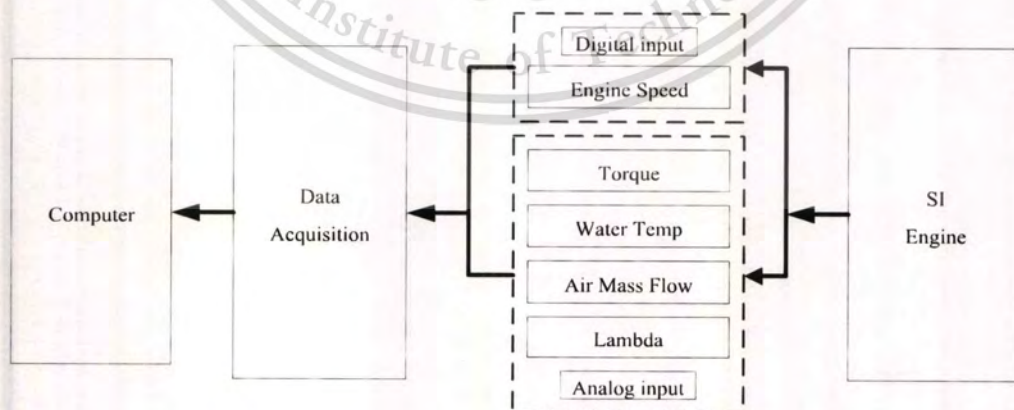


Figure 3.26 Data acquisition diagram (DAQ)

Figure 3.26 shows the data acquisition (DAQ) is used to collect the experiment data both analog signal and digital signal. An analog signal is measured response to change of voltage in this experiment are strain-gauge for calculate engine brake torque, air mass flow sensor for calculate air mass flow rate and cooling water temperature sensor. Digital signal is a signal waveform, in this experiment is crankshaft sensor for calculate engine speed.



Figure 3.27 Data acquisition module “MyOS01”

Figure 3.27 shows the data acquisition module “MyOS01” ECUs has been modified as data acquisition module. The module is based on “Microchip” dsPIC 30F6014A microcontroller, which is 12 bits resolution of analog to digital converter (ADC), 8 channels with the sampling rate of 25 Hz, connecting with computer via RS-232 port at baud rate 19.2 Kbps. The data are acquired in a 50 ms, which is provided record analog inputs (mass air flow, torque, water temperature) and digital input (engine speed from crankshaft sensor during the experiment).

The engine parameter logger is used to collect engine parameters. The air mass flow rate (g/s) has been shown in “A” section. The engine torque (N.m) as shown in “B” section. The engine speed (rpm) as shown in “C” section. The coolant water temperature ($^{\circ}\text{C}$), Throttle position voltage (0 V. for fully close and 3.99 V. for wide open throttle) as shown in “D” and “E”

sections. The “State Mem Data”, “Stop Mem” and Write to File” buttons are used to start record data, stop record data and save data into excel file respectively as shown in Figure 3.28.

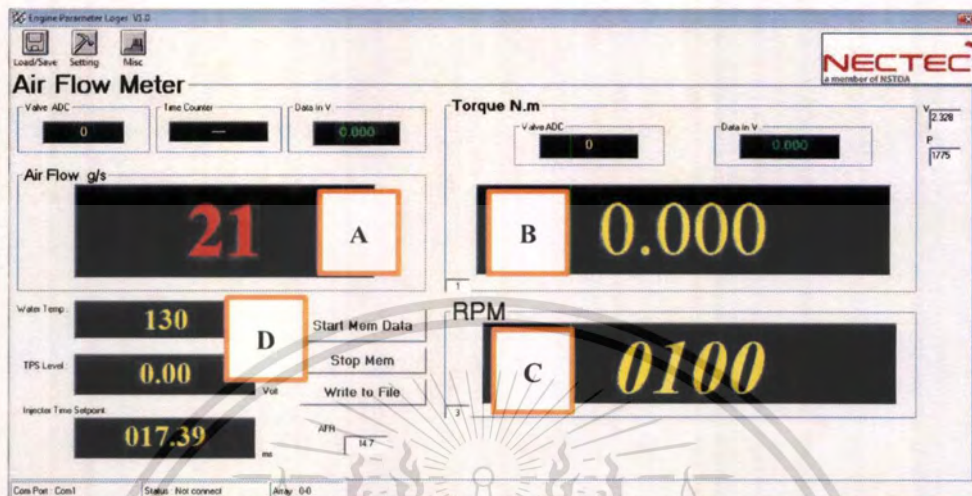


Figure 3.28 Engine parameter logger program

3.4 eMapnMod Program

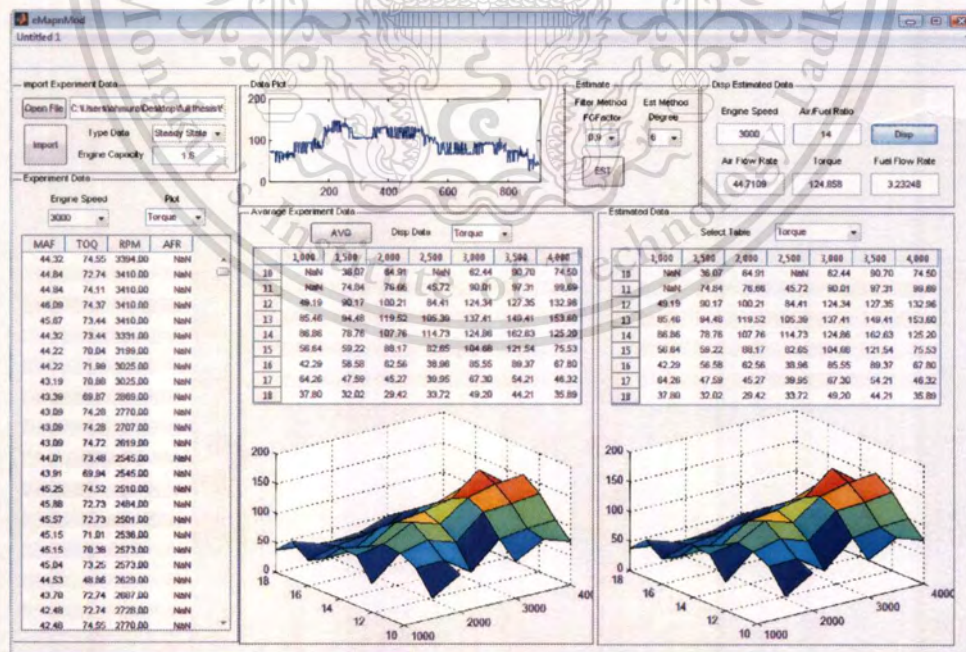


Figure 3.29 eMapnMod program

Figure 3.29 shows the eMapnMod program has been designed and developed for data estimation and display value. “Import data” panel is used for import experiment data from excel files and also display value in the table. “Data plot” panel is used for display input data graph. “Average data” panel is used for average value of experiment data compare with engine speed and air/ fuel ratio, display averaged data in table and plot averaged data in 3D graph. “Estimate” panel is used for selects forgetting factor for estimate data. “Disp Estimate Data” is used for interpolate value of estimate data. “Estimate Data” is used for display average estimate data and plot in 3D graph.

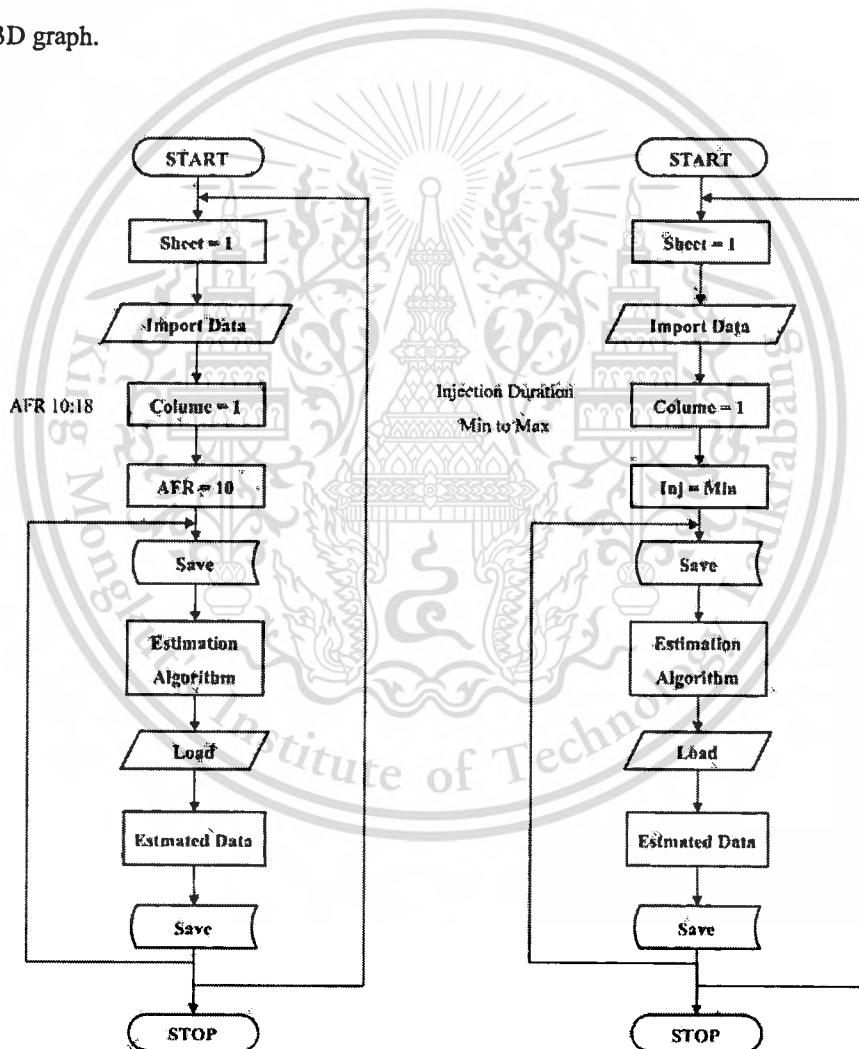


Figure 3.30 eMapnMod flow chart

Figure 3.30 shows the data selection flow chart of eMapnMod program. The left side is flow chart for steady state method and right side is flow chart of sweep test method.

3.5 Experimentations

In this experiment, the SI engine has been attached to the electric retarder via crankshaft which based on engine test stand and all of sensors and control systems have been already attached into the engine and electric retarder. The experiment methods for investigate engine behavior are divided into two methods, steady state test and sweep test.

3.5.1 Steady State

Warming up the engine and wide-band oxygen sensor at idle speed around 800 rpm until coolant water temperature should remain around 70 degrees Celsius. Engine speed condition from 1,000:4000, wide open throttle, adjust fuel inject duration timing until air fuel ratio since 10 to 18.

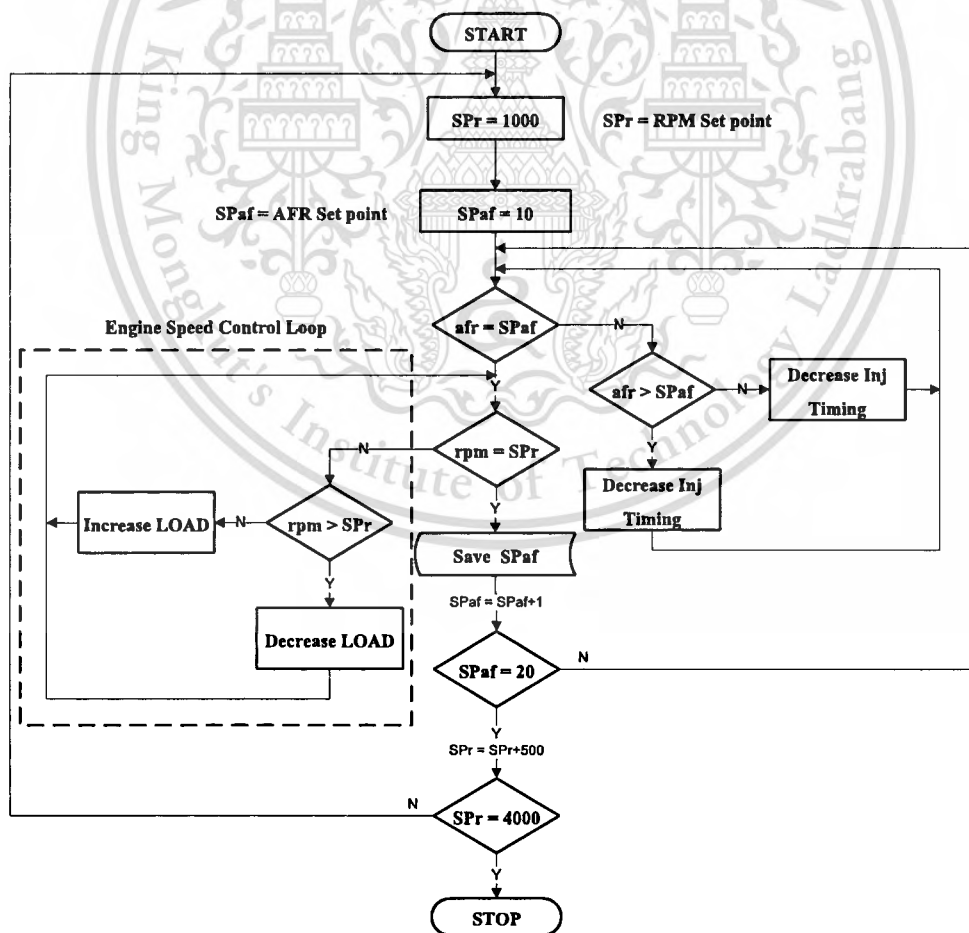


Figure 3.31 Steady state experiment flow chart

3.5.2 Sweep Test

In case of sweep test, warming up the engine and wide-band oxygen sensor at idle speed around 800 rpm until coolant water temperature should remain around 70 degrees Celsius. Engine speed condition from 1,000 to 4000, wide open throttle, and adjust injection timing until lambda value from 0.7 to 1.3.

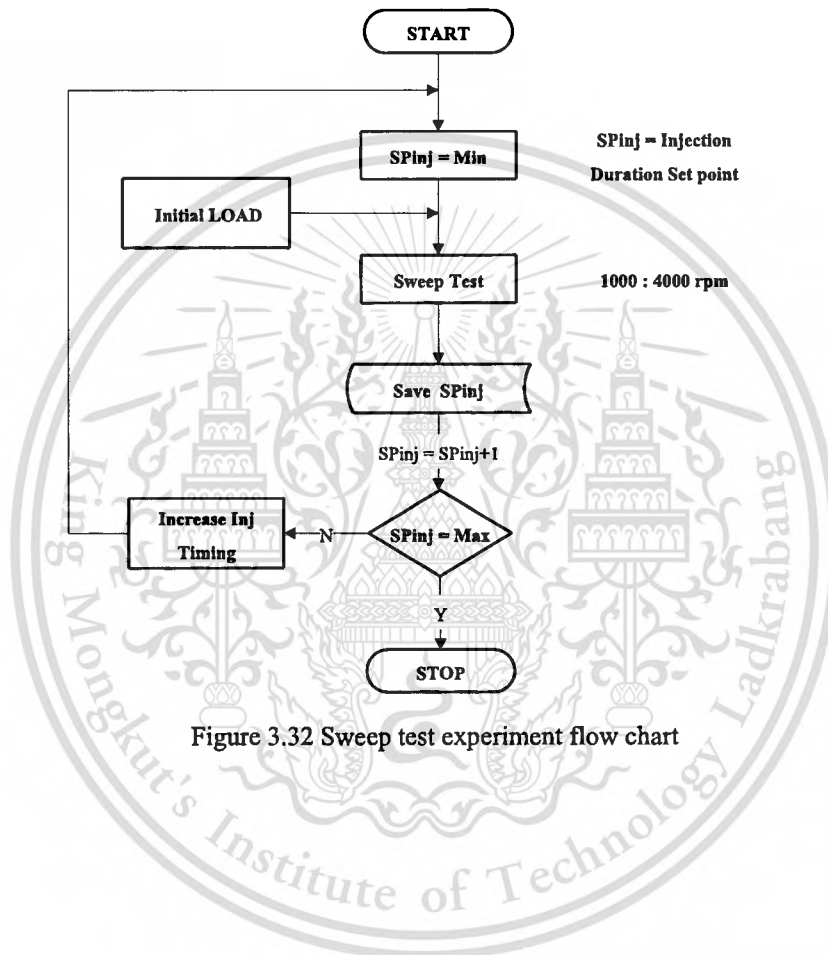


Figure 3.32 Sweep test experiment flow chart

CHAPTER 4

RESULTS AND DISCUSSIONS

This chapter shows the experimental results, simulation and validation data of SI engine when fueled gasoline and gasoline-ethanol blend. The air mass flow rate, fuel flow rate (injection duration), torque and air fuel ratio (λ) that implemented in this chapter, also the experimental results estimation result and validation results are discussed.

4.1 Steady State

4.1.1 Sampling Cycle Experiment “Steady State”

The data set has been selected reference with engine speed (RPM) and air fuel ratio (AFR). Identifications the engine parameters RPM, AFR, TORQUE and RPM, AFR, MAF at wide open throttle (WOT) a steady state experiment was performed. 7 equally spaced engine speeds (1000 to 4000 rpm) and 9 equally spaced air fuel ratios (AFR) (10 to 18) was used to building a torque map and air mass flow map. Each maps measurements in 63 different steady state operating points.

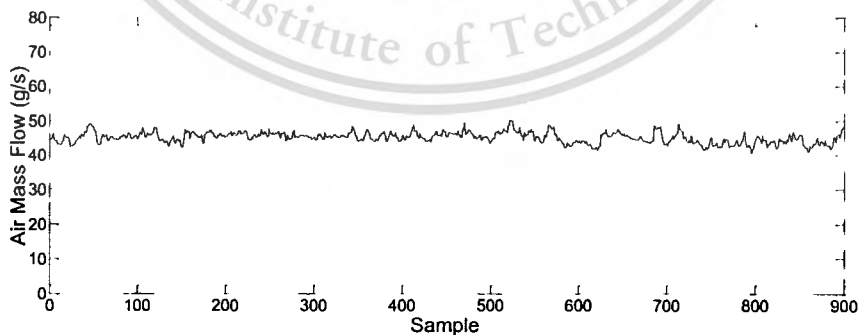


Figure 4.1 Air mass flow measurement at engine speed 3,000 rpm

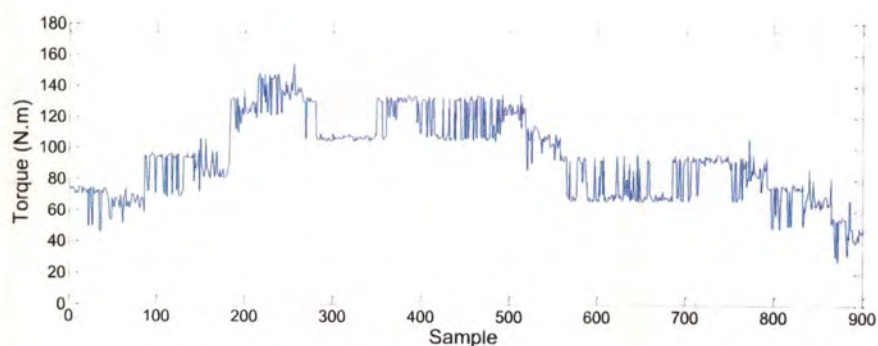


Figure 4.2 Torque measurement at engine speed 3,000 rpm

Figure 4.2 and Figure 4.2 shows, the example of sampling cycle of air mass flow and torque measurement at engine speed 3,000 rpm.

4.2 Sweep Test

4.2.1 Sampling Cycle Experiment "Sweep Test"

The data set has been selected reference with engine speed (RPM) and lambda (λ). Identifications the engine parameters RPM, LAMBDA, TORQUE and RPM, LAMBDA, MAF at wide open throttle (WOT) a sweep test experiment were performed. 7 equally spaced engine speeds (1000 to 4000 rpm) and 7 equally spaced lambdas (λ) (0.7 to 1.3) were used to building a torque map and air mass flow map. Each maps measurements in 49 different sweep test operating points.

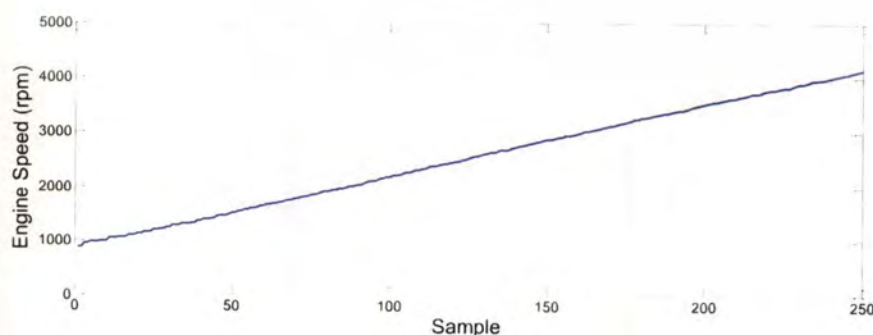


Figure 4.3 Engine speed at fuel injection duration 11 ms

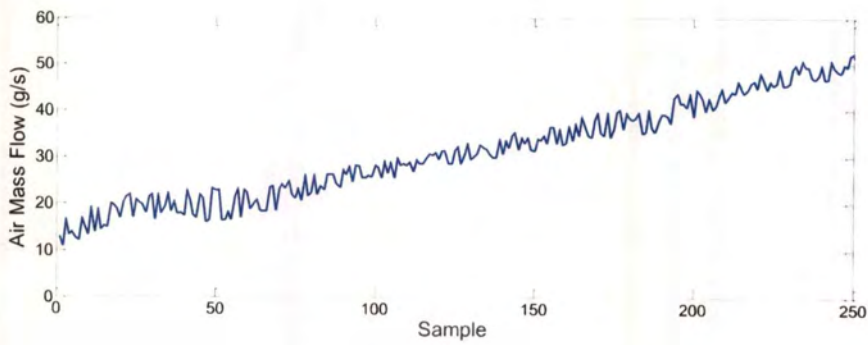


Figure 4.4 Air mass flow at fuel injection duration 11 ms

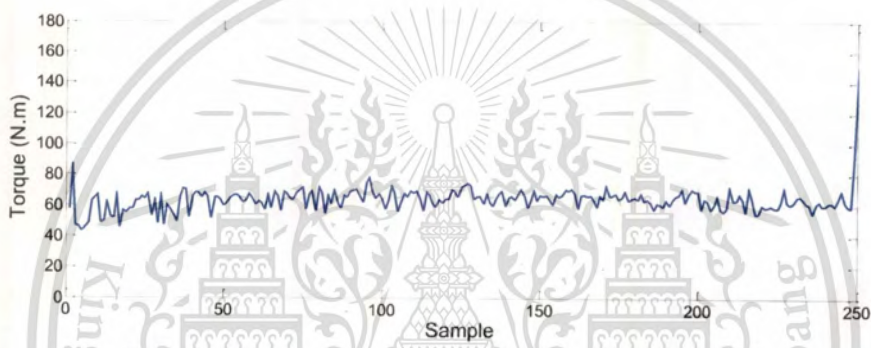


Figure 4.5 Torque measurement at fuel injection duration 11 ms

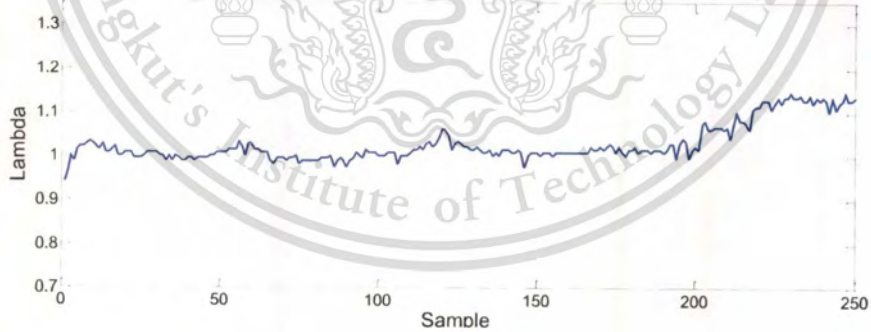


Figure 4.6 Lambda value at fuel injection duration 11 ms

Figure 4.3, Figure 4.4, Figure 4.5 and Figure 4.6 show the sampling cycle of engine speed, air mass flow, torque and lambda with sweep test method.

4.3 Experiment

The air mass flow measurement is depending on engine speed (RPM) and throttle angle (TPS). In this experiment, wide open throttle has been considered, and then the air mass flow rate is only depending on engine speed.

The fuel mass flow rate is depending on engine speed (RPM), air mass flow rate (AMFR) and air fuel ratio (AFR). In this experiment, the fuel mass flow rate is relation with average measurement air mass flow rate and air fuel ratio which can calculated by equation (2-7) in term \dot{m}_{fc} without transport delay and time lag associated with engine/sensor process.

The torque measurement is depending on engine speed (RPM), air fuel ratio (AFR) and spark ignition timing (SPK). In this experiment, the spark ignition timing has been neglected.

4.4 Estimation

4.4.1 eMapnMod Estimation Process

In this work, the recursive least square (RLS) algorithm has been considered to decrease the influence of input sample from the far past, a weighting factor for influence of each sample is used. The eMapnMod is dividing into 2 test methods; steady state and sweep test.

4.4.2 Forgetting Factor Identification

Power spectral density is selected to find the frequency components of a signal (torque measurement) buried in a noisy time domain signal when change forgetting factor with FFT (Fast Fourier Transform) MATLAB function. In this work, we defined the forgetting factor equal to 0.9 as show in Figure 4.7 and Figure 4.8.

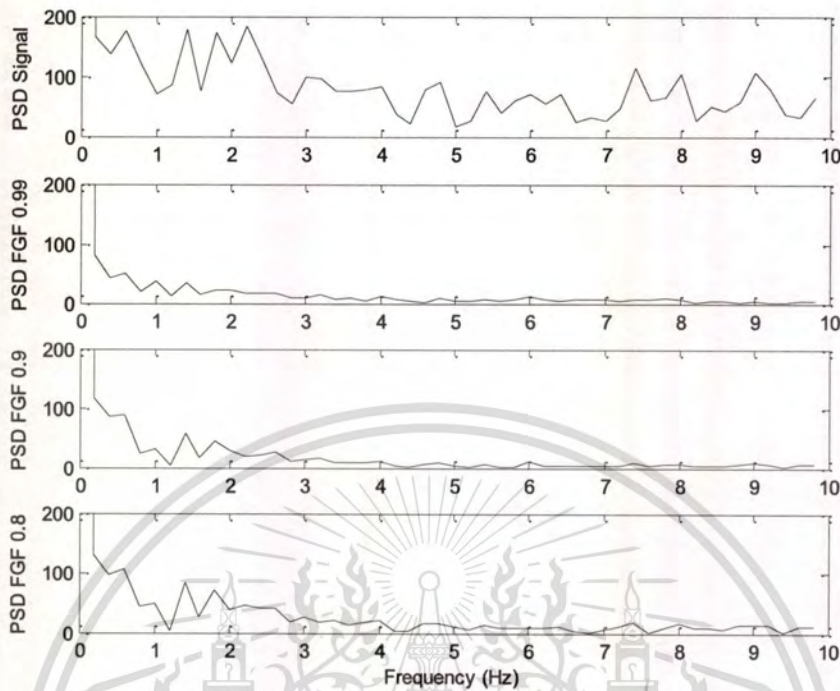


Figure 4.7 Power spectral density of experiment data (Torque)

Figure 4.7 shows the characteristic of power spectral density (PSD) from experiment data (torque) when the forgetting factor has been changed. The PSD signal shows the power spectral density of measurement data (torque). The PSD higher than 100, frequency are around 0 – 0.25 Hz. Then, we can assume from PSD Signal figure; the desired signal has frequency around 0 – 0.25 Hz. and other frequency is noise.

When change the forgetting factor value = 0.99 the signal is decreased lower than 100 as shown in Figure PSD FGF 0.99. So that means the both of signal and noise has been filtered.

When change the forgetting factor value = 0.9 the signal are still remain (higher than) 100 as shown in Figure PSD FGF 0.9. So that means just only noise has been filtered.

When change the forgetting factor value = 0.8 the both of signal and noise are still higher than 100 as shown in Figure PSD FGF 0.8. So that means the both of signal and noise has not been filtered enough.

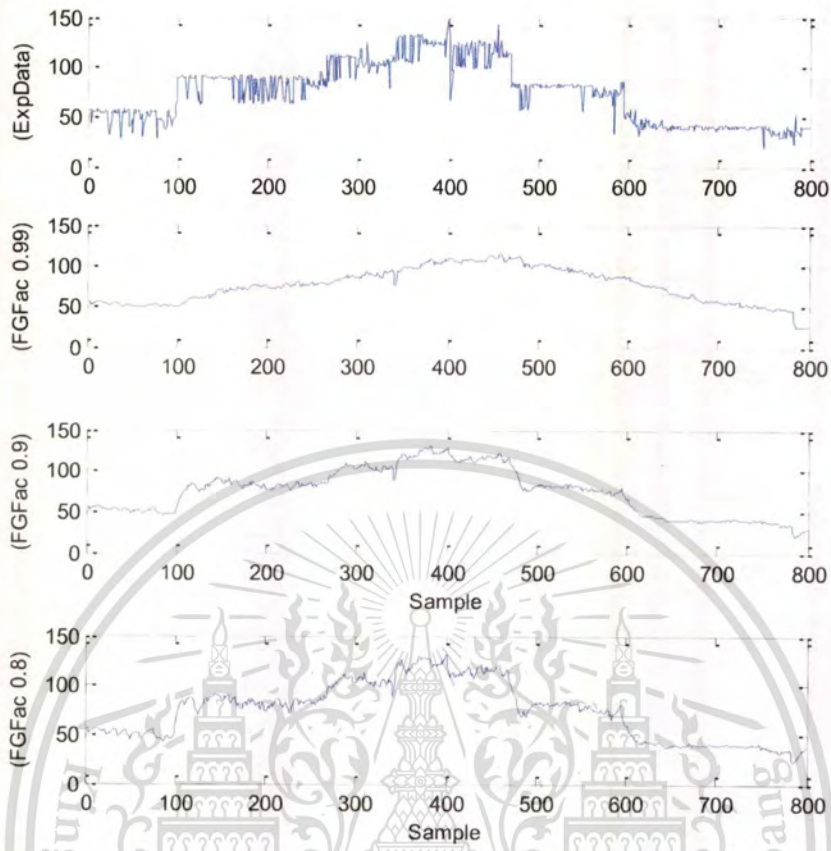


Figure 4.8 Torque estimation when change forgetting factor

Figure 4.8 shows the characteristic of experiment data (torque) when the forgetting factor has been changed. The ExpData figure shows the signal (torque measurement) is including noise and vibration.

When change the forgetting factor = 0.99, FGFac 0.99 Figure shows not only noise has been decreased but also the torque signal has been loss characteristic.

When change the forgetting factor = 0.9, FGFac 0.9 Figure shows only noise and vibration has been decreased and the torque signal are stilling in the characteristic.

When change the forgetting factor = 0.8, the FGFac 0.8 Figure shows the torque signals are stilling the characteristic and also noise and vibration are still high.

From Figure 4.7 and Figure 4.8, we can assume the optimum of forgetting factor for experiment data is 0.9 from PSD signal.

4.4.3 Steady State

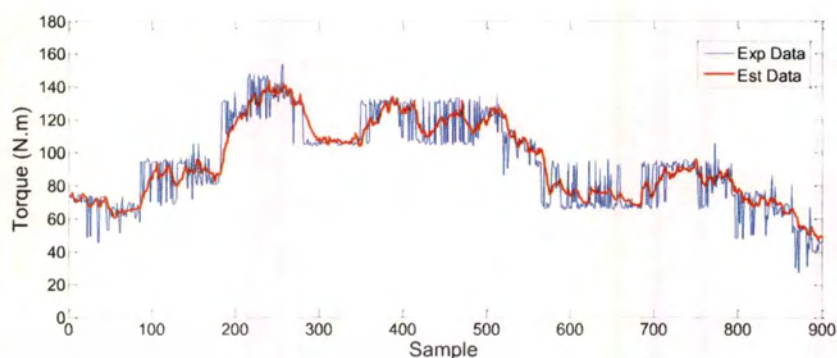


Figure 4.9 Torque measurement vs torque estimation at 3,000 rpm

4.4.4 Sweep Test

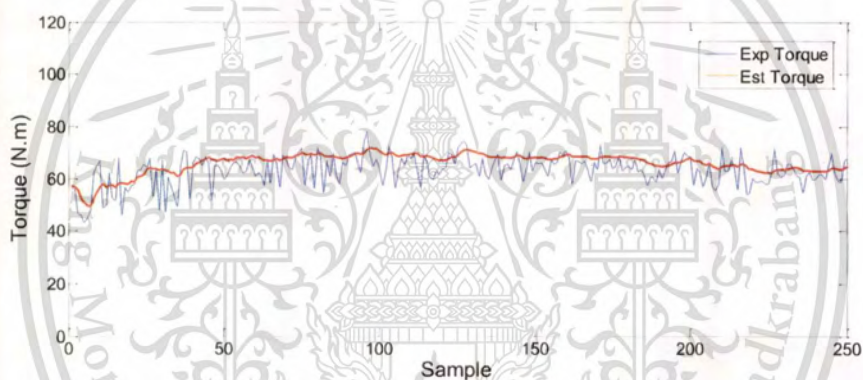


Figure 4.10 Torque measurement vs torque estimation at injection duration 11 ms

Figure 4.9 and Figure 4.10 show the example of sampling cycle and estimation data both steady state (3,000 rpm) and sweep test (11 ms) with recursive least square (RLS) with forgetting factor 0.9.

4.5 Experimental Results

This section we evaluate the air fuel ratio and performance of standard gasoline engine on actual engine. The experimental results have been separated 2 types; steady state test and sweep test. The steady state test method, only gasoline fuel has been considered. The both of gasoline and gasoline-ethanol blend (E-10, E-20 and E-85) have been considered in sweep test method.

4.5.1 Steady State (Gasoline)

For steady state testing the engine speed is controlled by the engine dynamometer (eddy-current). The gasoline results can be divided into 4 results. The air mass flow, fuel mass flow calculation, rotation torque, and volumetric efficiency.

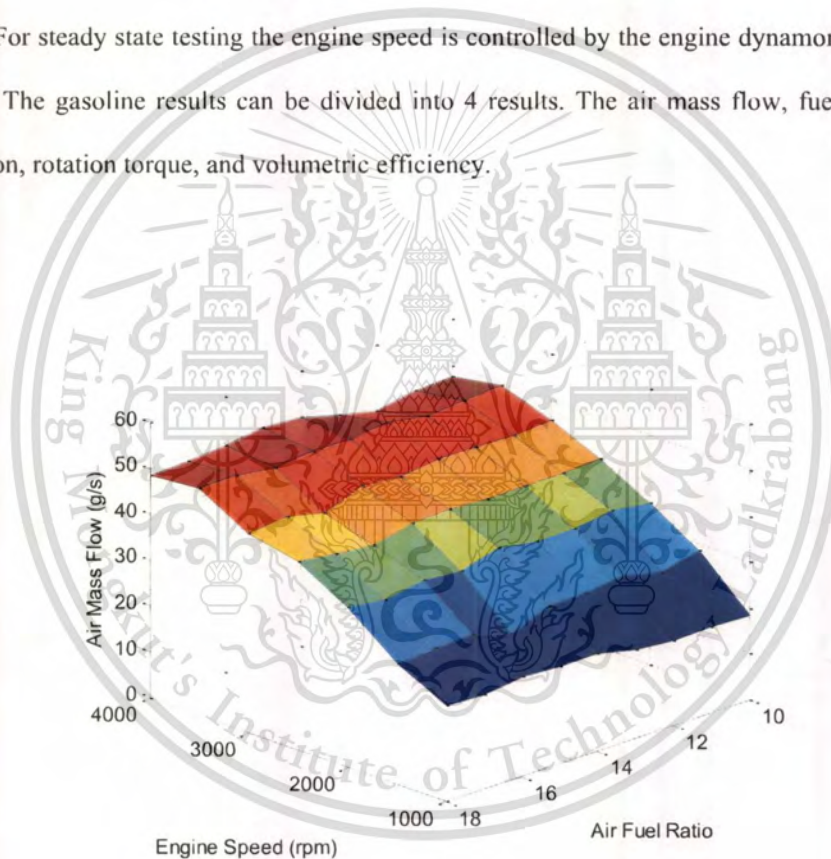


Figure 4.11 Air mass flow measurement (g/s)

Figure 4.11 shows the air mass flow rate measurement when gasoline used as fuel is increased due to increasing engine speed since 1,000 rpm to 3,500 rpm. The engine speed over 3,500 rpm, the air mass flow is slightly decreased.

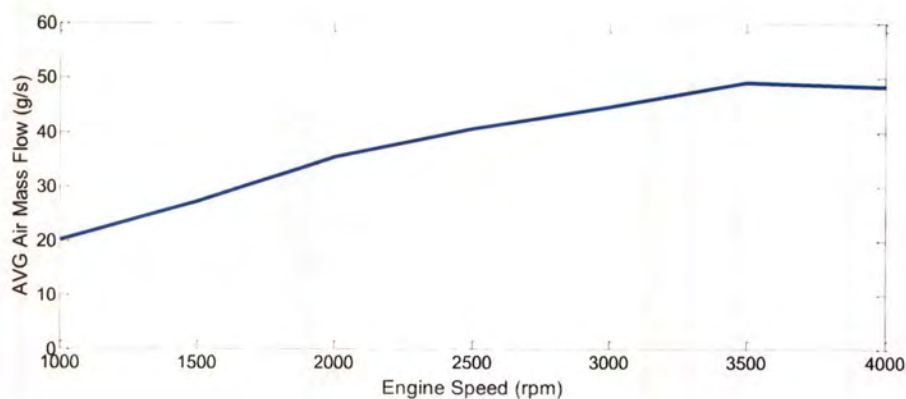


Figure 4.12 Average air mass flow (g/s)

Figure 4.12 shows the average of air mass flow when gasoline used as fuel. The maximum air mass flow is equal to 49.18 g/s at engine speed 3,500 rpm and minimum air mass flow is equal to 20.17 g/s at the engine speed 1,000 rpm. At engine speed 4,000 rpm the air mass flow is equal to 48.40 g/s. The difference of air mass flow between engine speed 3,500 rpm and 4,000 is equal to 1.5%.

In addition, the differences of air mass flows between air fuel ratios each engine speeds are (approximately) equal.

The air fuel mixture is entering in the cylinder due to the opening time of the intake valve and close. In this works, the engine test (MAZDA BP-ZE) is without variable valve timing system the parameters of valve opening, lifting and closing were fixed. This condition was optimum for normal engine speed, but unsuitable at high engine speed.

The high engine speed case the engine requires amounts of air into the combustion chamber, that valve timing should remain open for a longer period of time. This is may be explained to the air mass flow of engine speed 4,000 rpm, is less than engine speed 3,500 rpm.

The case of fuel injection duration, the fuel mass flow rate is calculated by equation (2-1) which depends on measurement air mass flow and air fuel ratio as shown in Figure 4.13.

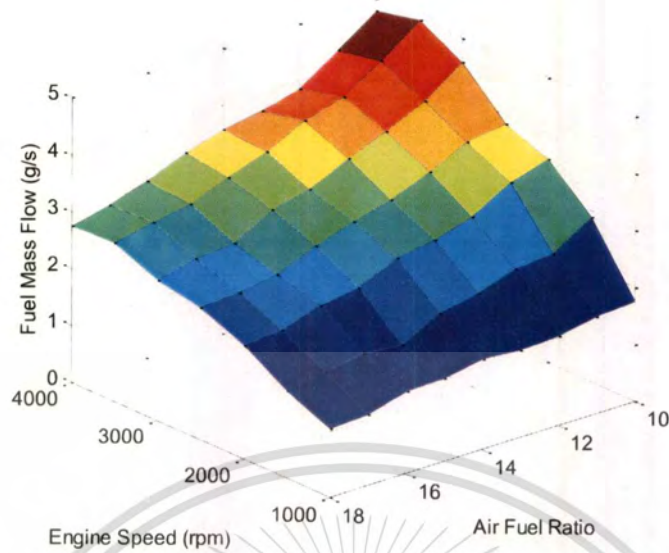


Figure 4.13 Fuel mass flow (g/s)

An increasing fuel mass flow rate is due to decreasing air fuel ratio and increasing engine speed. The minimum fuel mass flow is 1.23 g/s at air fuel ratio and engine speed equal to 18 and 1,000 rpm respectively. The maximum fuel mass flow is 4.99 g/s at air fuel ratio and engine speed equal to 10 and 3,500 rpm respectively.

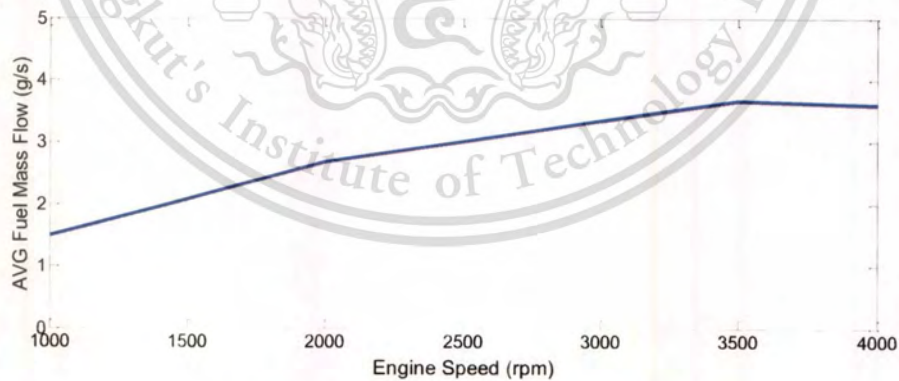


Figure 4.14 Average fuel mass flow (g/s)

Figure 4.14 shows the average of fuel mass flow when gasoline used as fuel. The maximum fuel mass flow is equal to 3.67 g/s at engine speed 3,500 rpm and minimum fuel mass

flow is equal to 1.50 g/s at the engine speed 1,000 rpm. At the engine speed 4,000 rpm the fuel mass flow is equal to 3.61 g/s. The difference of fuel mass flow between engine speed 3,500 rpm and 4,000 is equal to 1.63%.

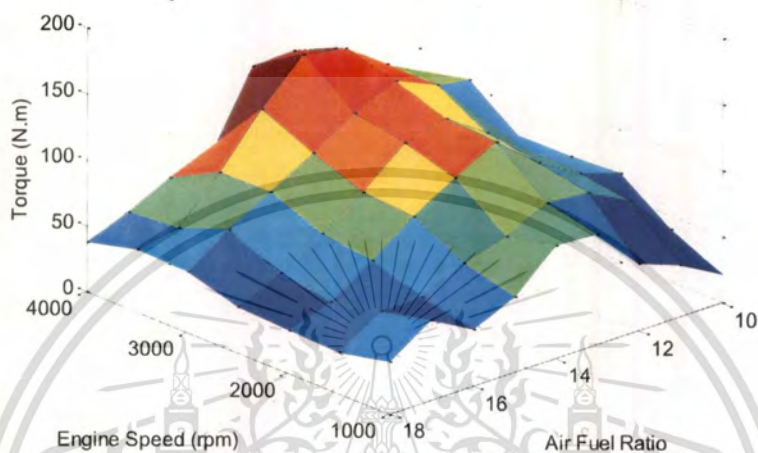


Figure 4.15 Torque measurement (Nm)

Figure 4.15 shows the torque measurement when gasoline used as fuel. The torque is increased since air fuel ratio is equal to 10 (rich) to the maximum torque at air fuel ratio 14-15. The torque is decreased due to air fuel ratio over 15 to 18 (lean). The torque is increased due to the increasing engine speed since 1,000 rpm to 3,500 rpm and over 3,500 rpm torque is slightly degraded which is related to quantity of air fuel mixture into the combustion chamber.

Figure 4.16 shows the average torque and maximum torque at air fuel ratio is equal to 14 when gasoline used as fuel. The case of average torque, the maximum torque is equal to 100.52 N.m at engine speed 3,500 rpm and minimum torque is equal to 53.60 N.m. at engine speed 1,000 rpm.

The case of air fuel ratio is equal to 14 (maximum torque), the maximum torque is equal to 140.42 N.m at engine speed 3,500 rpm and minimum torque is equal to 85.84 N.m. at engine speed 1,000 rpm.

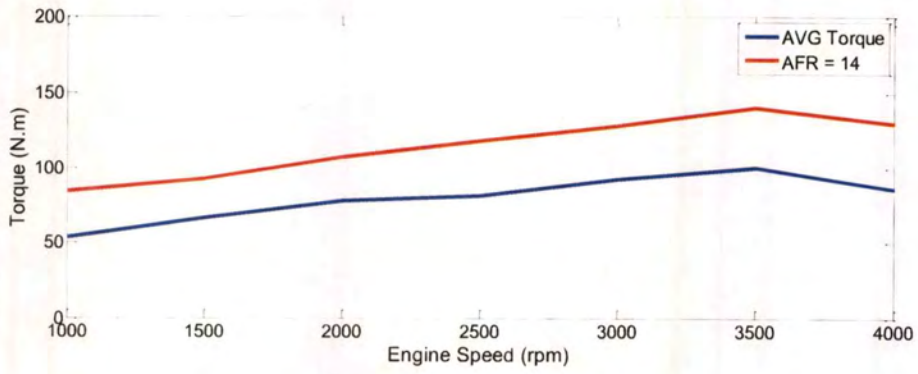


Figure 4.16 Average torque vs. maximum torque (AFR = 14)

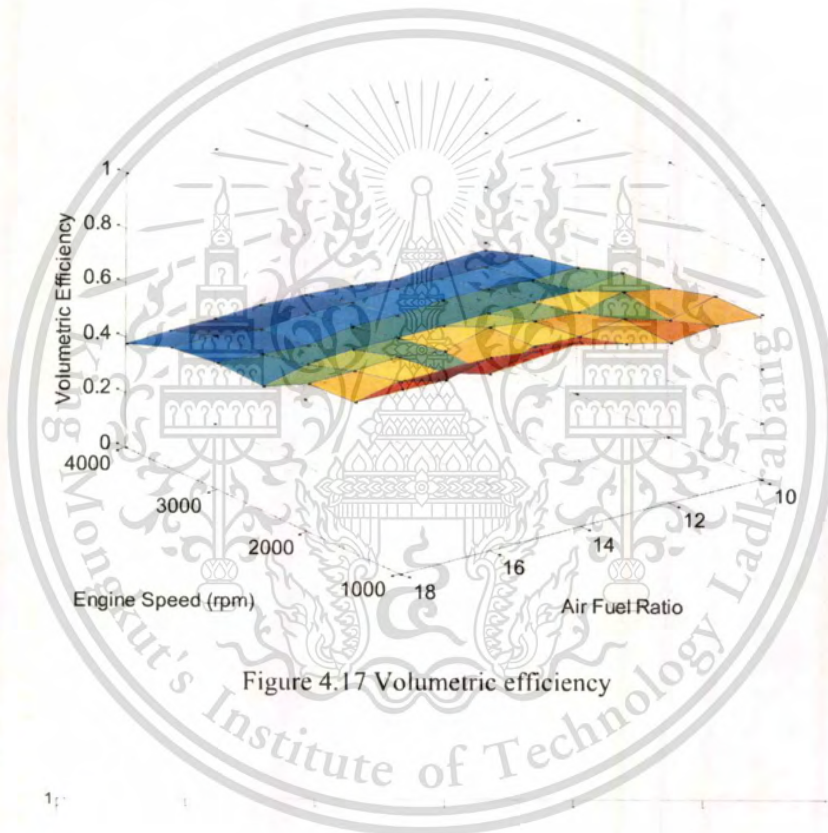


Figure 4.17 Volumetric efficiency

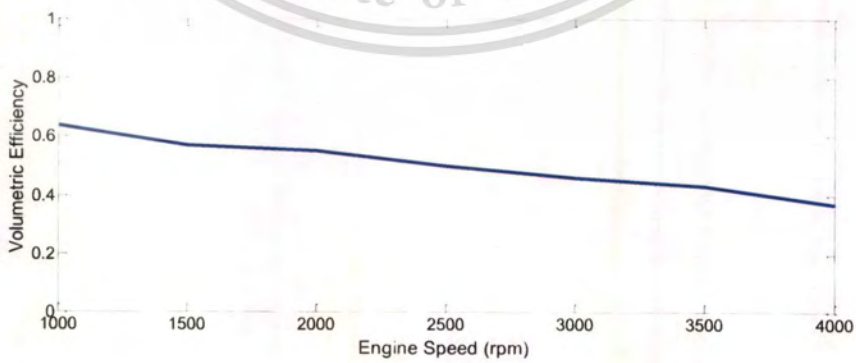


Figure 4.18 Average volumetric efficiency

Figure 4.17 and Figure 4.18 show the volumetric efficiency when gasoline used as fuel. The volumetric efficiency is decreased due to increasing engine speed since 1,000 to 4,000 rpm. The maximum volumetric efficiency is equal to 0.64 and minimum is equal to 0.37 at engine speed 1,000 and 4,000 rpm respectively.

4.5.2 Sweep Test (Gasoline)

Sweep test is ramped the engine speed between two operating point while data is logged continuously. The sweep test (gasoline) results can be divided into 4 results. The air mass flow, fuel injection duration, rotation torque, and volumetric efficiency.



Figure 4.19 Air mass flow measurement (g/s)

Figure 4.19 shows the air mass flow measurement when gasoline used as fuel is increased due to increasing engine speed since 1,000 rpm to 4,000 rpm.

Figure 4.20 shows the average air mass flow measurement when gasoline used as fuel. The maximum air mass flow is equal to 48.59 g/s at engine speed 4,000 rpm and minimum air mass flow is equal to 14.81 g/s at engine speed 1,000 rpm.

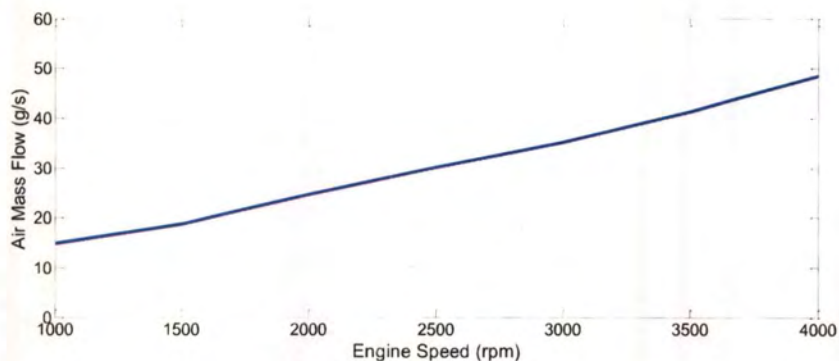


Figure 4.20 Average air mass flow (g/s)

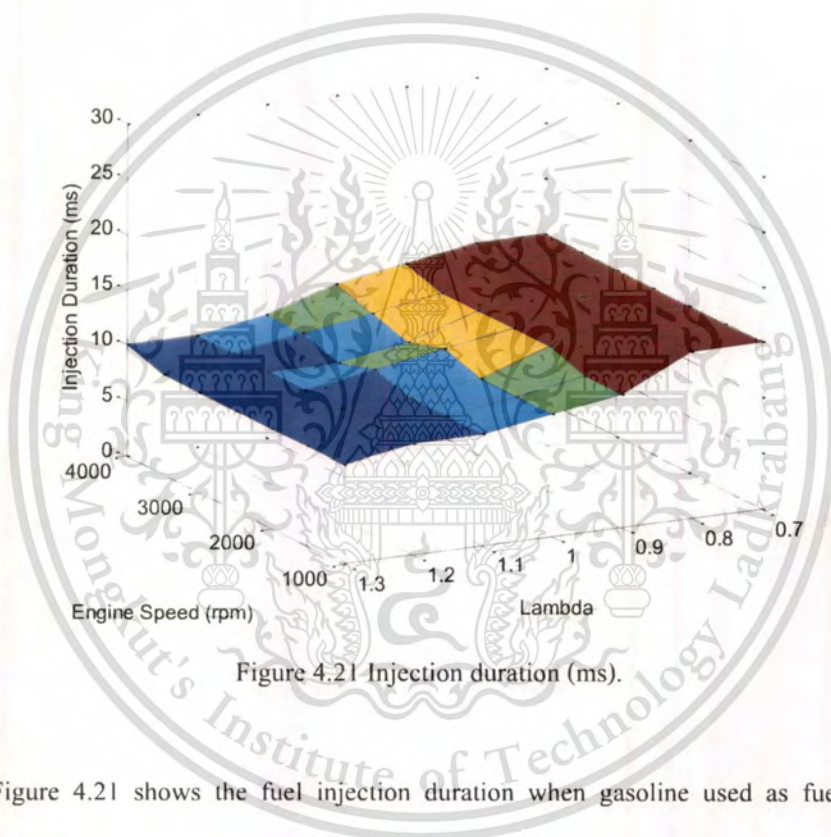


Figure 4.21 Injection duration (ms).

Figure 4.21 shows the fuel injection duration when gasoline used as fuel. The fuel injection duration is increased due to the decreasing lambda value and increasing engine speed. The maximum injection duration is equal to 15 ms at engine speed and lambda value are equal to 4,000 rpm and 0.7 (too rich) respectively. The minimum injection duration is equal to 9 ms at engine speed and lambda value are equal to 1,000 and 1.3 (too lean) respectively.

Figure 4.22 shows the torque when gasoline used as fuel. The torque is increased due to increasing lambda value is equal to 0.7 (rich) to the maximum torque at lambda value is equal to 0.9. The torque is decreased due to increasing lambda value over 0.9.

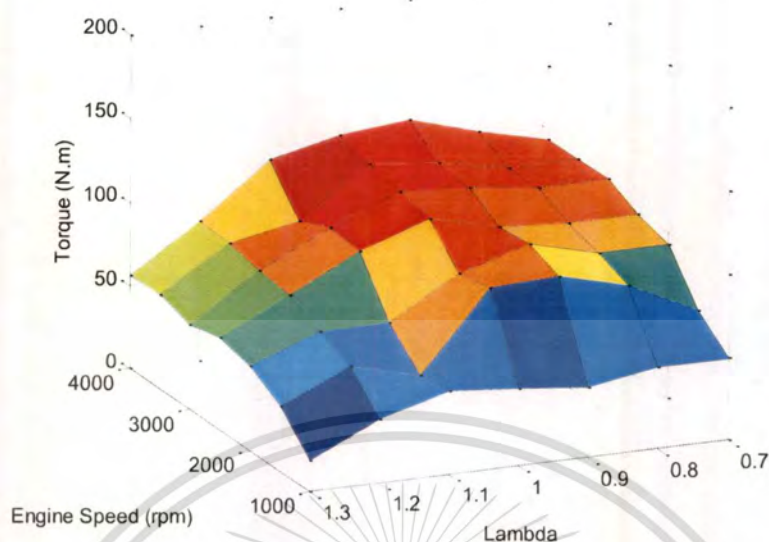


Figure 4.22 Torque measurement (N.m)

An increasing the engine speed since 1,000 to 4,000 the torque is increased since minimum torque at engine speed 1,000 rpm to maximum torque at 4,000 rpm. It is related with air mass flow and fuel injection duration into the combustion chamber.

Figure 4.23 shows the average torque and maximum torque at lambda value is equal to 0.9 when gasoline used as a fuel. The case of average torque, the maximum torque is equal to 104.46 N.m at engine speed 4,000 rpm and minimum torque is equal to 42.16 N.m at engine speed 1,000 rpm.

The case of lambda value is equal to 0.9 (maximum torque), the maximum torque is equal to 128.62 N.m at engine speed 4,000 rpm and minimum torque is equal to 42.42 N.m. at engine speed 1,000 rpm.

Figure 4.24 and Figure 4.25 show the volumetric efficiency when gasoline used as fuel. The volumetric efficiency is decreased due to increasing engine speed since 1,000 to 3,000 rpm. The engine speed over 3,000 is increased slightly in volumetric efficiency. The maximum volumetric efficiency is equal to 0.46 and minimum is equal to 0.40 at engine speed 1,000 and 3,000 rpm respectively.

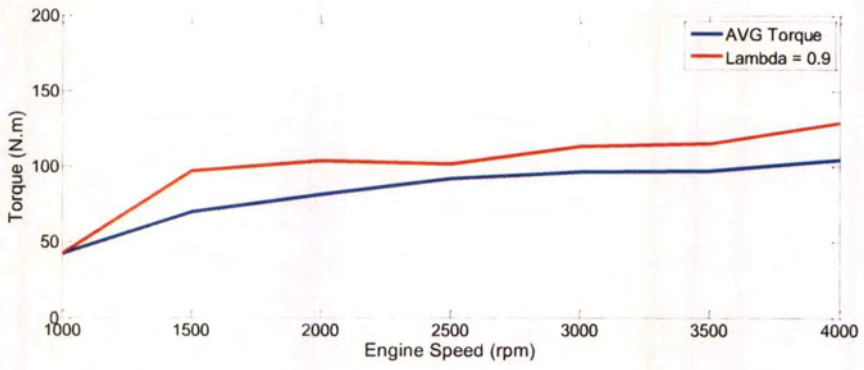


Figure 4.23 Average torque vs. maximum torque (lambda = 0.9)

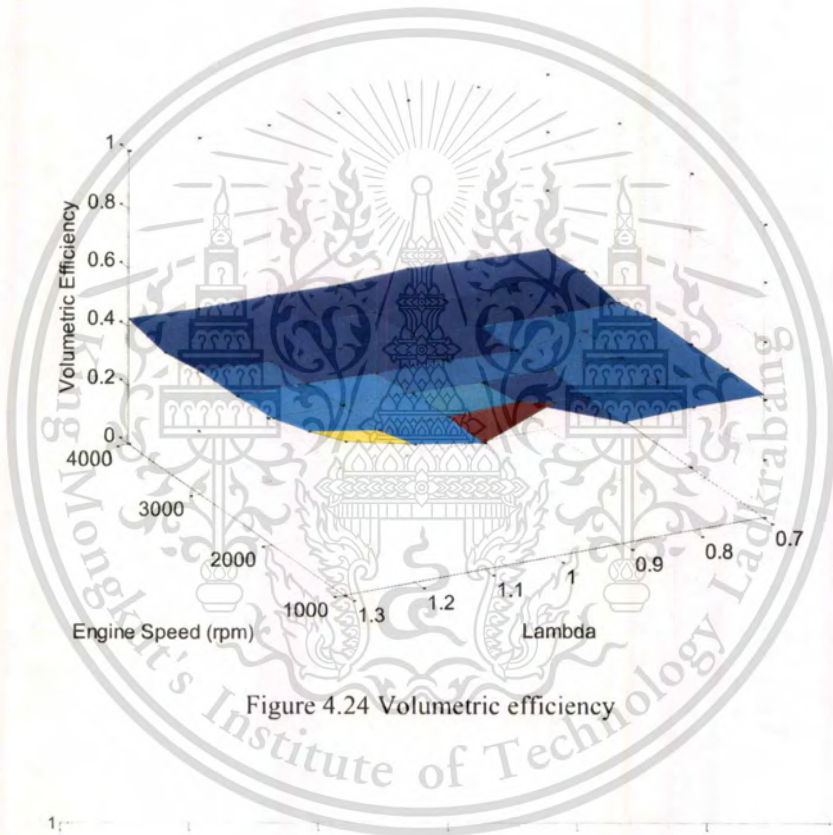


Figure 4.24 Volumetric efficiency

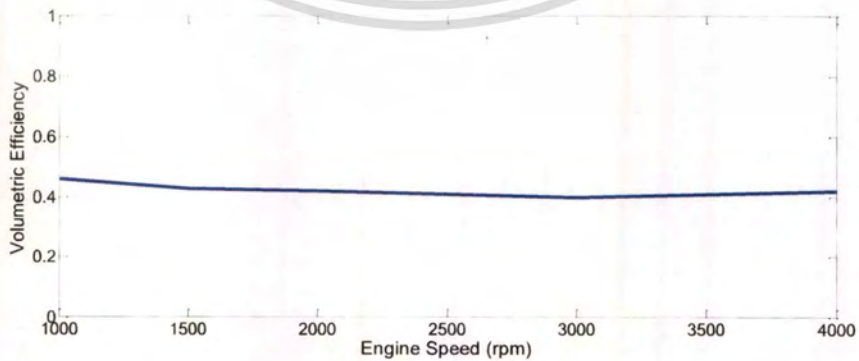


Figure 4.25 Average volumetric efficiency

4.5.3 Sweep Test (Gasoline-Ethanol Blend E-10)

The sweep test (Gasoline-Ethanol Blend E-10) results can be divided into 4 results. The air mass flow, fuel injection duration, rotation torque, and volumetric efficiency.



Figure 4.26 Air mass flow measurement (g/s)

Figure 4.26 shows the air mass flow measurement when gasoline-ethanol blend E-10 used as fuel is increased due to increasing engine speed since 1,000 rpm to 4,000 rpm.

Figure 4.27 shows the average air mass flow measurement when gasoline-ethanol blend E-10 used as fuel. The maximum air mass flow is equal to 47.18 g/s at engine speed 4,000 rpm and minimum air mass flow is equal to 13.90 g/s at engine speed 1,000 rpm.

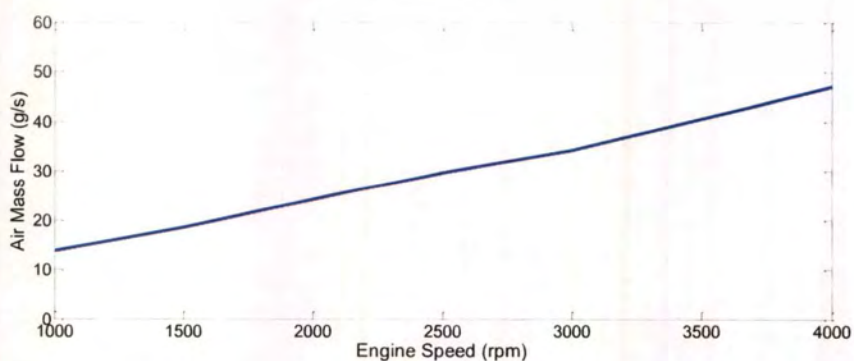


Figure 4.27 Average air mass flow (g/s)

This material is reserved for educational use only, not allowed for commercial use.

Forbidden to modify the content, and cite the document when use.

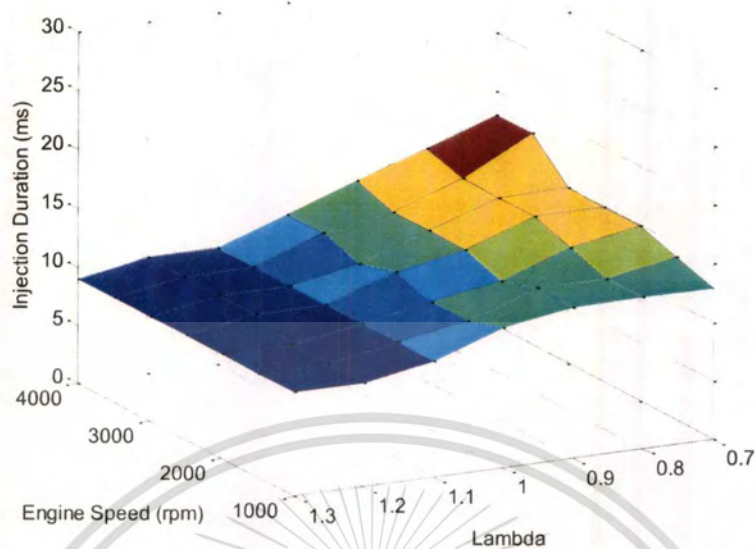


Figure 4.28 Injection duration (ms)

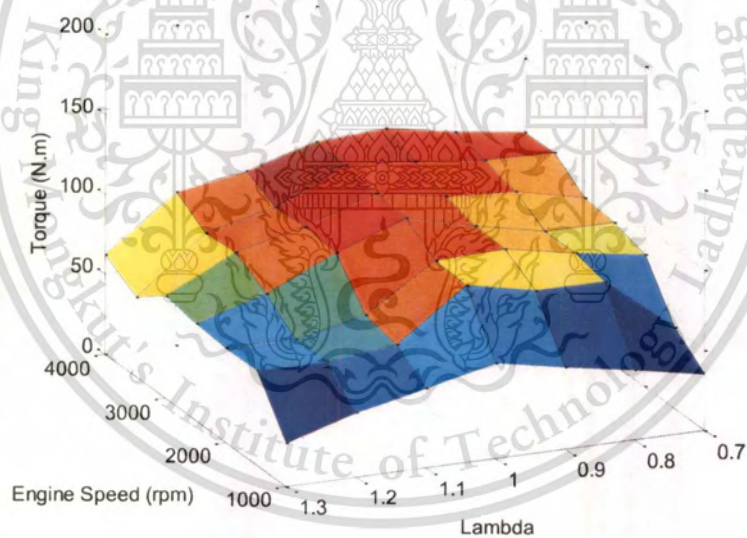


Figure 4.29 Torque measurement (N.m)

Figure 4.28 shows the fuel injection duration when gasoline-ethanol blend E-10 used as fuel. The fuel injection duration is increased due to the decreasing lambda value and increasing engine speed.

The maximum injection duration is equal to 17 ms at engine speed and lambda value are equal to 4,000 rpm and 0.7 (too rich) respectively. The minimum injection duration is equal to 9 ms at engine speed and lambda value are equal to 1,000 and 1.3 (too lean) respectively.

Figure 4.29 shows the torque measurement when gasoline-ethanol blend E-10 used as fuel. The torque is increased due to increasing lambda value is equal to 0.7 (rich) to the maximum torque at lambda value is equal to 0.9. The torque is decreased due to increasing lambda value over 0.9.

An increasing the engine speed since 1,000 to 4,000 the torque is increased since minimum torque at engine speed equal to 1,000 rpm to maximum torque at 4,000 rpm. It is related with air mass flow and fuel injection duration into the combustion chamber.

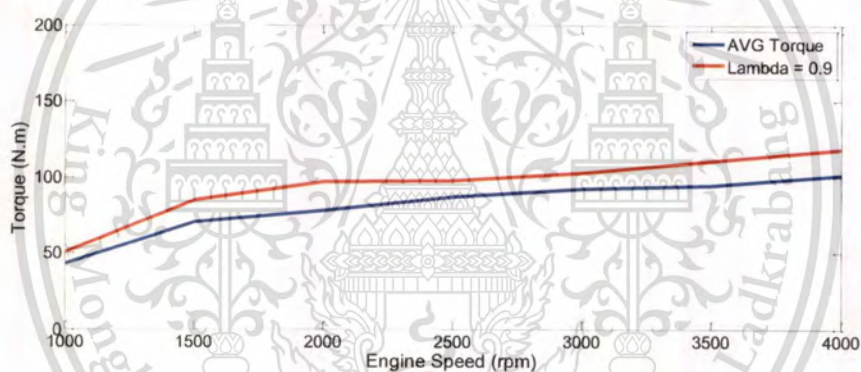


Figure 4.30 Average torque vs. maximum torque (lambda = 0.9)

Figure 4.30 shows the average torque and maximum torque at lambda value is equal to 0.9 when gasoline-ethanol E-10 used as fuel. The case of average torque, the maximum torque is equal to 101.45 N.m at engine speed 4,000 rpm and minimum torque is equal to 43.38 N.m at engine speed 1,000 rpm.

The case of lambda value is equal to 0.9 (maximum torque), the maximum torque is equal to 118.34 N.m at engine speed 4,000 rpm and minimum torque is equal to 51.04 N.m. at engine speed 1,000 rpm.

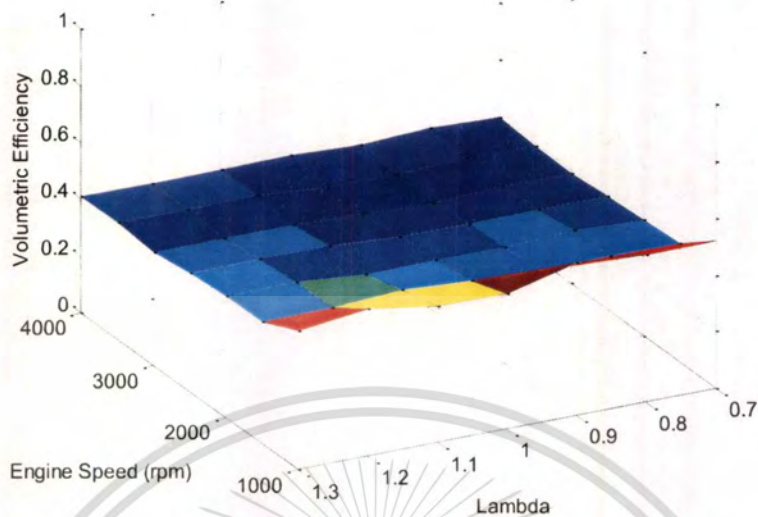


Figure 4.31 Volumetric efficiency

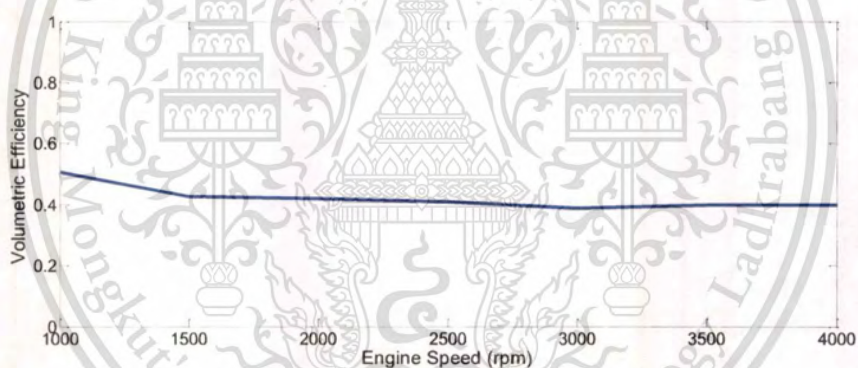


Figure 4.32 Average volumetric efficiency

Figure 4.31 and Figure 4.32 show the volumetric efficiency when gasoline-ethanol blend E-10 used as fuel. The volumetric efficiency is decreased due to increasing engine speed since 1,000 to 3,000 rpm. The engine speed over 3,000 is increased slightly in volumetric efficiency. The maximum volumetric efficiency is equal to 0.49 and minimum is equal to 0.40 at engine speed 1,000 and 3,000 rpm respectively.

4.5.4 Sweep Test (Gasoline-Ethanol Blend E-20)

The sweep test (Gasoline-ethanol blend E-20) results can be divided into 4 results. The air mass flow, fuel injection duration, rotation torque, and volumetric efficiency.

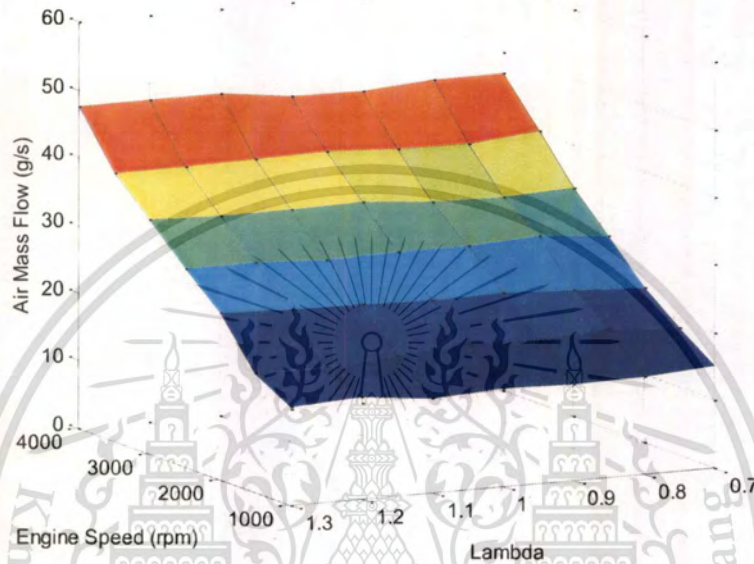


Figure 4.33 Air mass flow measurement (g/s)

Figure 4.33 shows the air mass flow measurement when gasoline-ethanol blend E-20 used as fuel is increased due to increasing engine speed since 1,000 rpm to 4,000 rpm.

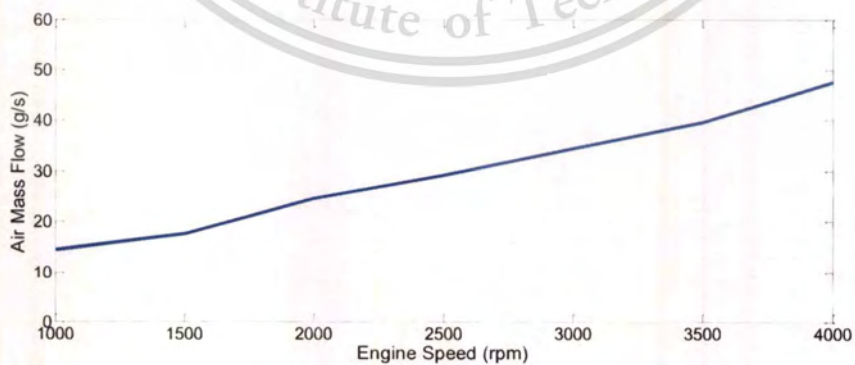


Figure 4.34 Average air mass flow (g/s)

Figure 4.34 shows the average air mass flow when gasoline-ethanol blend E-20 used as fuel. The maximum air mass flow is equal to 47.04 g/s at engine speed 4,000 rpm and minimum air mass flow is equal to 14.64 g/s at engine speed 1,000 rpm

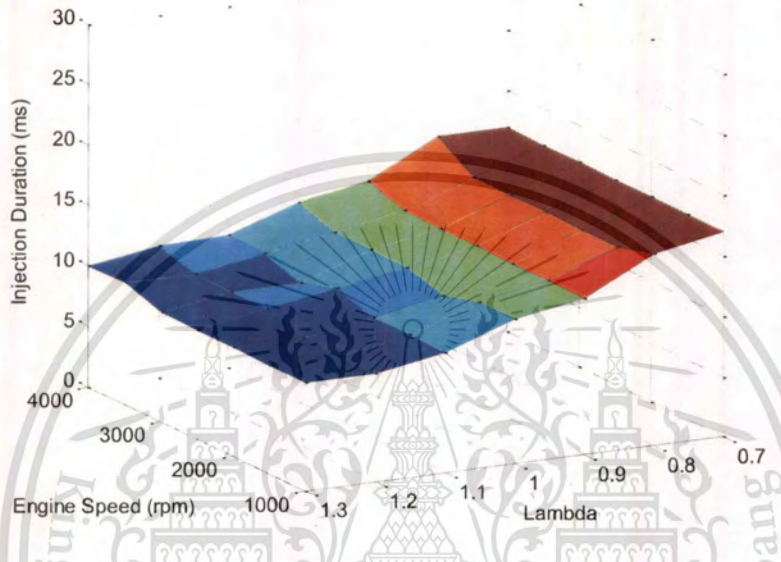


Figure 4.35 Injection duration (ms)

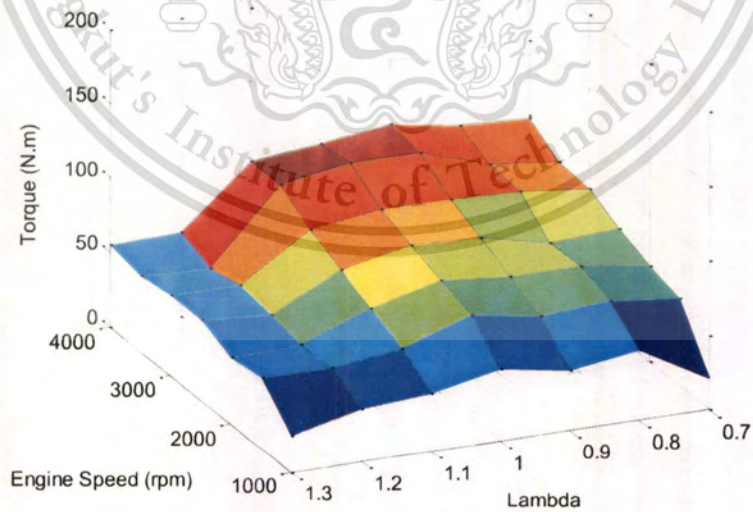


Figure 4.36 Torque measurement (N.m)

Figure 4.35 shows the fuel injection duration when gasoline-ethanol blend E-20 used as fuel. The fuel injection duration is increased due to the decreasing lambda value and increasing engine speed. The maximum injection duration is equal to 17 ms at engine speed and lambda value are equal to 4,000 rpm and 0.7 (too rich) respectively. The minimum injection duration is equal to 9 ms at engine speed and lambda value are equal to 1,000 and 1.3 (too lean) respectively.

Figure 4.36 shows the torque measurement when gasoline-ethanol blend E-20 used as fuel. The torque is increased due to increasing lambda value is equal to 0.7 (rich) to the maximum torque at lambda value is equal to 0.9. The torque is decreased due to increasing lambda value over 0.9.

An increasing the engine speed since 1,000 to 4,000 the torque is increased since minimum torque at engine speed equal to 1,000 rpm to maximum torque at 4,000 rpm. It is related with air mass flow and fuel injection duration into the combustion chamber.

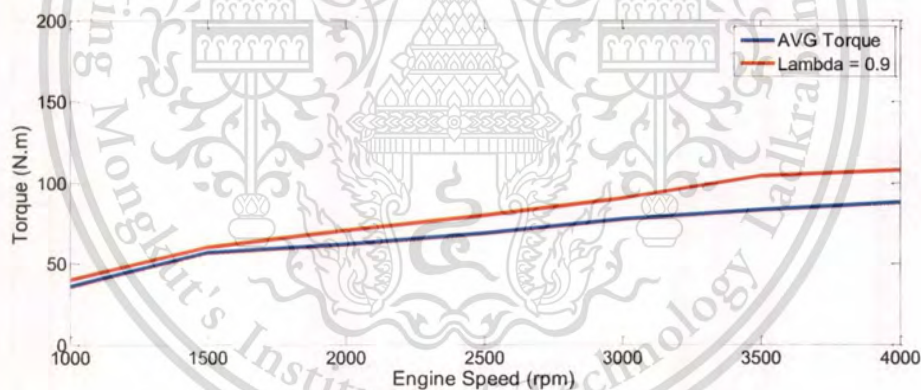


Figure 4.37 Average torque vs. maximum torque (lambda = 0.9)

Figure 4.37 shows the average torque and maximum torque at lambda value is equal to 0.9 when gasoline-ethanol blend E-20 used as fuel. The case of average torque, the maximum torque is equal to 88.24 N.m at engine speed 4,000 rpm and minimum torque is equal to 36.47 N.m at engine speed 1,000 rpm. The case lambda value is equal to 0.9 (maximum torque), the maximum torque is equal to 108.40 N.m at engine speed 4,000 rpm and minimum torque is equal to 40.44 N.m. at engine speed 1,000 rpm.

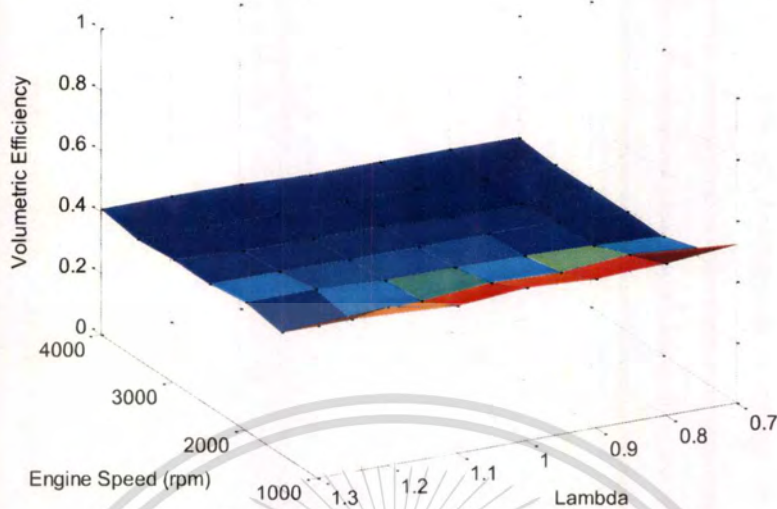


Figure 4.38 Volumetric efficiency

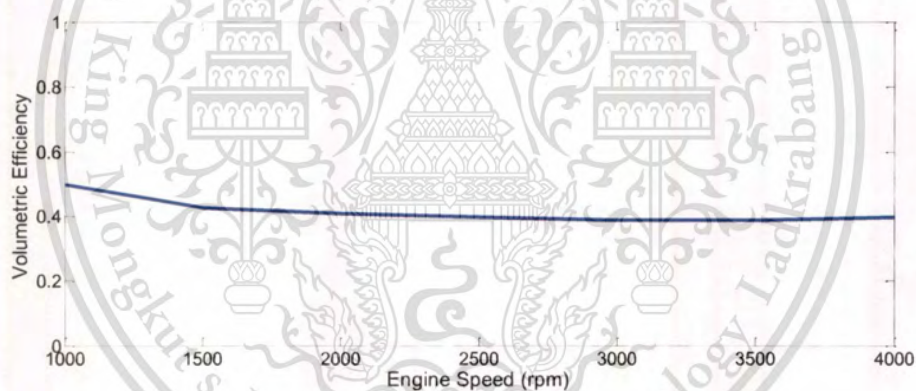


Figure 4.39 Average volumetric efficiency

Figure 4.38 and Figure 4.39 show the volumetric efficiency when gasoline-ethanol blend E-20 used as fuel. The volumetric efficiency is decreased due to increasing engine speed since 1,000 to 3,000 rpm. The engine speed over 3,000 is slightly increased in volumetric efficiency. The maximum volumetric efficiency is equal to 0.50 and minimum is equal to 0.39 at engine speed 1,000 and 3,000 rpm respectively.

4.5.5 Sweep Test (Gasoline-Ethanol Blend E-85)

The sweep test (Gasoline-ethanol blend E-85) results can be divided into 4 results. The air mass flow, fuel injection duration, rotation torque, and volumetric efficiency.

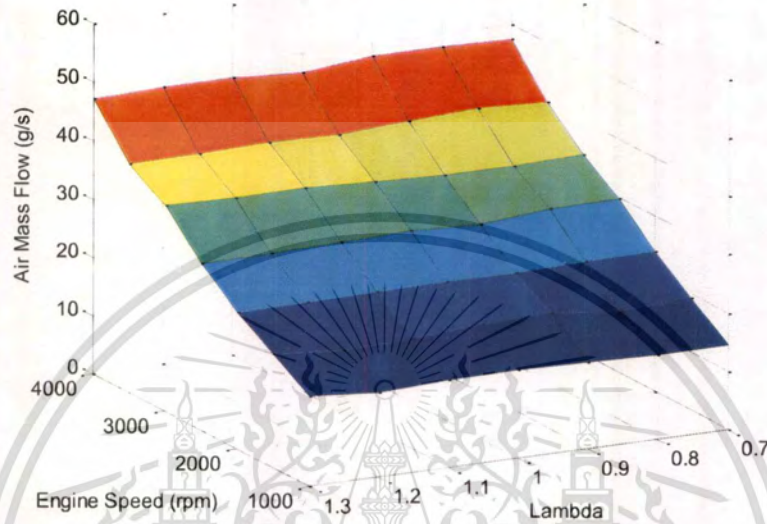


Figure 4.40 Air mass flow measurement (g/s)

Figure 4.40 shows the air mass flow measurement when gasoline-ethanol blend E-85 used as fuel is increased due to increasing engine speed since 1,000 rpm to 4,000 rpm.

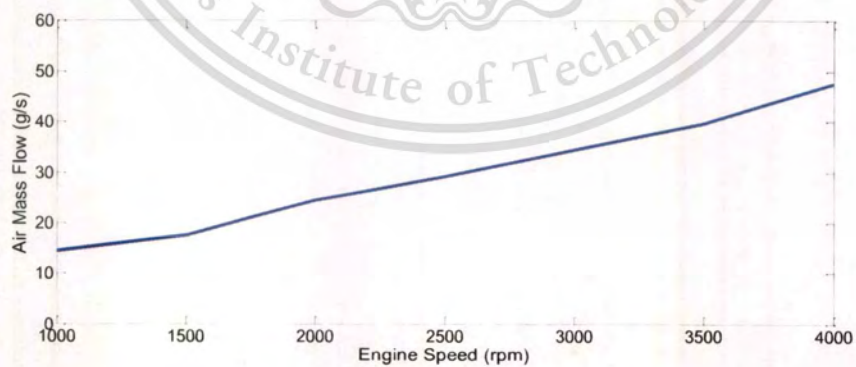


Figure 4.41 Average air mass flow (g/s)

Figure 4.41 shows the average air mass flow when gasoline-ethanol blend E-85 used as fuel. The maximum air mass flow is equal to 47.56 g/s at engine speed 4,000 rpm and minimum air mass flow is equal to 14.92 g/s at engine speed 1,000 rpm.

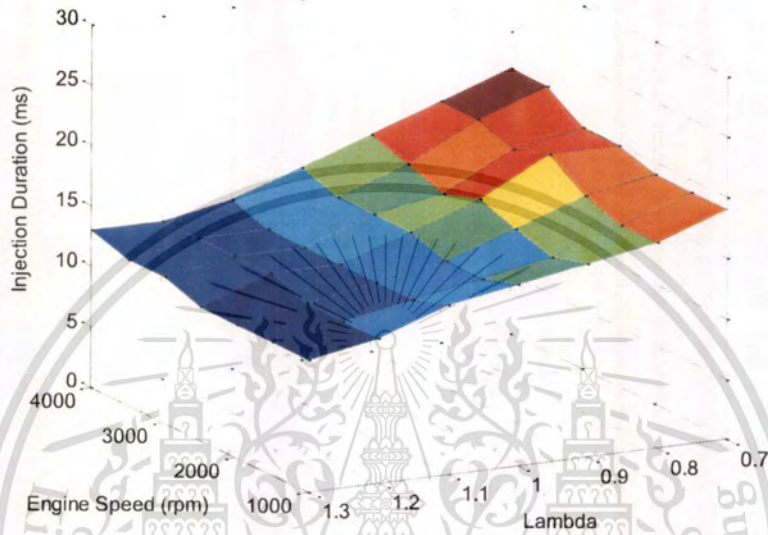


Figure 4.42 Injection duration (ms)

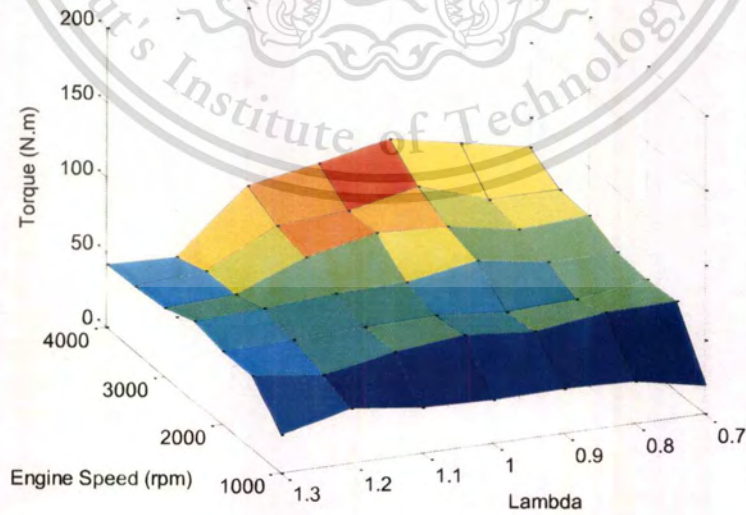


Figure 4.43 Torque measurement (N.m)

Figure 4.42 shows the fuel injection duration when gasoline-ethanol blend E-85 used as fuel. The fuel injection duration is increased due to the decreasing lambda value and increasing engine speed. The maximum injection duration is equal to 22 ms at engine speed and lambda value are equal to 4,000 rpm and 0.7 (too rich) respectively. The minimum injection duration is equal to 11 ms at engine speed and lambda value are equal to 1,000 and 1.3 (too lean) respectively.

Figure 4.43 shows the torque when gasoline-ethanol blend E-85 used as fuel. The torque is increased due to increasing lambda value is equal to 0.7 (rich) to the maximum torque at lambda value is equal to 0.9. The torque is decreased due to increasing lambda value over 0.9.

An increasing the engine speed since 1,000 to 4,000 the torque is increased since minimum torque at engine speed equal to 1,000 rpm to maximum torque at 4,000 rpm. It is related with air mass flow and fuel injection duration into the combustion chamber.

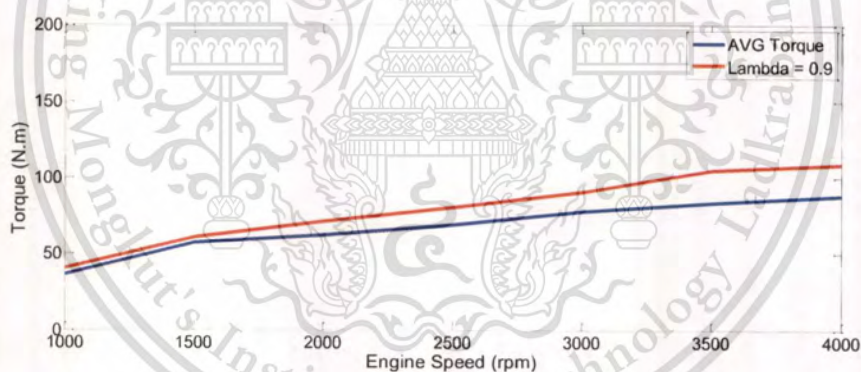


Figure 4.44 Average torque vs. maximum torque (lambda = 0.9)

Figure 4.44 shows the average torque and maximum torque at lambda value is equal to 0.9 when gasoline-ethanol blend E-85 used as a fuel. The case of average torque, the maximum torque is equal to 74.55 N.m at engine speed 4,000 rpm and minimum torque is equal to 29.19 N.m at engine speed 1,000 rpm. The case lambda value is equal to 0.9 (maximum torque), the maximum torque is equal to 98.94 N.m at engine speed 4,000 rpm and minimum torque is equal to 31.05 N.m. at engine speed 1,000 rpm.

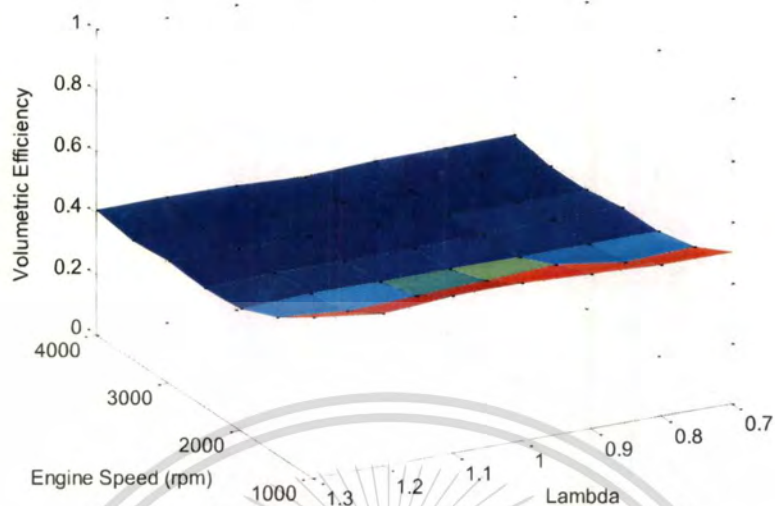


Figure 4.45 Volumetric efficiency

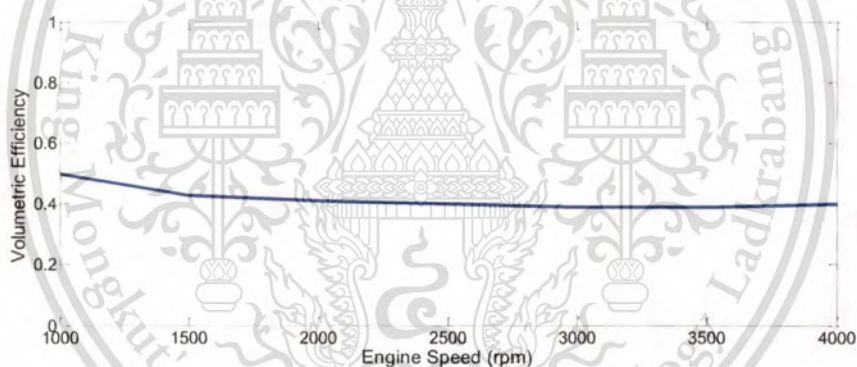


Figure 4.46 Average volumetric efficiency

Figure 4.45 and Figure 4.46 show the volumetric efficiency when gasoline-ethanol blend E-85 used as fuel. The volumetric efficiency is decreased due to increasing engine speed since 1,000 to 3,000 rpm. The engine speed over 3,000 is increased slightly in volumetric efficiency. The maximum volumetric efficiency is equal to 0.51 and minimum is equal to 0.39 at engine speed 1,000 and 3,000 rpm respectively.

4.6 Simulation Results

This section we evaluate the air fuel ratio and performance of standard gasoline engine when simulation on eMapnMod program based on MATLAB software. The only forgetting factor has been used to reduce noise and vibration during experimental process. The simulation results have been separated 2 types; the data from steady state test (only gasoline) and sweep test (gasoline and gasoline-ethanol blend E-10, E-20 and E-85). The only torque parameter has been compared between test methods and fuel types.

4.6.1 Steady State (Gasoline)

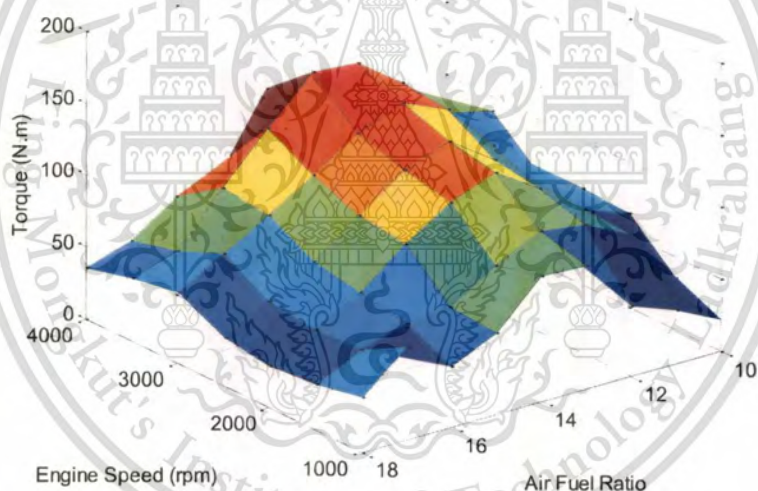


Figure 4.47 Torque estimation (N.m)

Figure 4.47 shows the torque estimation when gasoline used as fuel by eMapnMod program with forgetting factor is equal to 0.9. The torque is increased since air fuel ratio is equal to 10 (rich) to the maximum torque at air fuel ratio 14-15. The torque is decreased due to air fuel ratio over 15 to 18 (lean). The torque is increased due to the increasing engine speed since 1,000 rpm to 3,500 rpm and over 3,500 rpm torque is slightly decreased which is related to quantity of air fuel mixture into the combustion chamber.

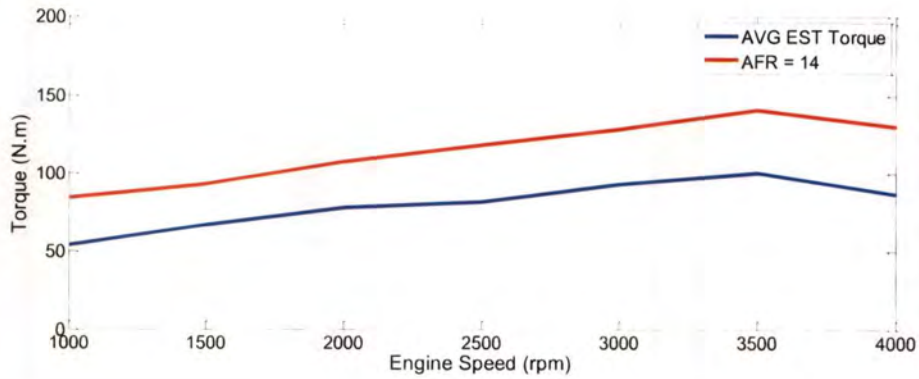


Figure 4.48 Average torque estimation vs. maximum torque estimation (AFR = 14)

Figure 4.48 shows the average torque estimation and maximum torque estimation at air fuel ratio is equal to 14 when gasoline used as a fuel. The case of average torque, the maximum torque is equal to 100.53 N.m at engine speed 3,500 rpm and minimum torque is equal to 52.57 N.m. at engine speed 1,000 rpm.

The case of air fuel ratio equal to 14 (maximum torque), the maximum torque is equal to 140.41 N.m at engine speed 3,500 rpm and minimum torque is equal to 86.86 N.m. at engine speed 1,000 rpm.

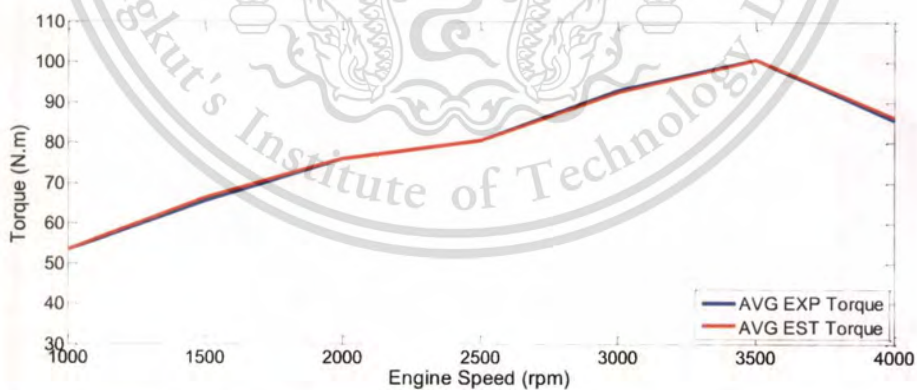


Figure 4.49 Average torque measurement vs. average torque estimation

Figure 4.49 shows the average torque measurement vs. average torque estimate when gasoline used as a fuel. The difference error between average measurement and average estimation torque is 0.21%.

4.6.2 Sweep Test (Gasoline)

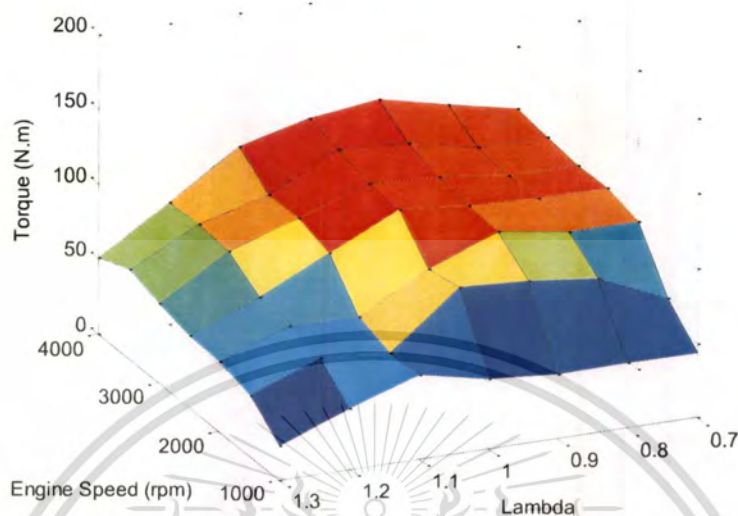


Figure 4.50 Torque estimation (N.m).

Figure 4.50 shows the torque estimation when gasoline used as fuel by eMapnMod program with forgetting factor is equal to 0.9. The torque is increased due to increasing lambda value is equal to 0.7 (rich) to the maximum torque at lambda value is equal to 0.9. The torque is decreased due to increasing lambda value over 0.9. An increasing the engines speed since 1,000 to 4,000 the torque is increased since minimum torque at engine speed is equal to 1,000 rpm to maximum torque at 4,000 rpm. It is related with air mass flow and fuel injection duration into the combustion chamber.

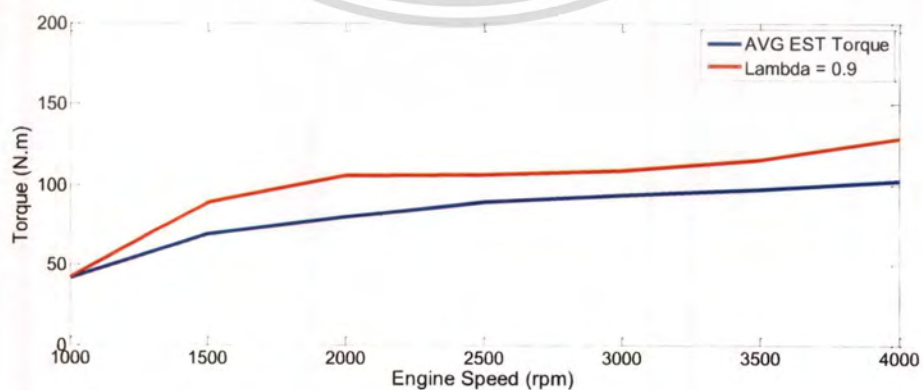


Figure 4.51 Average torque estimation vs. maximum torque estimation (lambda = 0.9)

Figure 4.51 shows the average torque estimation vs. maximum torque estimation ($\lambda = 0.9$). The case average torque estimate, the maximum torque is equal to 103.10 N.m at engine speed 4,000 rpm and minimum average torque estimate is equal to 42.43 N.m. at engine speed 1,000 rpm

The case of λ value is equal to 0.9 (maximum torque estimate), the maximum torque is equal to 128.62 N.m at engine speed 4,000 rpm and minimum torque is equal to 42.95 N.m. at engine speed 1,000 rpm.

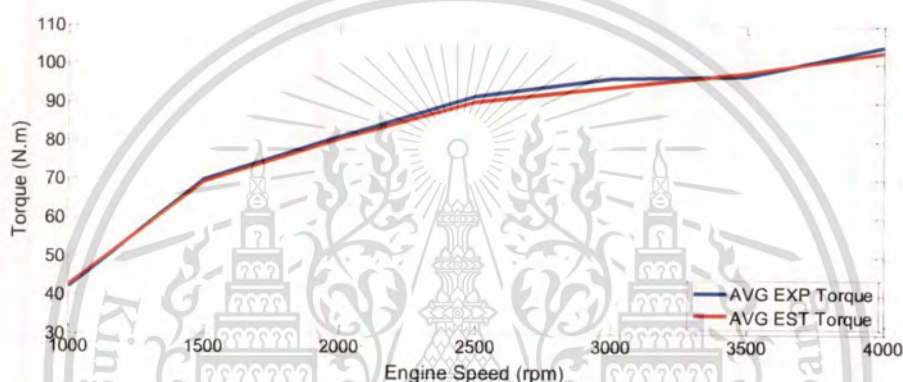


Figure 4.52 Average torque measurement vs. average torque estimation

Figure 4.52 shows the average torque measurement vs. average torque estimation. The difference error between average measurement and average estimation torque is equal to 0.92%.

4.6.3 Sweep Test (Gasoline-Ethanol Blend E-10)

The Figure 4.53 shows the torque estimation when gasoline-ethanol blend E-10 used as fuel by eMapnMod program with forgetting factor is equal to 0.9. The torque is increased due to increasing λ value is equal to 0.7 (rich) to the maximum torque at λ value is equal to 0.9. The torque is decreased due to increasing λ value over 0.9.

An increasing the engine speed since 1,000 to 4,000 the torque is increased since minimum torque at engine speed 1,000 rpm to maximum torque at 4,000 rpm. It is related with air mass flow and fuel injection duration into the combustion chamber.

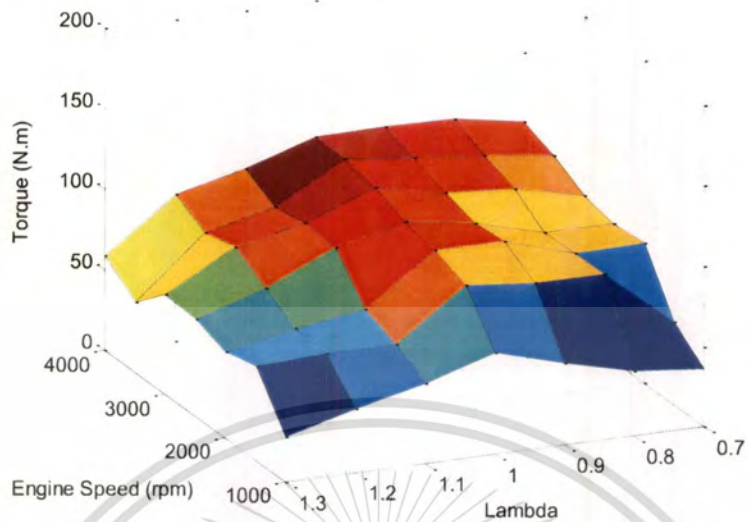


Figure 4.53 Torque estimation (N.m)

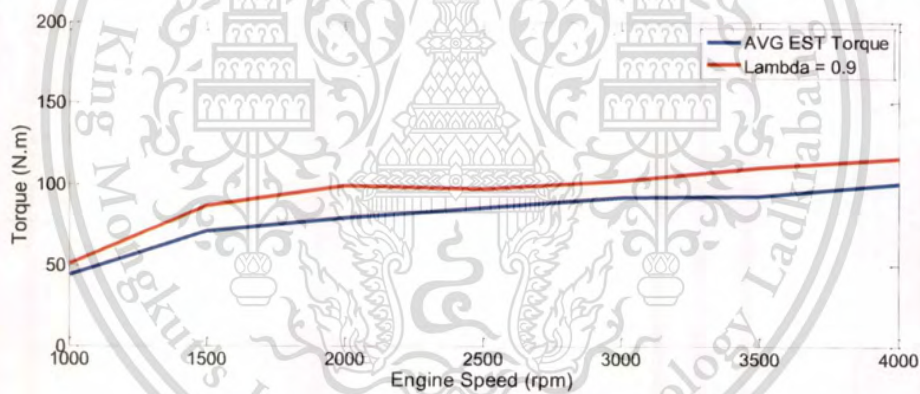


Figure 4.54 Average torque estimate vs. maximum torque (lambda = 0.9)

Figure 4.54 shows the average torque estimation vs. maximum torque estimation (lambda = 0.9). The case average torque estimate, the maximum torque is equal to 100.84 N.m at engine speed 4,000 rpm and minimum average torque estimate is equal to 44.05 N.m. at engine speed 1,000 rpm.

The case of lambda value is equal to 0.9 (maximum torque estimate), the maximum torque is equal to 116.07 N.m at engine speed 4,000 rpm and minimum torque is equal to 51.13 N.m. at engine speed 1,000 rpm.

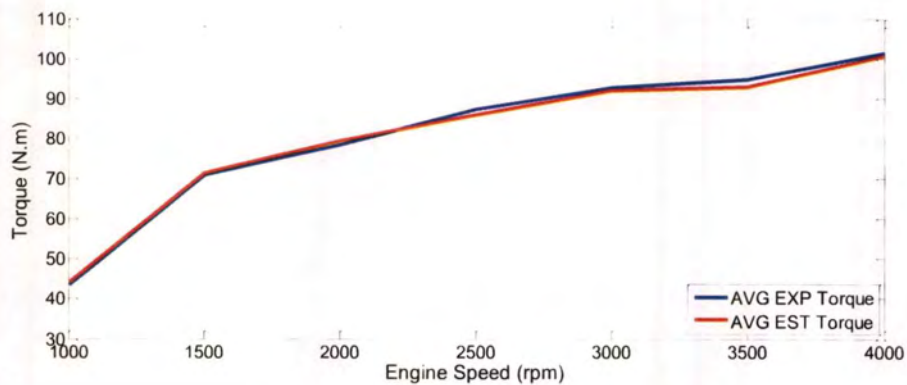


Figure 4.55 Average torque measurement vs. average torque estimation

Figure 4.55 shows the average torque measurement vs. average torque estimation. The difference error between average measurement and average estimation torque is equal to 0.46%.

4.6.4 Sweep Test (Gasoline-Ethanol Blend E-20)

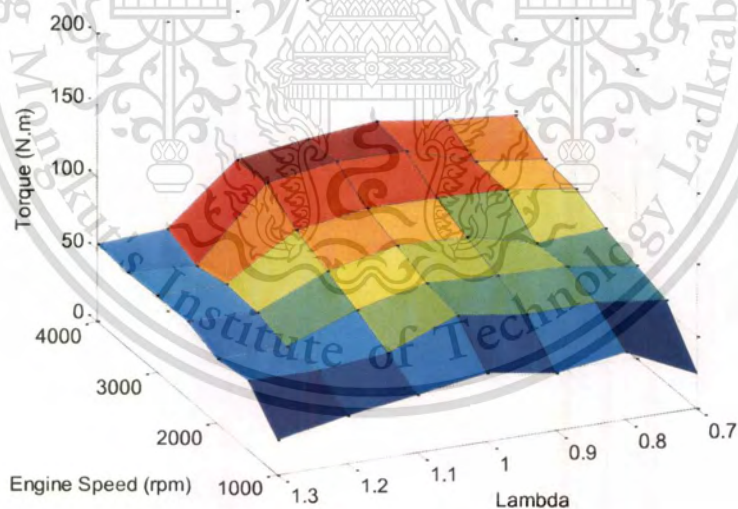


Figure 4.56 Torque estimation (N.m)

Figure 4.56 shows the torque estimation when gasoline-ethanol blend E-20 used as fuel by eMapnMod program with forgetting factor is equal to 0.9. The torque is increased due to

increasing lambda value is equal to 0.7 (rich) to the maximum torque at lambda value is equal to 0.9. The torque is decreased due to increasing lambda value over 0.9.

An increasing the engine speed since 1,000 to 4,000 the torque is increased since minimum torque at engine speed equal to 1,000 rpm to maximum torque at 4,000 rpm. It is related with air mass flow and fuel injection duration into the combustion chamber.

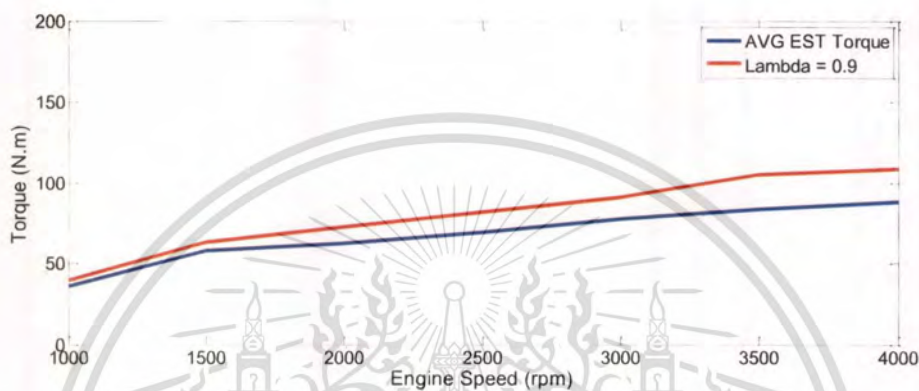


Figure 4.57 Average torque estimation vs. maximum torque (lambda = 0.9)

Figure 4.57 shows the average torque estimation vs. maximum torque estimation (lambda = 0.9). The case average torque estimate, the maximum torque is equal to 88.24 N.m at engine speed 4,000 rpm and minimum average torque estimate is equal to 36.03 N.m. at engine speed 1,000 rpm. The case lambda value equal to 0.9 (maximum torque estimate), the maximum torque is equal to 108.40 N.m at engine speed 4,000 rpm and minimum torque is equal to 39.44 N.m. at engine speed 1,000 rpm.

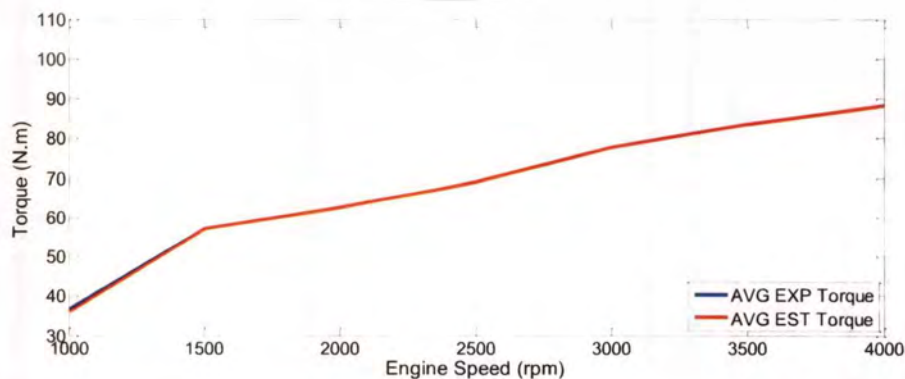


Figure 4.58 Average torque measurement vs. average torque estimation

Figure 4.58 shows the average torque measurement vs. average torque estimation. The difference error between average measurement and average estimation torque is equal to 0.14%.

4.6.5 Sweep Test (Gasoline-Ethanol Blend E-85)

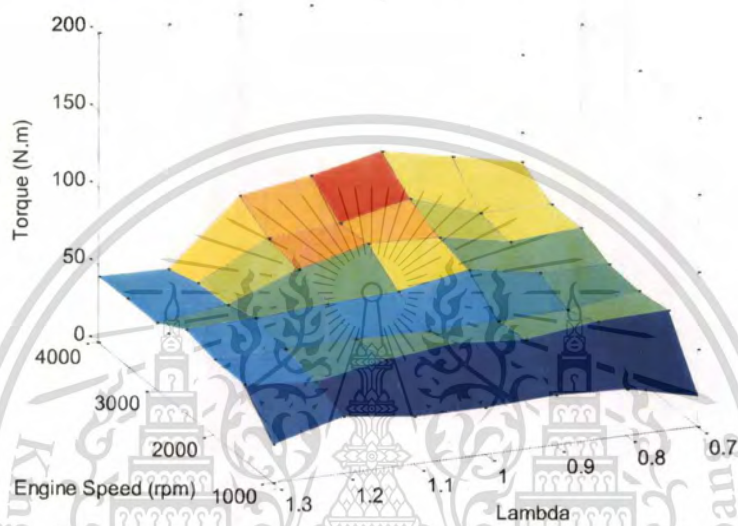


Figure 4.59 Torque estimation (N.m)

Figure 4.59 shows the torque estimation when gasoline-ethanol blend E-85 used as a fuel by eMapnMod program with forgetting factor equal to 0.9. The torque is increased due to increasing lambda value is equal to 0.7 (rich) to the maximum torque at lambda value is equal to 0.9. The torque is decreased due to increasing lambda value over 0.9.

An increasing the engine speed since 1,000 to 4,000 the torque is increased since minimum torque at engine speed equal to 1,000 rpm to maximum torque at 4,000 rpm. It is related with air mass flow and fuel injection duration into the combustion chamber.

Figure 4.60 shows the average torque estimation vs. maximum torque estimation (lambda = 0.9). The case of average torque estimate, the maximum torque is equal to 75.26 N.m at engine speed 4,000 rpm and minimum average torque estimation is equal to 29.19 N.m. at engine speed 1,000 rpm

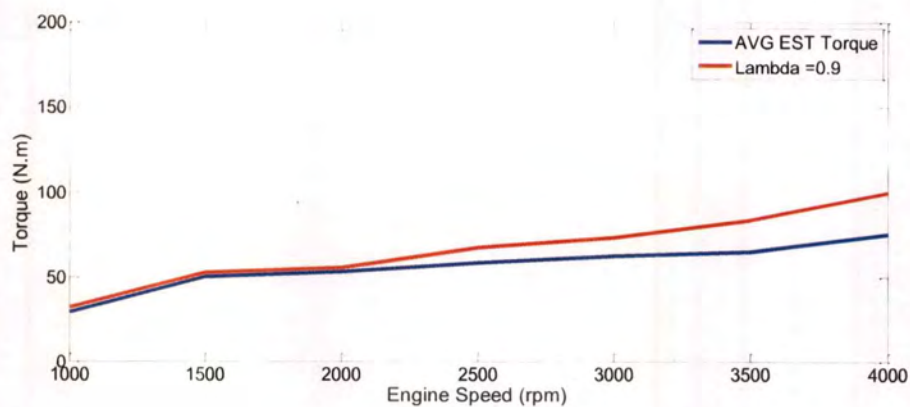


Figure 4.60 Average torque estimation vs. maximum torque (lambda = 0.9)

The case of lambda value equal to 0.9 (maximum torque estimation), the maximum torque is equal to 99.94 N.m at engine speed 4,000 rpm and minimum torque is equal to 32.05 N.m. at engine speed 1,000 rpm.

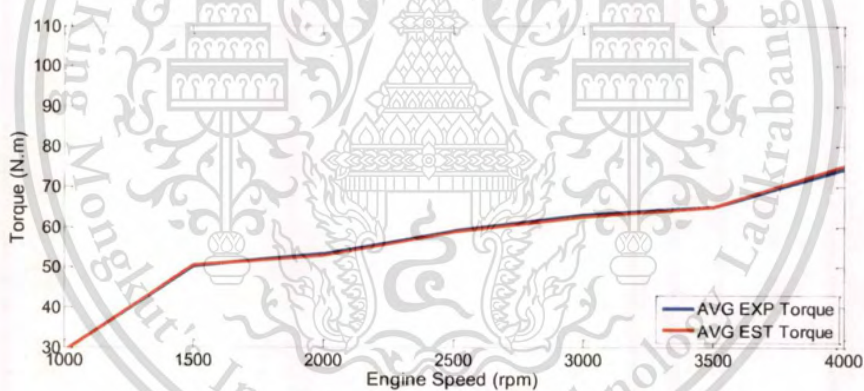


Figure 4.61 Average torque measurement vs. average torque estimation

Figure 4.61 shows the average torque measurement vs. average torque estimation. The difference error between average measurement and average estimation torque is equal to 0.68%.

4.7 Validation Results

This section the polynomial regression used to validated the torque estimation from previous section. The validation result has been separated into 2 types; the data from steady state test (only gasoline used as fuel) and sweep test (gasoline and gasoline-ethanol blend E-10, E-20 and E-85). The only torque parameter has been compared with test methods and fuel types.

4.7.1 Steady State (Gasoline)

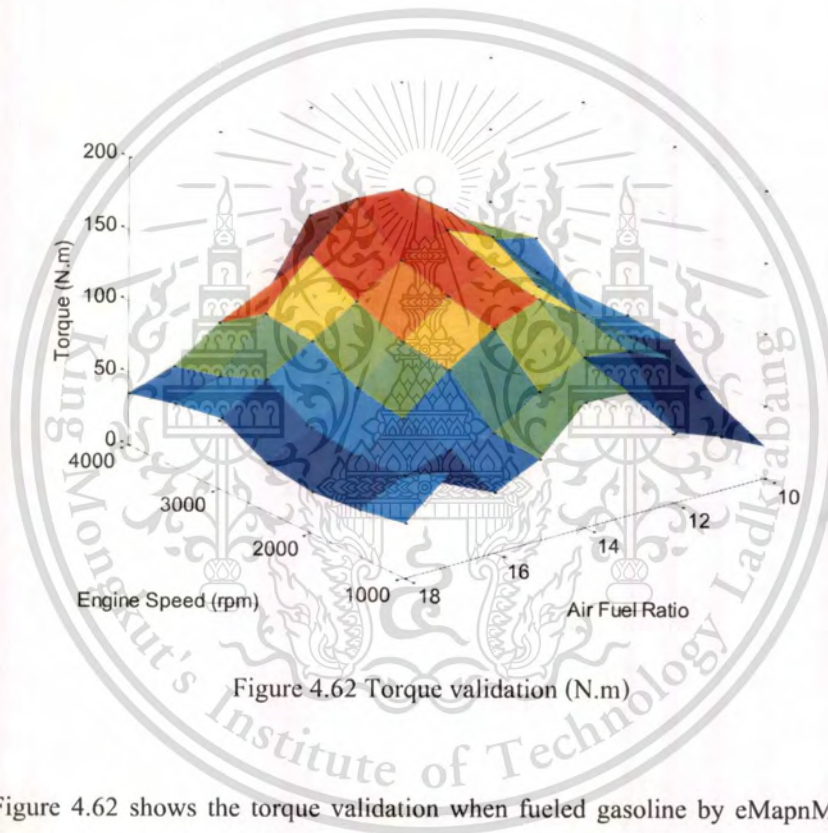


Figure 4.62 shows the torque validation when fueled gasoline by eMapnMod program with polynomial degree 6. The torque is increased since air fuel ratio = 10 (rich) to the maximum torque at air fuel ratio 14-15. The torque is decreased due to air fuel ratio over 15 to 18 (lean). The torque is increased due to the increasing engine speed since 1,000 rpm to 3,500 rpm and over 3,500 rpm torque is slightly decreased which is related to quantity of air fuel mixture into the combustion chamber.

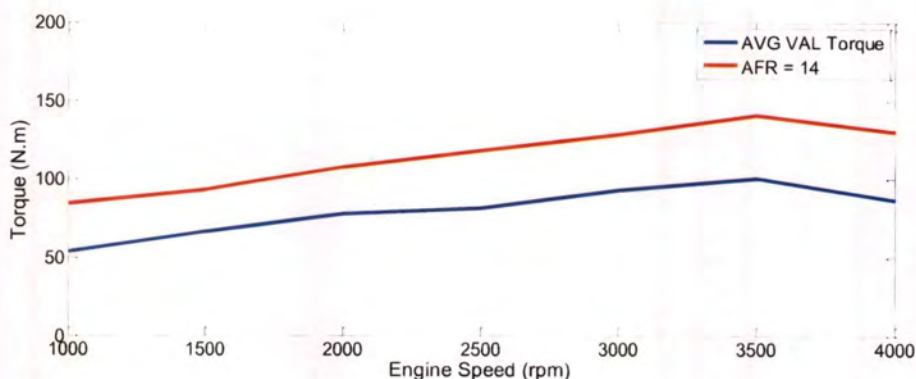


Figure 4.63 Average torque validation vs. maximum torque validation (AFR = 14)

Figure 4.63 shows the average torque validation and maximum torque validation at air fuel ratio is equal to 14 when fueled gasoline. The case of average torque, the maximum torque is equal to 99.83 N.m at engine speed 3,500 rpm and minimum torque is equal to 54.27 N.m. at engine speed 1,000 rpm. The case of air fuel ratio equal to 14 (maximum torque), the maximum torque is equal to 140.90 N.m at engine speed 3,500 rpm and minimum torque is equal to 85.66 N.m. at engine speed 1,000 rpm.

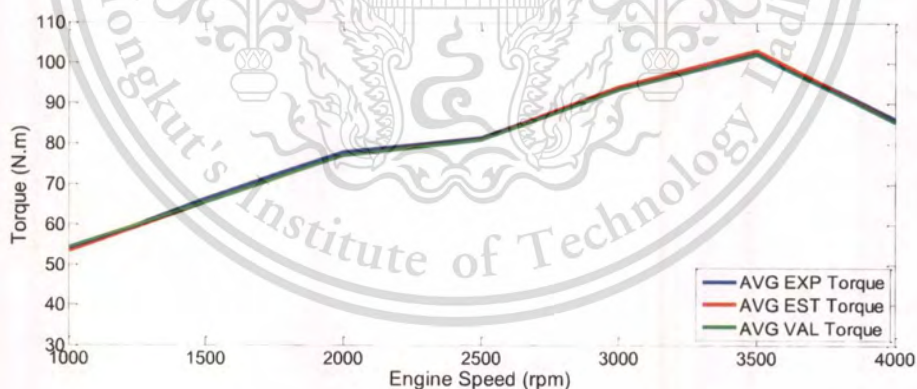


Figure 4.64 The measurement, estimated and validated torque

Figure 4.64 shows the average torque measurement, average torque estimation and average validation torque when gasoline used as fuel. The difference error between average measurement and average estimation torque is 0.60% and the difference error between average torque estimation and average torque validation is 0.36%.

4.7.2 Sweep Test (Gasoline)

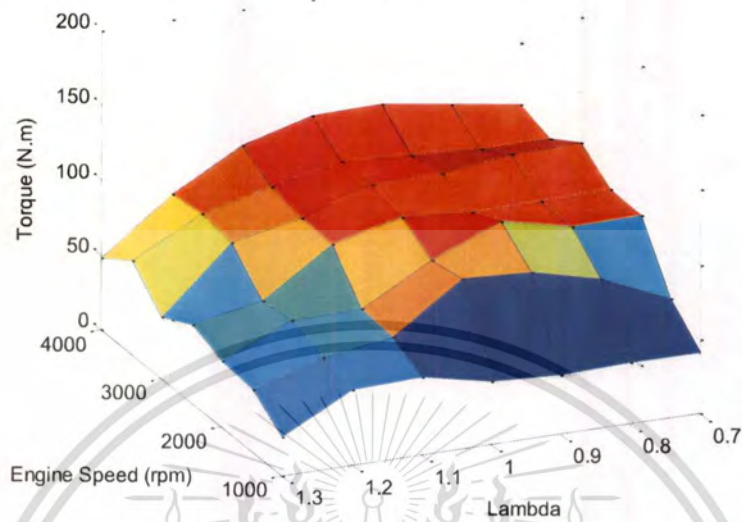


Figure 4.65 Torque validation (N.m).

Figure 4.65 shows the torque validation when gasoline used as fuel by eMapnMod program with polynomial degree 6. The torque is increased due to increasing lambda value is equal to 0.7 (rich) to the maximum torque at lambda value is equal to 0.9. The torque is decreased due to increasing lambda value over 0.9.

An increasing the engine speed since 1,000 to 4,000 the torque is increased since minimum torque at engine speed equal to 1,000 rpm to maximum torque at 4,000 rpm. It is related with air mass flow and fuel injection duration into the combustion chamber.

Figure 4.66 shows the average torque validation vs. maximum torque validation (lambda value is equal to 0.9). The case of average torque estimate, the maximum torque is equal to 102.20 N.m at engine speed 4,000 rpm and minimum average torque estimate is equal to 41.48 N.m. at engine speed 1,000 rpm

The case of lambda value equal to 0.9 (maximum torque estimate), the maximum torque is equal to 128.45 N.m at engine speed 4,000 rpm and minimum torque is equal to 39.91 N.m. at engine speed 1,000 rpm.

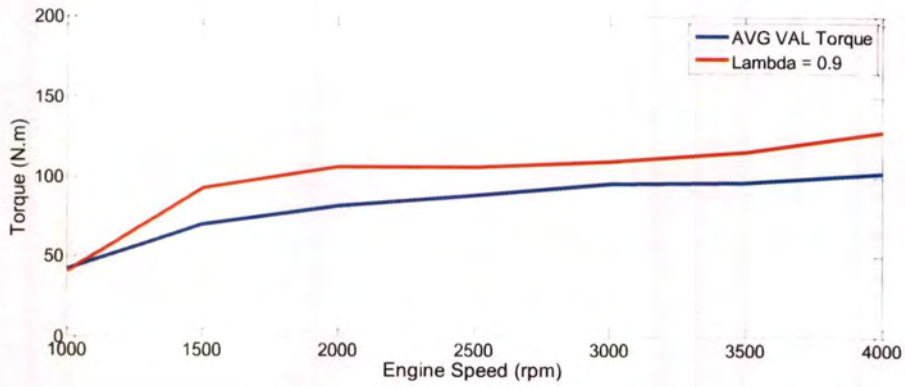


Figure 4.66 Average torque validation vs. maximum torque validation (lambda = 0.9)

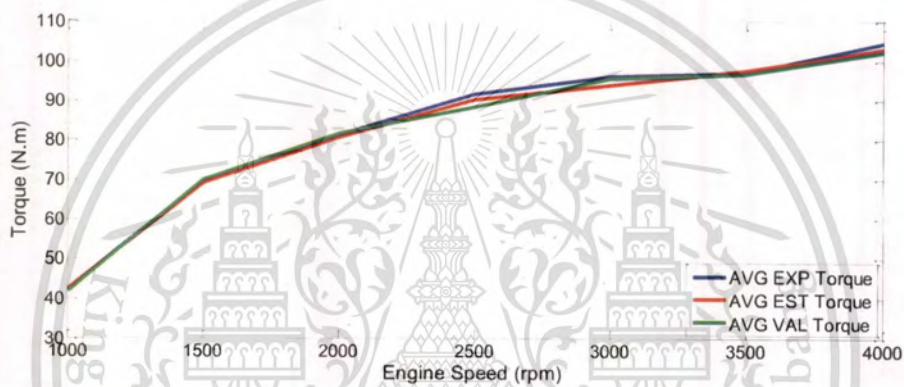


Figure 4.67 Average measurement, estimate and validate torque

Figure 4.67 shows the average torque measurement, average torque estimation and average validation torque when fueled gasoline. The difference error between average measurement and average torque estimation is equal to 1.08% and the difference error between average torque estimation and average torque validation is equal to 0.15%.

4.7.3 Sweep Test (Gasoline-Ethanol Blend E-10)

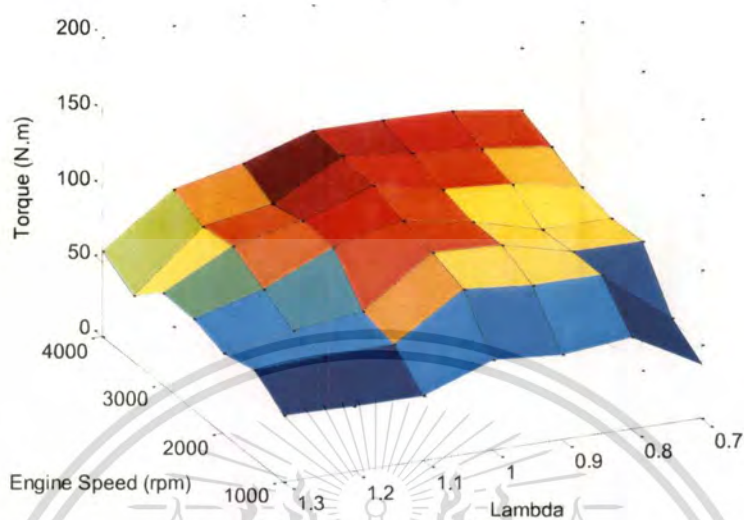


Figure 4.68 Torque validation (N.m)

Figure 4.68 shows the torque validation when gasoline-ethanol blend E-10 used as fuel by eMapnMod program with polynomial degree 6. The torque is increased due to increasing lambda value is equal to 0.7 (rich) to the maximum torque at lambda value is equal to 0.9. The torque is decreased due to increasing lambda value over 0.9.

An increasing the engine speed since 1,000 to 4,000 the torque is increased since minimum torque at engine speed equal to 1,000 rpm to maximum torque at 4,000 rpm. It is related with air mass flow and fuel injection duration into the combustion chamber.

Figure 4.69 shows the average torque validation vs. maximum torque validation (lambda = 0.9). The case of average torque estimate, the maximum torque is equal to 100.70 N.m at engine speed 4,000 rpm and minimum average torque estimate is equal to 49.58 N.m. at engine speed 1,000 rpm.

The case of lambda value equal to 0.9 (maximum torque estimate), the maximum torque is equal to 116.07 N.m at engine speed 4,000 rpm and minimum torque is equal to 56.07 N.m. at engine speed 1,000 rpm.

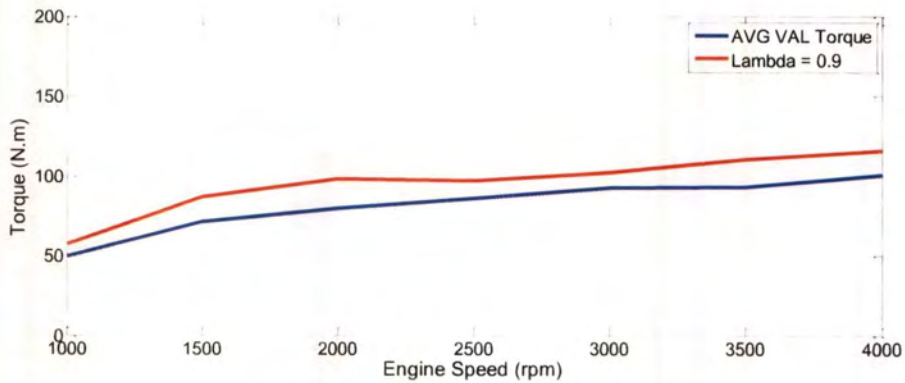


Figure 4.69 Average torque validation vs. maximum torque validation (lambda = 0.9)

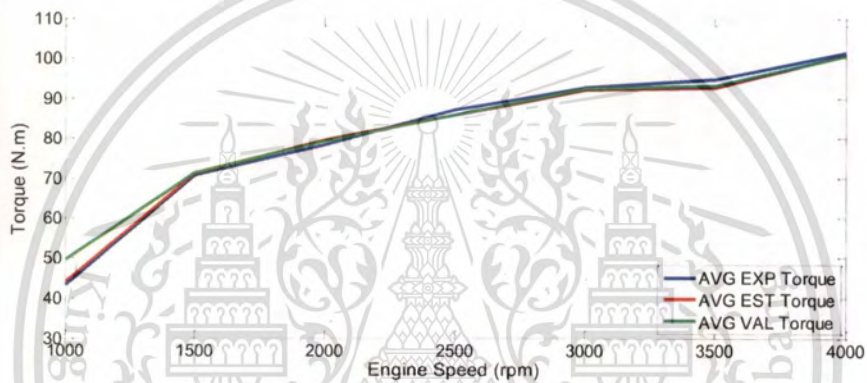


Figure 4.70 Average measure, estimated and validated of torque

Figure 4.70 shows the average torque measurement, average torque estimation and average validation torque when fueled gasoline. The difference error between average measurement and average estimation torque is equal to 0.6% and the difference error between average torque estimate and average torque validation is equal to 1.07%.

4.7.4 Sweep Test (Gasoline-Ethanol Blend E-20)

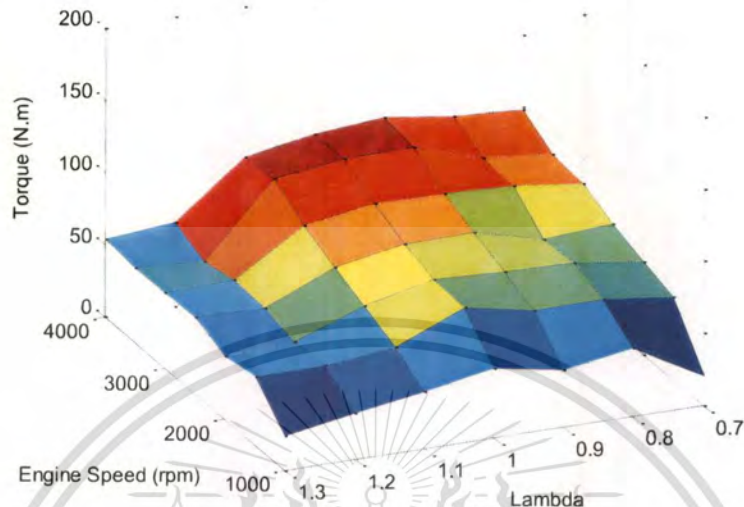


Figure 4.71 Torque validation (N.m)

Figure 4.71 shows the torque validation and gasoline-ethanol blend E-20 used as fuel by eMapnMod program with polynomial degree 6. The torque is increased due to increasing lambda value is equal to 0.7 (rich) to the maximum torque at lambda value is equal to 0.9. The torque is decreased due to increasing lambda value over 0.9.

An increasing the engine speed since 1,000 to 4,000 the torque is increased since minimum torque at engine speed equal to 1,000 rpm to maximum torque at 4,000 rpm. It is related with air mass flow and fuel injection duration into the combustion chamber.

Figure 4.72 shows the average torque validation vs. maximum torque validation (lambda = 0.9). The case of average torque estimate, the maximum torque is equal to 88.53 N.m at engine speed 4,000 rpm and minimum average torque estimate is equal to 35.89 N.m. at engine speed 1,000 rpm.

The case of lambda value equal to 0.9 (maximum torque estimate), the maximum torque is equal to 108.40 N.m at engine speed 4,000 rpm and minimum torque is equal to 39.44 N.m. at engine speed 1,000 rpm.

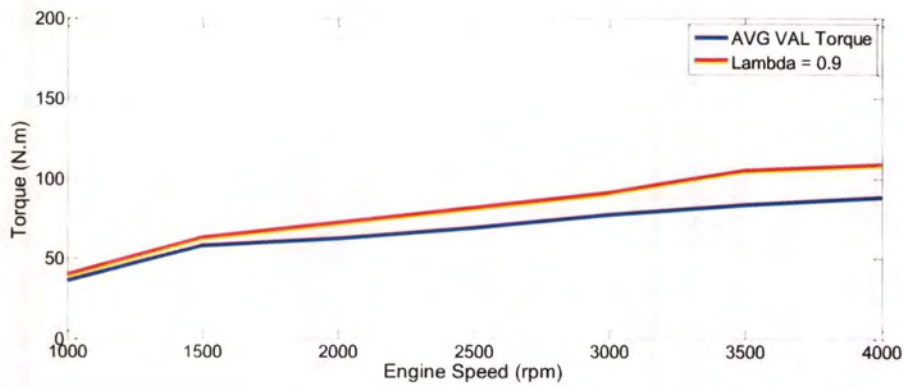


Figure 4.72 Average torque validation vs. maximum torque (Lambda = 0.9)

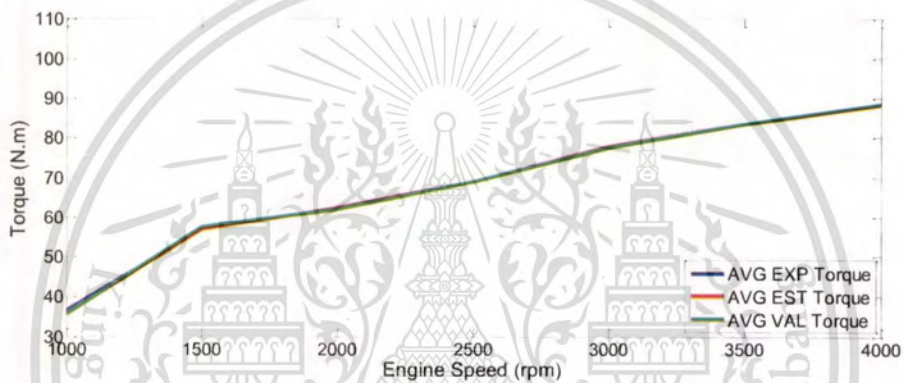


Figure 4.73 Average measure, estimated and validated torque

Figure 4.73 shows the average torque measurement, average torque estimation and average validation torque when gasoline-ethanol blend E-20 used as a fuel. The difference error between average torque measurement and average torque estimation is 0.08% and the difference error between average torque estimation and average torque validation is 0.06%.

4.7.5 Sweep Test (Gasoline-Ethanol Blend E-85)

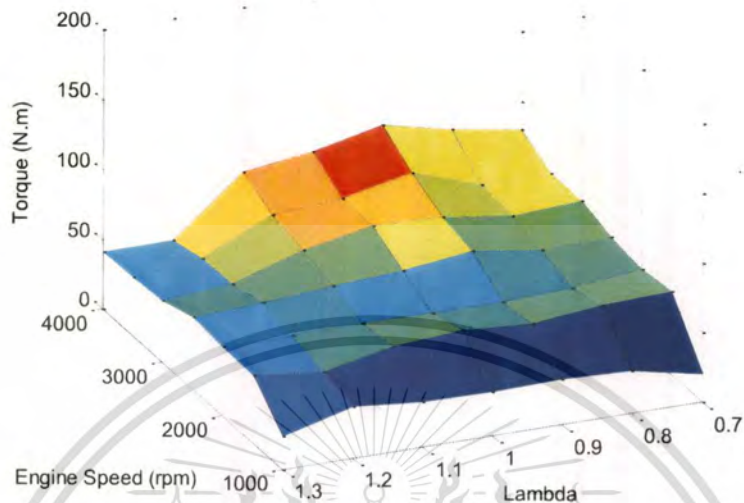


Figure 4.74 Torque validation (N.m)

Figure 4.74 shows the torque validation and gasoline-ethanol blend E-85 used as fuel by eMapnMod program with polynomial degree 6. The torque is increased due to increasing lambda value is equal to 0.7 (rich) to the maximum torque at lambda value is equal to 0.9. The torque is decreased due to increasing lambda value over 0.9.

An increasing the engine speed since 1,000 to 4,000 the torque is increased since minimum torque at engine speed equal to 1,000 rpm to maximum torque at 4,000 rpm. It is related with air mass flow and fuel injection duration into the combustion chamber.

Figure 4.75 shows the average torque validation vs. maximum torque validation (lambda = 0.9). The case of average torque estimation, the maximum torque is equal to 74.98 N.m at engine speed 4,000 rpm and minimum average torque estimate is equal to 29.38 N.m. at engine speed 1,000 rpm.

The case of lambda value is equal to 0.9 (maximum torque estimate), the maximum torque is equal to 99.94 N.m at engine speed 4,000 rpm and minimum torque is equal to 32.05 N.m. at engine speed 1,000 rpm.

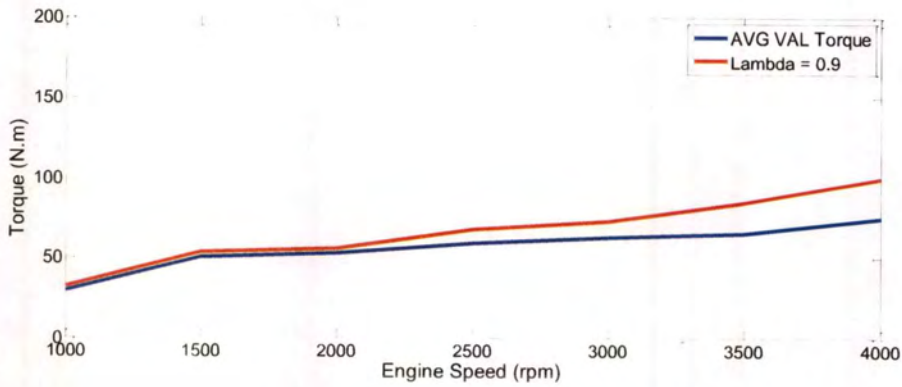


Figure 4.75 Average torque validation vs. maximum torque validation (lambda = 0.9)

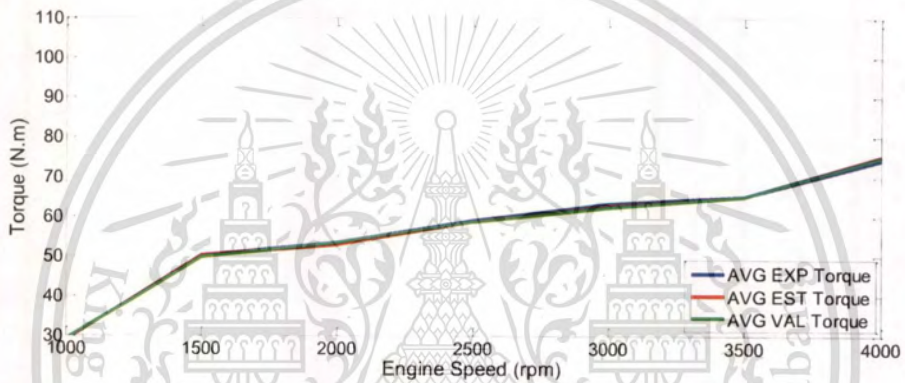


Figure 4.76 Average measure, estimated and validated of torque

Figure 4.76 shows the average torque measurement, average torque estimation and average validation torque when fueled gasoline. The difference error between average measurement and average torque estimation is 0.45% and the difference error between average torque estimation and average torque validation is 0.23%.

4.8 Summary

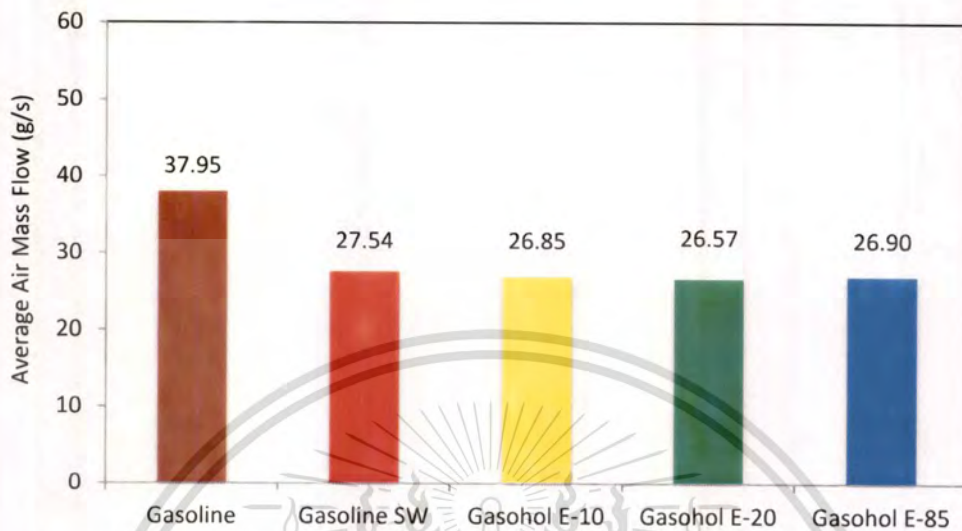


Figure 4.77 Average air mass flow (g/s)

The average air mass flows are decreased in accordance with the test method as shown in Figure 4.77. The average air mass flow of steady state experiment is equal to 37.95 g/s. and other columns shows the air mass flows of sweep test method gasoline and gasoline-ethanol blend used as fuel are approximately to 27 g/s. In case of the sweep test, the air mass flows are approximately to 27% less than the steady state test condition and do not depend on fuel types.

Figure 4.78 shows the average injection duration are increased in accordance with quantity of mixed ethanol. The average fuel injection duration of gasoline by sweep test method (red column) is equal to 12 ms, gasoline-ethanol blend (yellow column) is equal to 11.98 ms. The difference of injection duration between gasoline and gasoline-ethanol blend E-10 is small.

In case of gasoline-ethanol blend E-20 (green column) and E-85 (blue column), the average injection duration of both fuel type are equal to 12.43 ms and 15.37 ms which injection duration has been increased approximately to 3.5% for E-20 and 28% for E-85 respectively when compare with gasoline.

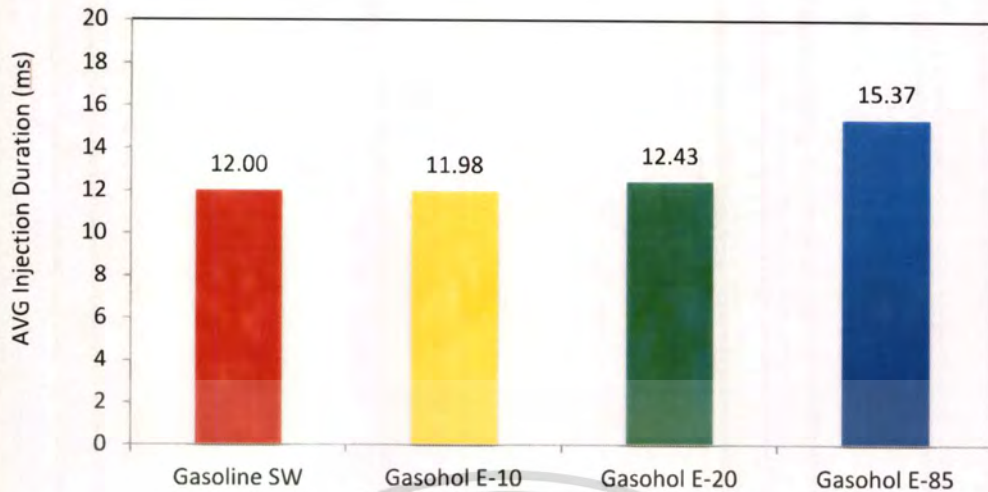


Figure 4.78 Average injection duration (ms)

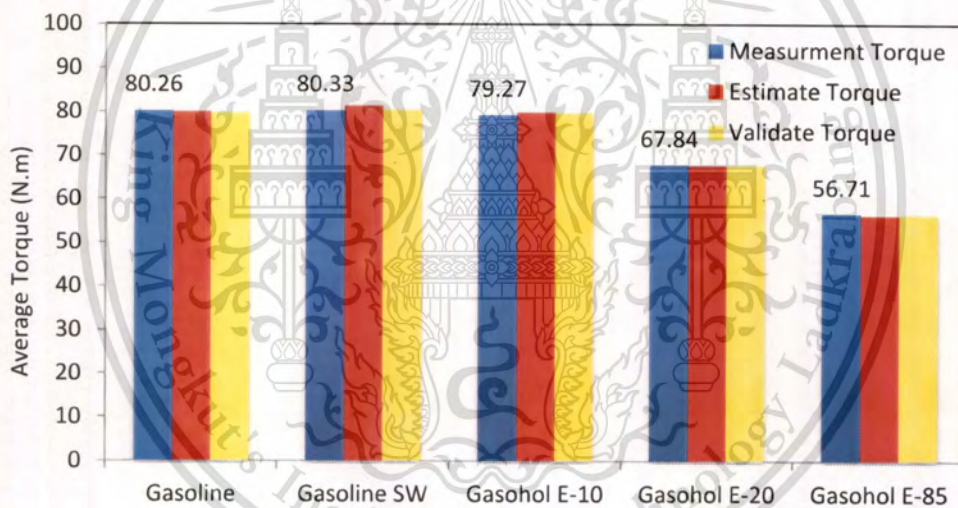


Figure 4.79 Average torque (N.m)

Figure 4.79 shows the average torque due to test method and fuel types. The average torque of steady state test and sweep test method are roughly equal (80.26 N.m. and 80.33 N.m.). In case of fuel types, the average torque of gasoline-ethanol blend E-10 is equal to 79 N.m. which small different with gasoline around 0.9% (compare with average of gasoline between steady state and sweep test method). Average torque are decrease due to increase the ethanol percentage, average torque of gasoline-ethanol blend E-20 is equal to 67 N.m. less than gasoline around 16%

and average torque of gasoline-ethanol blend E-85 is equal to 56.71 N.m. less than gasoline around 29%.

The simulation results from recursive least square when forgetting factor is equal to 0.9. The estimation results are roughly equal to the experiment results (measurement). The maximum error between experiment and estimation results is equal to 0.92% (gasoline sweep test). The polynomial regression used as validate the estimation results. The maximum error between estimation and validation result is equal to 1.07% (gasoline-ethanol blend E-10).



CHAPTER 5

CONCLUSIONS AND SUGGESTIONS

5.1 Conclusion

This thesis presents the development of observation data engine model by using engine mapping. The empirical study was done on eddy current dynamometer in order to explore torques and air fuel ratios of a spark ignition engine which ran on gasoline and gasoline-ethanol blends, E-10, E-20 and E-85. The experiment data was captured while the fuel injection durations and engine speed were controlled to obtain the air fuel ratio in the ranges of between 0.7 and 1.3, whereas the required engine speeds were in between 1,000 and 4,000 rpm. In this thesis, the data sets were collected by two experimental methods: steady state test and sweep test. The spark ignition timing was calibrated according to the optimum condition for the gasoline fuel and throttle was set at the wide open throttle position (WOT) only. However, the cold start, idle speed, a compensation of natural atmosphere (i.e. air temperature and humidity of engine test room), term of emission and fuel consumption were not considered in this work.

The sweep test is alternative techniques which can take less effort in creating engine model and give similar results when comparing to the steady state method. However, the sweep test is not suitable for signals which have slow response, such as air mass flow. The comparisons between both data-capturing methods are described as the following:

- The average injection duration has increased in accordance with quantity of mixed ethanol. The difference of injection duration between gasoline and gasoline-ethanol blend E-10 is small (approximately to 12 ms). The average injection durations of E-20 and E-85 are equal to 12.43 ms and 15.37 ms and are different from gasoline 3.5% and 28% respectively.

- The average torque of steady state test and sweep test methods are roughly equal (80.26 N.m and 80.33 N.m). Torques varied according to fuel types. The average torque of gasoline-ethanol blend E-10 is equal to 79 N.m, average torque of gasoline-ethanol blend E-20 is equal to

67 N.m and average torque of gasoline-ethanol blend E-85 is equal to 56.71 N.m. The difference of torque between gasoline and gasoline-ethanol blend E-10 is small (less than 0.9%). The average torques is decreased due to the increasing in ethanol percentage. The average torques of gasoline-ethanol E-20 and gasoline-ethanol E-85 are approximately to 16% and 29% less than gasoline.

- The average air mass flow of steady state experiment is equal to 37.95 g/s and for the sweep test experiment are approximately to 27 g/s. In case of the sweep test, the air mass flows are approximately 27% less than the steady state test condition and do not depend on fuel types.

The “eMapnMod” program, based on MATLAB, has been developed as a tool for engine identification which employs recursive least square (RLS) to filter noise and vibration on captured data. To adjust the RLS, the forgetting factor has been applied for signal processing.

With RLS forgetting factor 0.9 and polynomial regression, the simulation results of torque given by the eMapnMod were significantly closed to the experimental results. The maximum average error of torques between the experiment and estimation is 0.92% (gasoline sweep test) and the maximum error between the estimation and validation result is 1.07% (gasoline-ethanol blend E-10).

5.2 Suggestion

The sweep test typically took 12.5 seconds for increasing speed from 1000 rpm to 4000 rpm which was very short time for reading air mass flow parameter. The air mass flow reading errors between steady state and sweep test in this study could be caused from 2 issues.

First, in the steady state test, the intake manifold pressure was relatively stable and it had enough time for drawing air into the engine cylinder under atmospheric pressure while the pressure in the sweep test had rapidly change and then caused air-flow problem.

Second, the response of air flow sensor, hot wire type, used in the study was slow because the fast air flow removed the heat from the hot wire faster than heat generation. The

electronic circuit could compensate this by increasing more current to the wire for producing heat. This solution might give the better dynamic response of air mass flow device.

For the strain gauge issue, the vibration of engine test stand during the experiment may effect to the torque measurement data. This can be improved by replacing the strain gauge with the internal combustion pressure sensor for measuring the pressure in combustion chamber.

In the future work, to improve performance of the engine when ethanol or gasoline-ethanol blend on the standard gasoline engine, adjusting spark timing advance should be considered rather than controlling fuel injection duration only.



REFERENCES

- [1] J.B. Heywood. **Internal Combustion Engine Fundamental**, New York, 1988.
- [2] Byungho Lee, Ann Arbor and Yann G. Guezennec. "Rapid Engine Mapping and Modeling." **US. Patent**, 2007.
- [3] "http://encarta.msn.com/encyclopedia_761553622_2/Internal-Combustion_Engine/html"
Encarta Encyclopedia, 2009
- [4] Uwe Kiencke and Lar Nielsen. **Automotive Control Systems for Engine, Driving and Vehicle**, 2nd ed., Springer-Verlag, 2005.
- [5] Jack Erjavec. **Automotive Technology a System**. 4th. Thomson Delmar Learning, 2005.
- [6] Timothy Holliday and Anthony J. Lawrance. "Engine-Mapping Experiment:A two-Stage Regression Approach." **American Statistical Association and the American Society for Quality**. Vol. 40, 2006.
- [7] Jeff B Burl. "A State Model for the Air-Fuel Ratio." n.d.
- [8] Owen K, Coley T. **Automotive Fuels Reference Book**. 2nd ed. **USA Society of Automotive Engineers, Inc.**, 1995
- [9] B. Saerens, J. Vandersteen, T. Persoons, J. Swevers, M. Diehl and E Van den Bulck. "Minimization of The Fuel Consumption of a Gasoline Engine Using Dynamic Optimization." **Applied Energy** 86, 2009. pp 1582-1588
- [10] Jacob Benestry and Tomas Gansler. "A Recursive Estimation of The Condition Number in the RLS Algorithm." **IEEE Transaction Automotive Control**, 2005.
- [11] Christan Fedbauer, Franz Pernkopf, and Erhard Rank. "Adaptive Filters." n.d.
- [12] James E. Bobrow and Walter Murry. "An Algorithm for RLS Identification of Parameter that Very Quickly with Time." **IEEE Transaction Automotive Control**, 1993.
- [13] S. Gunnarson. "Combining Tracking and Regularization in Recursive Least Square Identification." Sweden, n.d.
- [14] Kremer FG, Fachetti A. "Alcohol as Automotive Fuel-Brazilian Experience." State of Alternative Fuel Technologies 2000 (SP-1545). **Society of Automotive Engineers, Inc.** SAE 2000-01-1965, 2000

REFERENCES (CONT.)

- [15] Dai W, Cheemalamarri S, Curtis EW, Boussarsar R, Morton RK. "Engine Cycle Simulation of Ethanol and Gasoline Blends." SAE Technical Paper 2003-01-3093. **Society of Automotive Engineers, Inc., USA, 2003**
- [16] Li L, Liu Z, Wang H, Deng B, Xiao Z, Gong C, Su Y. "Combustion and Emissions of Ethanol Fuel (E100) in a Small SI Engine." SAE Technical Paper 2003-01-3262. **Society of Automotive Engineers, Inc., USA, 2003.**
- [17] Marco Campi. "Performance of RLS Identification Algorithm with Forgetting Factor : A Phi-Mixing Approach." n.d.
- [18] Dan J. Dechene. "First Transversal Recursive Least-Square (FT-RLS) Algorithm." Department of Electrical and Computer Engineering, University of Western Ontario London, n.d.
- [19] L.Guzzella and Christopher H. Onder. "Introduction to Modeling and Control of IC Engine Systems" New York: Springer Berlin Heidelberg, 2007.
- [20] Walt Boyes. **Instrumentation reference book**. 4 th. Butterworth-Heinemann, 2010.
- [21] M. Chatpoj, P. Pongkacha, S.Downgpummate, J. Janpaiboon, T. Pattrapornnant. "Eddy Current & DC Regenerative Dynamometer System." Embedded System Technology, NECTEC, 2010.
- [22] "LM-1 Digital Air fuel Ratio (Lambda) Meter Manual." Innovate Motorsports, n.d.
- [23] M. Chatpoj, J. Janpaiboon, N. Kririksh, P. Pumvisate, P. Sira-uksorn. "Ignition Control Unit Pre-Commercial." Embedded System Technology, NECTEC, 2008.
- [24] E. Hendricks and S. C. Sorenson. "Mean Value Modeling of Spark Ignition Engine." SAE Technical Paper, 1990.
- [25] A. Brahma, D. Upadhyay, A. Serrani and G. Rizzoni. "Modeling, Identification and State Estimation of Diesel Engine Torque and NOx Dynamic in Response to Fuel Quantity and Timing Excitations." **American Control Conference**. Vol 3, 2004.
- [26] M. Ayeb, D. Lichtenthaler, T. Winsel and H. Theuerkauf. "SI Engine Modeling Using Neural Network." SAE Technical Paper 980790, 1998.

REFERENCES (CONT.)

- [27] B. Hariri, A.T. Shenton and R.E. Dorey. "Parameter Identification, Estimation, and Dynamometer Validation of the Nonlinear Dynamics of an Automotive Spark-Ignition Engine." **Journal of Vibration and Control**, January 1998. pp. 47-59.
- [28] Ward M.C., Brace C.J. Shaddick G., Finch A.J. Akehurst S. Ceen R. Hale T. and Kennedy G. "Bayesian Statistics in Engine Mapping." n.d.
- [29] M. Suporn. "Estimation of Flex Fuel injection Period Using Artificial Neural Networks." **Kasetsart University Conference 44**, 2010
- [30] H.Bayraktar and O.Durgun. "Mathematical Modeling of SI Engine Cycle." **Energy Sources**, 25, 2003. pp. 439-445
- [31] Ward M.C., Brace C.J., Vanughan N.D., Ceen R., Hale T. and Kennedy G. "Invertigation of 'Sweep' Mapping Approach on Engine Testbed." **Society of Automotive Engineers, Inc.**, 2002.
- [32] Jone, Kenneth R. Muske and James C. Peyton. "A Model-Based SI Engine Air Fuel Ratio Controller." **American Control Conference**. Minneapolis, Minnesota, USA, June 14-16, 2006.
- [33] Perihan Sekmen and Yakup Sekmen. "Mathematical Modeling of a SI Engine Cycle with Actual Air-Fuel Cycle Analysis." **Mathematical and Computational Applications**, 2007. pp. 161-171
- [34] Wanida Norasethasopon. "Effect of Gasohol Production on the Sugarcane Industry in Thailand." **Journal of Asia Pacific Studies**, Vol 1, No 2, 2010. pp. 101-131
- [35] Rodrigo C. Costa and José R. Sodr . "Hydrous Ethanol vs. Gasoline-Ethanol Blend: Engine Performance and Emissions." **Fuel** Vol. 89, Issue 2, 2010. pp. 287-293
- [36] Muharrem Eyidogan, Ahmet Necati Ozsezen, Mustafa Canakci and Ali Turkcan. "Impact of Alcohol-Gasoline Fuel Blends on the Performance and Combustion Characteristics of an SI Engine." **Fuel** Vol. 89, 2010. pp. 2713-2720
- [37] M. Al-Hasan. "Effect of Ethanol–Unleaded Gasoline Blends on Engine Performance and Exhaust Emission." **Energy Conversion and Management** 44, 2003. pp. 1547–1561



This material is reserved for educational use only, not allowed for commercial use.

Forbidden to modify the content, and cite the document when use.

APPENDIX A

Gasoline-Ethanol Blend (Gasohol)

In this study we applied Gasohol for experiment on real engine. There have 2 types of mixtures, first alcohol or ethanol 99.5% and second is gasoline. For example, E85 contains 85 percent ethanol and 15 percent gasoline. Other blends may include E10, which contains 10 percent ethanol and 90 percent gasoline, and E20, which contains 20 percent ethanol and 80 percent gasoline.

Table A-1 Specifications of Standard Gasoline, Ethanol and Gasohol

Specifications	Gasoline	Ethanol	E-10	E-20	E-85
%Ethanol	-	99.50	10	20	85
Formula	C ₄ to C ₁₂	C ₂ H ₅ OH	-	-	CH _{2.822} O _{0.425}
Stoichiometric AFR	14.7	9	14.13	13.29	9.86
RON	91	108.6	95	95	95
LHV (MJ/kg)	44.4	26.9	43.47	41.38	33.1
HOV (kJ/kg)	349	840	410	-	-

Ethanol has a higher octane number than gasoline and when blended with gasoline can effectively operate at higher compression ratios with subsequent improvement in power output, efficiency, and fuel consumption. It may be impractical to raise the compression ratio, but if the engine is knock-limited with standard gasoline, advancing the spark may offer improvements in performance similar to those obtained with a small increase in compression ratio.

Cold starting is highly dependent on the fuels ability to vaporize effectively at low temperatures and provide an ignitable mixture at the time of ignition. For ethanol blends, cold starting depends on the vaporization of the more volatile gasoline fractions. However, when

alcohol is present, the vapor contains a greater concentration of alcohol than would be expected based on the vapor pressure of the alcohol or its concentration in the gasoline. Due to ethanol's higher heat of vaporization than gasoline, more heat is required to vaporize ethanol blends. Effectively, the mixture suffers from enleanment due to the higher concentration of alcohol (because the chemically correct fuel/air ratio is higher). Raising the compression ratio and valve timing optimization are considered to be practical methods to improve cold starting.

Enleanment: The addition of oxygenates to gasoline has the effect of enleaning the fuel/air mixture on engines that are not adjusted to optimize this ratio. If an engine operates at a mixture that is significantly leaner than it is designed for, it will run at a higher temperature, which can lead to engine damage.

Vapor lock: the vapor pressure of ethanol is low, the Reid Vapor Pressure (RVP) of gasoline-ethanol blends rises depending on the ethanol proportion in the blend. Low RVP can cause starting problems, but high RVP can cause vapor lock in warm weather. Depending upon the degree, vapor blockage can cause engine performance problems ranging from poor to erratic power output to engine overheating to full engine stall due to fuel starvation and hot-start problems

Engine and Fuel system Deposits: Ethanol gasoline blends increase the solubility of gasoline fuel deposits leading to the release of gum-bound debris followed by blockage of filters and fuel metering components. Gum formation during equipment storage is a particular concern for equipment that does not get used on a regular basis. The majority of engine manufacturers recommend draining unused fuel from equipment or adding a fuel-stabilizing additive that prevents oxidation prior to storage of equipment. The solvent action of the oxygenated fuel may dissolve some of the fuel system deposits, which will plug fuel filters.

Material Compatibility: The materials used in engine fuels systems are diverse Ethanol in gasoline can cause elastomers to swell and lose tensile strength, causing fuel pumps, accelerator pumps, and hoses to fail. Materials such as tern plate (lead/tin-coated steel used in fuel tanks) zinc die castings, and aluminum fuel system components are attacked by alcohols and require

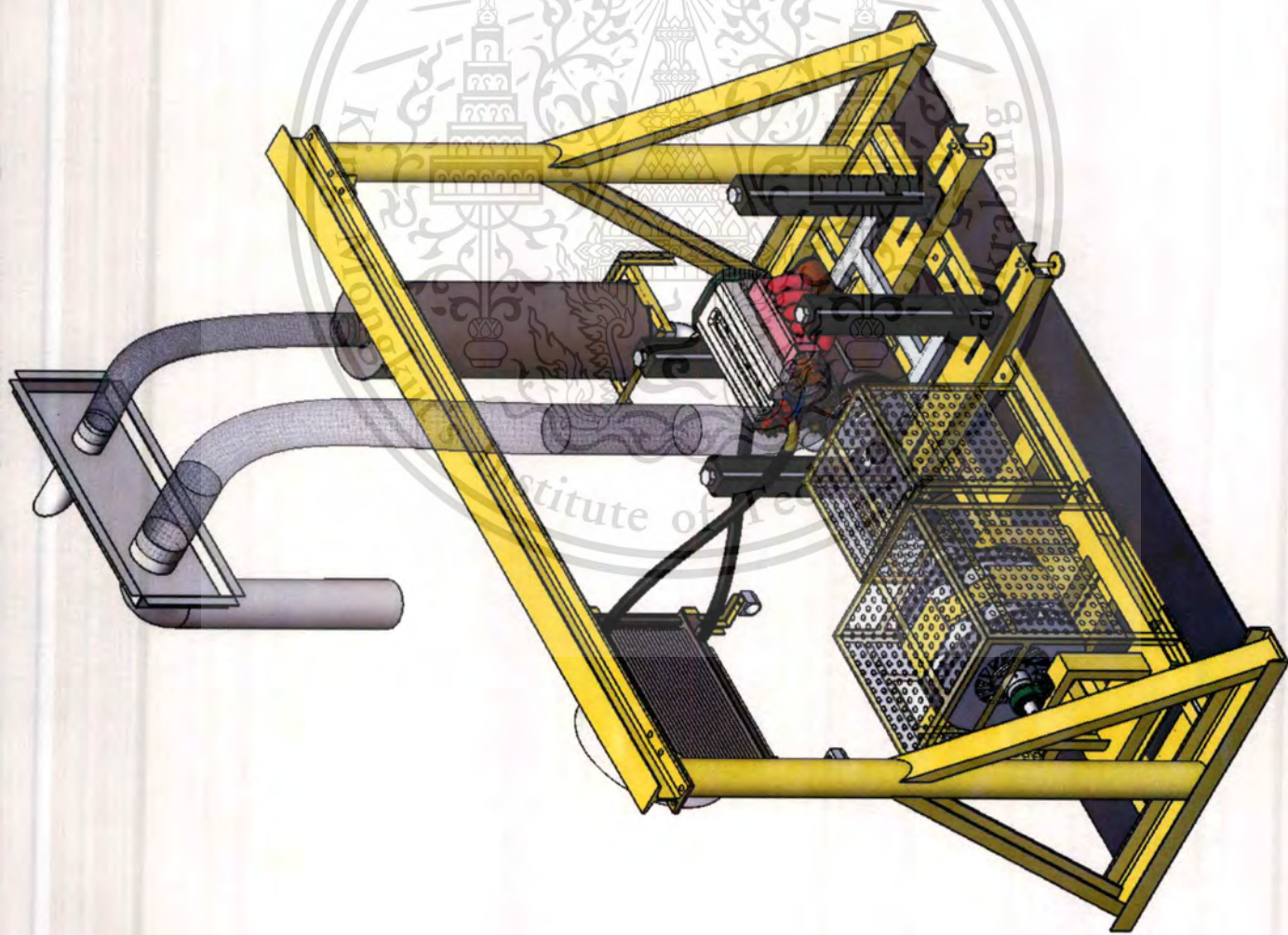
corrosion inhibitors to minimize this effect. Corrosion of steel is accelerated by the presence of alcohols in the fuel, partly because of the increased water content of the fuel. Only testing of representative components along with long-term durability and testing with the E20 ethanol blend can provide accurate information of the possible impact.

Phase Separation (of fuel): Ethanol has a high affinity for water, thus it contains a certain amount of water. Since gasoline and water do not mix, even small amounts of water in gasoline will result in a separate phase of water in a fuel tank, which, if pumped into the engine, could cause damage. However, years of experience have resulted in this concern being minimized. Oxygenated gasoline (ethanol blends), will tend to dry out fuel tanks by blending with the water allowing it to be combusted in the engine. Only with comparatively large amounts of water in ethanol-blended gasoline will a separate alcohol/water phase occur. There is a wide range of recommendations by manufacturers for the use of oxygenated fuels depending on the specific engine application. Water contamination can also cause corrosion on metal components. Solubility improvers, such as isopropanol, can prevent these problems.



APPENDIX B

Engine Test Stand Drawing



ECU Test Unit

Part No. Assam

Dimension. mm.

Discription

Sheet No. 00

Materal.

Scale. 1:22

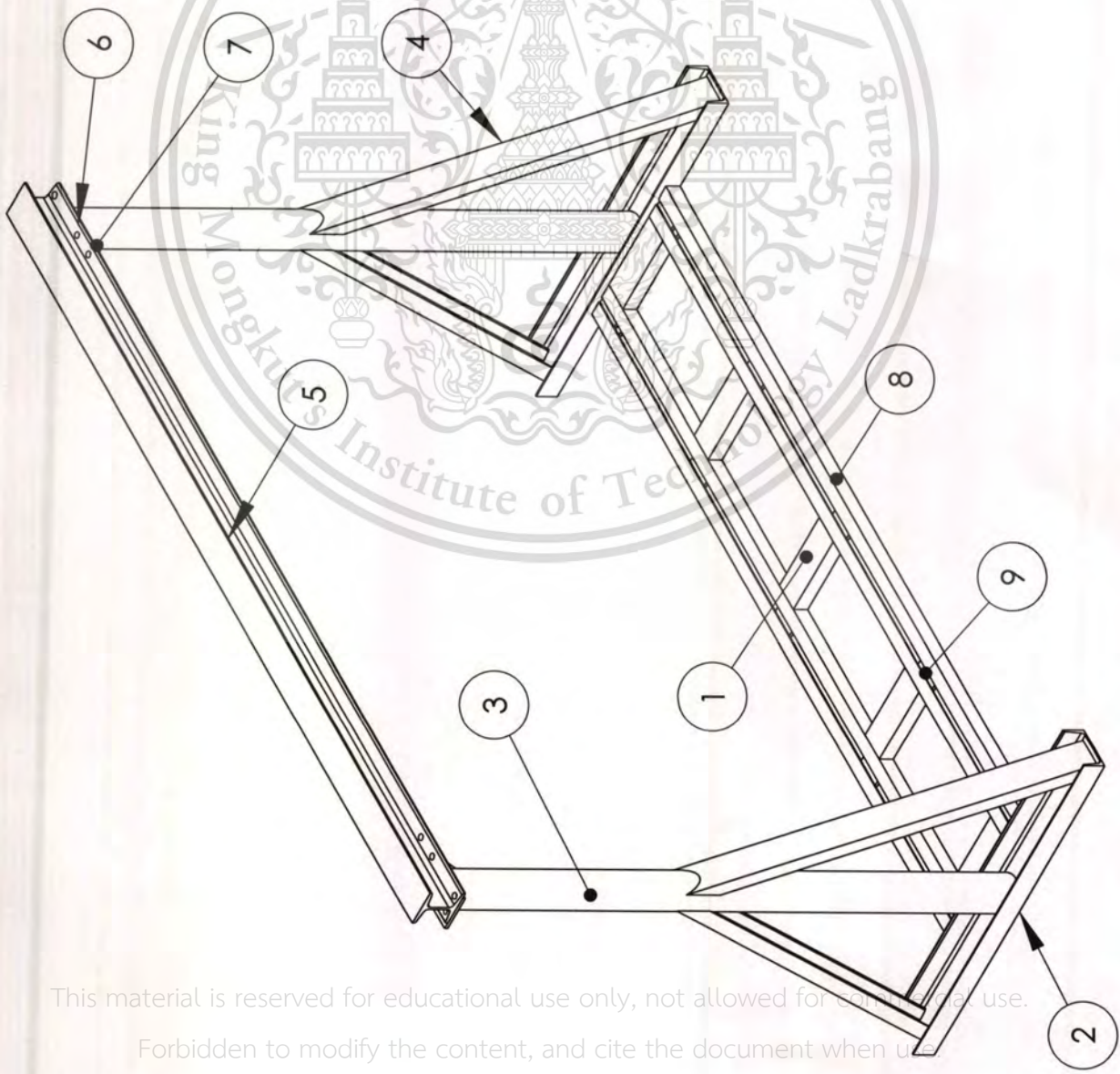
Size.

Qty.1

This material is reserved for educational use only, not allowed for commercial use.

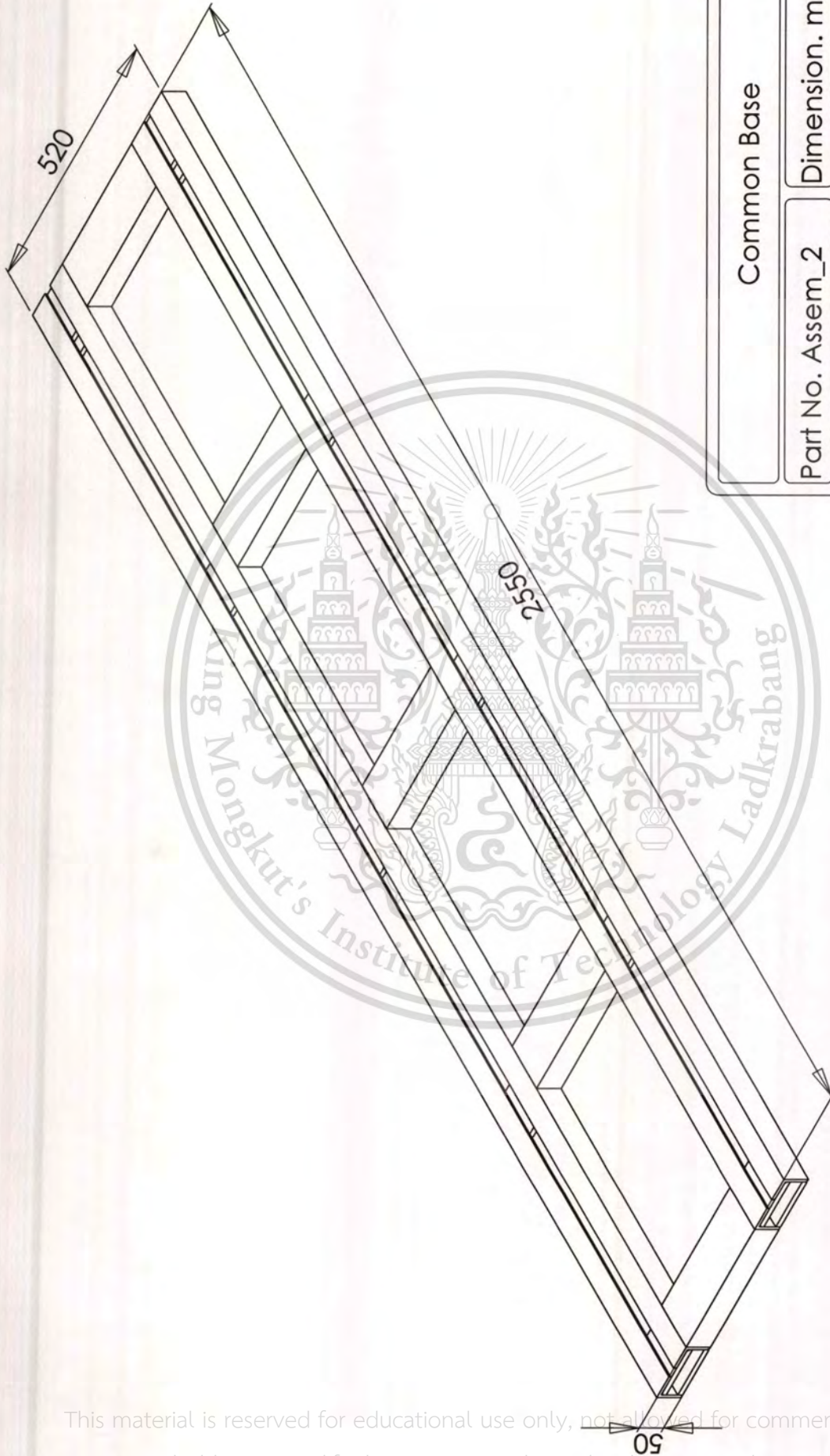
Forbidden to modify the content, and cite the document when use.

ITEM NO.	PART NUMBER	QTY.
1	rail_1_tie	5
2	gentry_crane_base_1	2
3	colome	2
4	gentry_crane_base_2	4
5	bar	1
6	bar vs colome spacer	2
7	gentry_crane_wing	2
8	rail_base_1_angle	4
9	rail_connector	14



Base_Engine_Test	
Part No. Assem_1	Dimension. mm.
Description.	Sheet No. 1
Material.	Scale. 1:20
Size. 1200x2850x2150	Qty. 1

This material is reserved for educational use only, not allowed for commercial use.
 Forbidden to modify the content, and cite the document when used.



Common Base

Part No. Assem_2

Dimension. mm.

Discription

Sheet No. 2

Material. Steel

Scale. 1:10

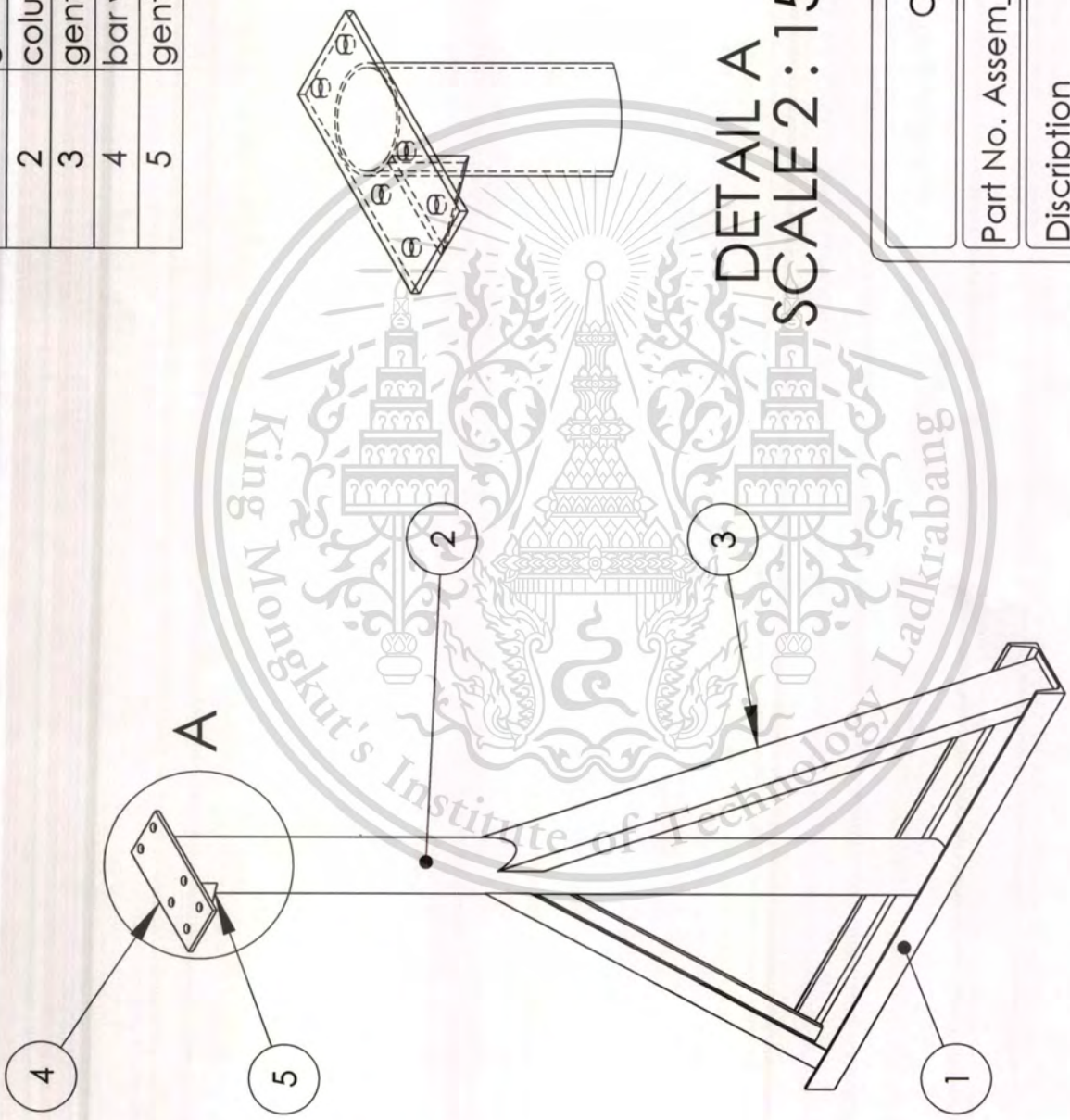
Size. 520x2550x50

Qty. 1

This material is reserved for educational use only, not allowed for commercial use.

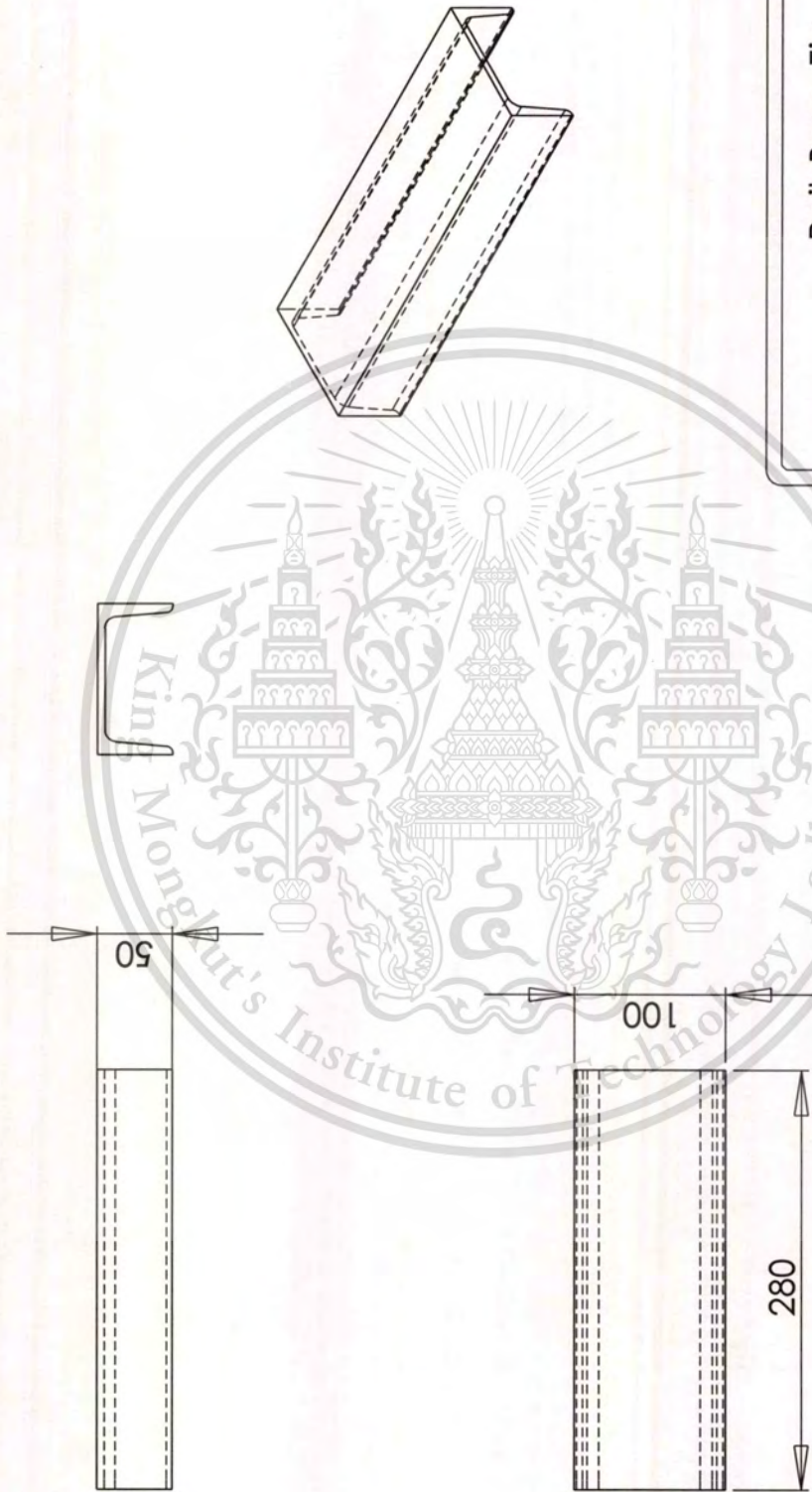
Forbidden to modify the content, and cite the document when use.

ITEM NO.	PART NUMBER	QTY.
1	gentry_crane_base_1	1
2	colume	1
3	gentry_crane_base_2	2
4	bar vs colume spacer	1
5	gentry_crane_wing	1



DETAIL A SCALE 2:15

Colume_Assem	
Part No. Assem_3	Dimension. mm.
Discription	Sheet No. 3
Materal. Steel	Scale. 1:15
Size.	Qty. 2



Rail_Base_Tie

Part No. 1

Dimension. mm.

Discription

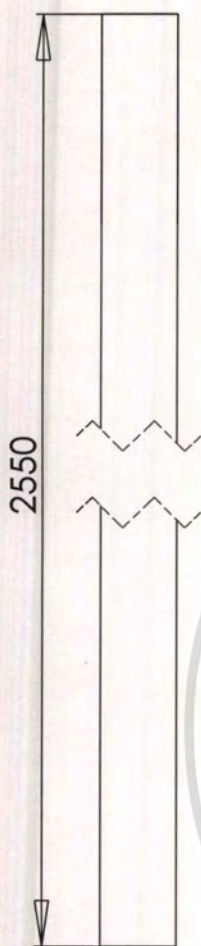
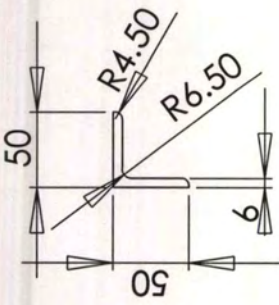
Sheet No. 4

Materal. Channel 100x50x5

Scale. 1:5

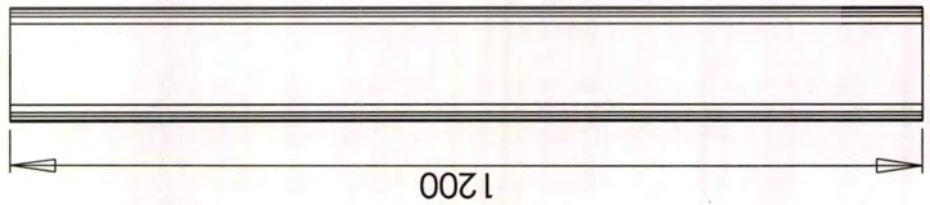
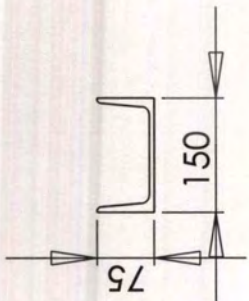
Size. 320

Qty. 5



Rail_Base_1	
Part No. 2	Dimension. mm.
Discription.	Sheet No. 5
Materral. Angle 50x50 t6	Scale. 1:5
Size. 2550mm.	Qty. 4

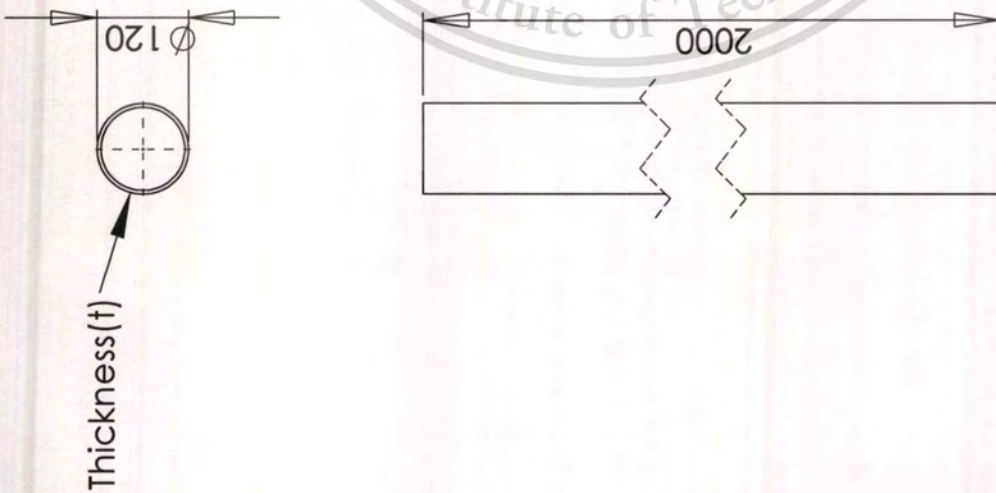
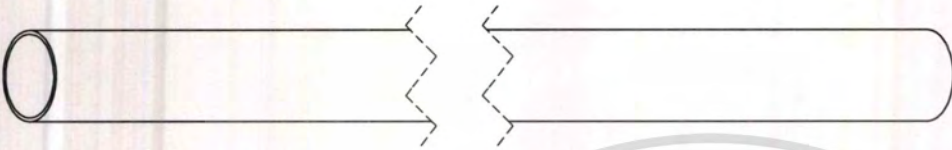
This material is reserved for educational use only, not allowed for commercial use.
 Forbidden to modify the content, and cite the document when use.



Gentry_Crane_Base_1	
Part No. 3	Dimension. mm.
Description	Sheet No. 6
Materal. Channel150x75x6.5	
Scale. 1:10	
Size. 1200.	Qty. 2

This material is reserved for educational use only, not allowed for commercial use.

Forbidden to modify the content, and cite the document when use.

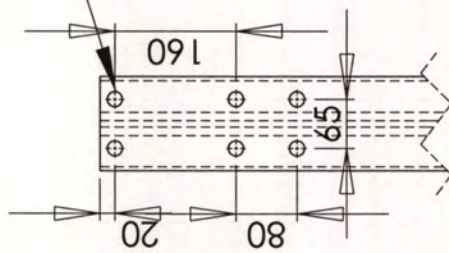
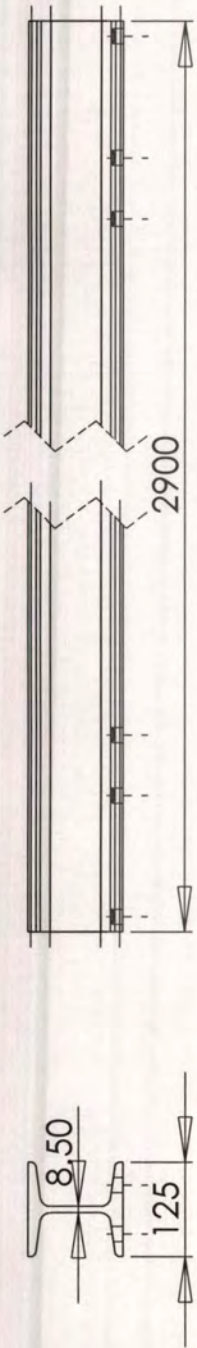


Colume	
Part No. 4	Dimension. mm.
Description Thickness Depend on Size of Round Bar	Sheet No. 7
Material. Round Bar 120xt	Scale. 1:10
Size. 2000	Qty. 2

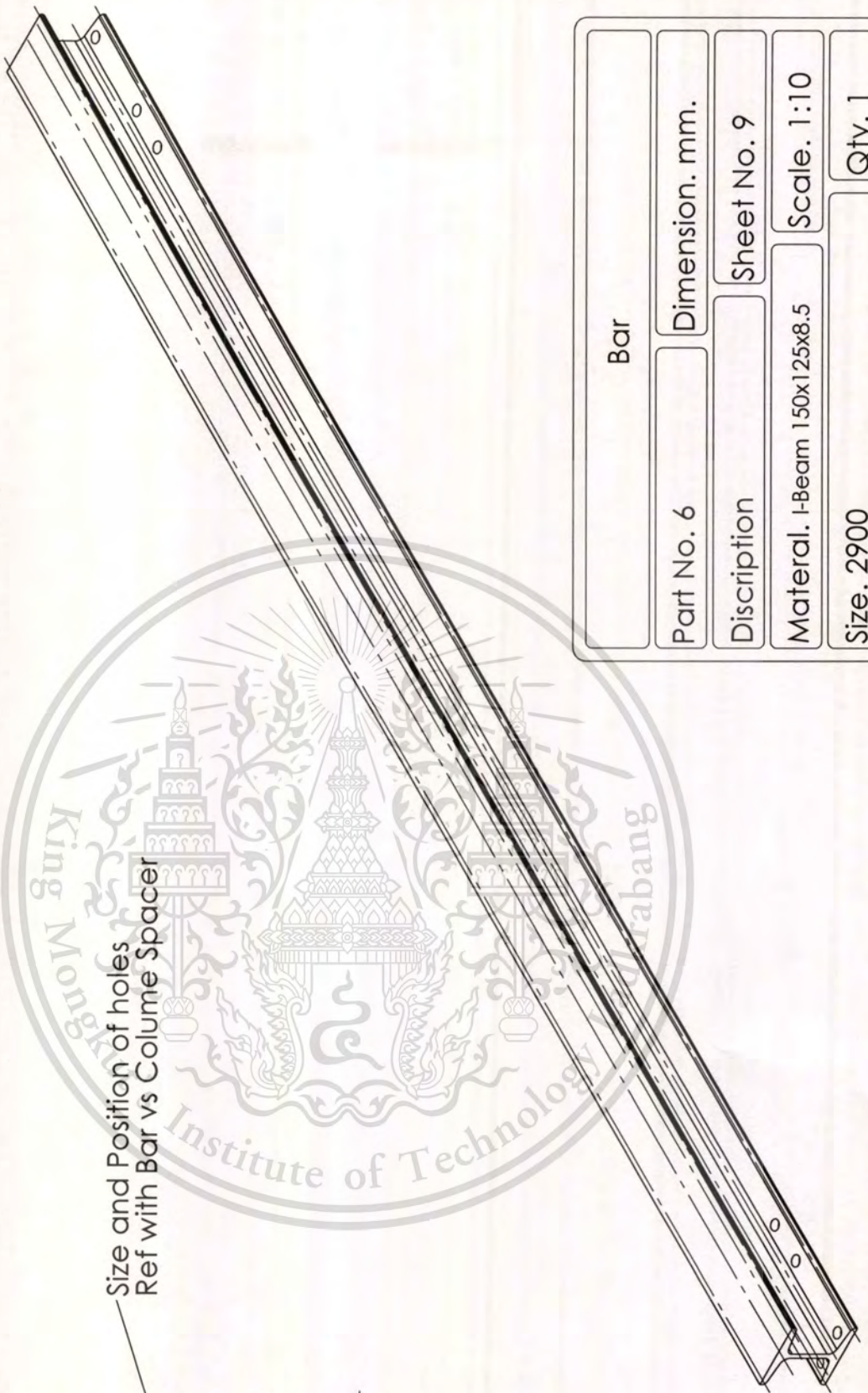


Curve Reference
with Colum Dia

Gentry_Crane_base_2	
Part No. 5	Dimension. mm.
Discription. <small>Curve reference with Colum Dia.</small>	Sheet No. 8
Materal. Channel 100x50x5	Scale. 1:10
Size. 1300	Qty. 4



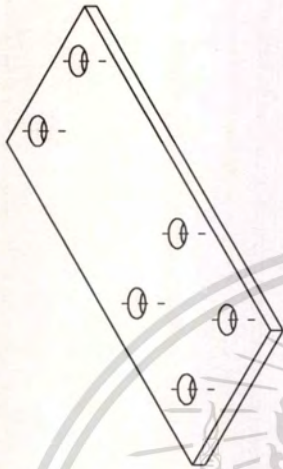
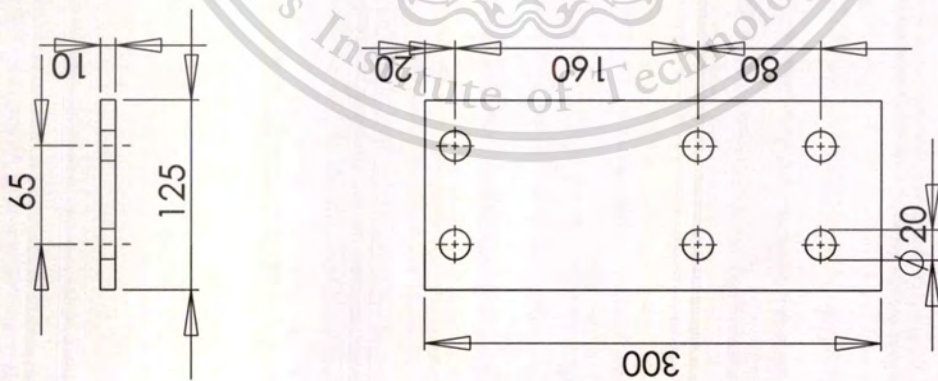
Size and Position of holes
Ref with Bar vs Colume Spacer



Bar	
Part No. 6	Dimension. mm.
Discription	Sheet No. 9
Material. I-Beam 150x125x8.5	Scale. 1:10
Size. 2900	Qty. 1

This material is reserved for educational use only, not allowed for commercial use.

Forbidden to modify the content, and cite the document when use.



Bar vs Colume_Spacer

Part No. 7

Dimension. mm.

Discription
Should Compare
with Bar

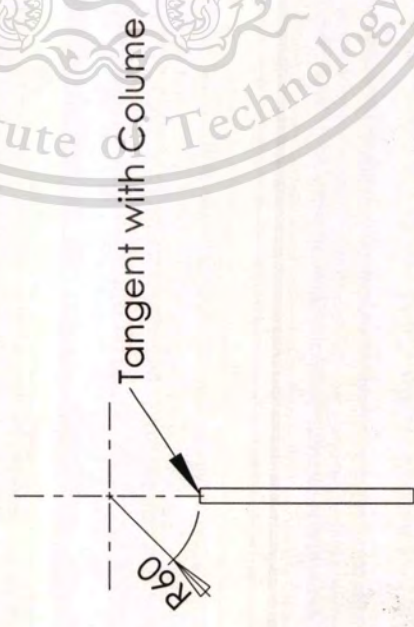
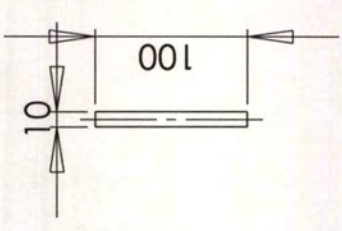
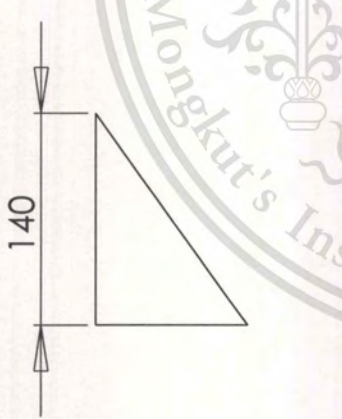
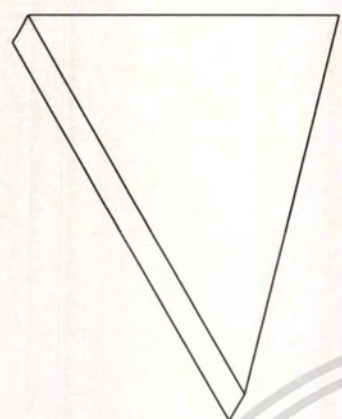
Sheet No. 10

Material. Sheet 10 mm

Scale. 1:5

Size. 125x300

Qty. 2



Gentry_Crane_wing

Part No. 8

Dimension. mm.

Discription
Curve Reference
with Colume

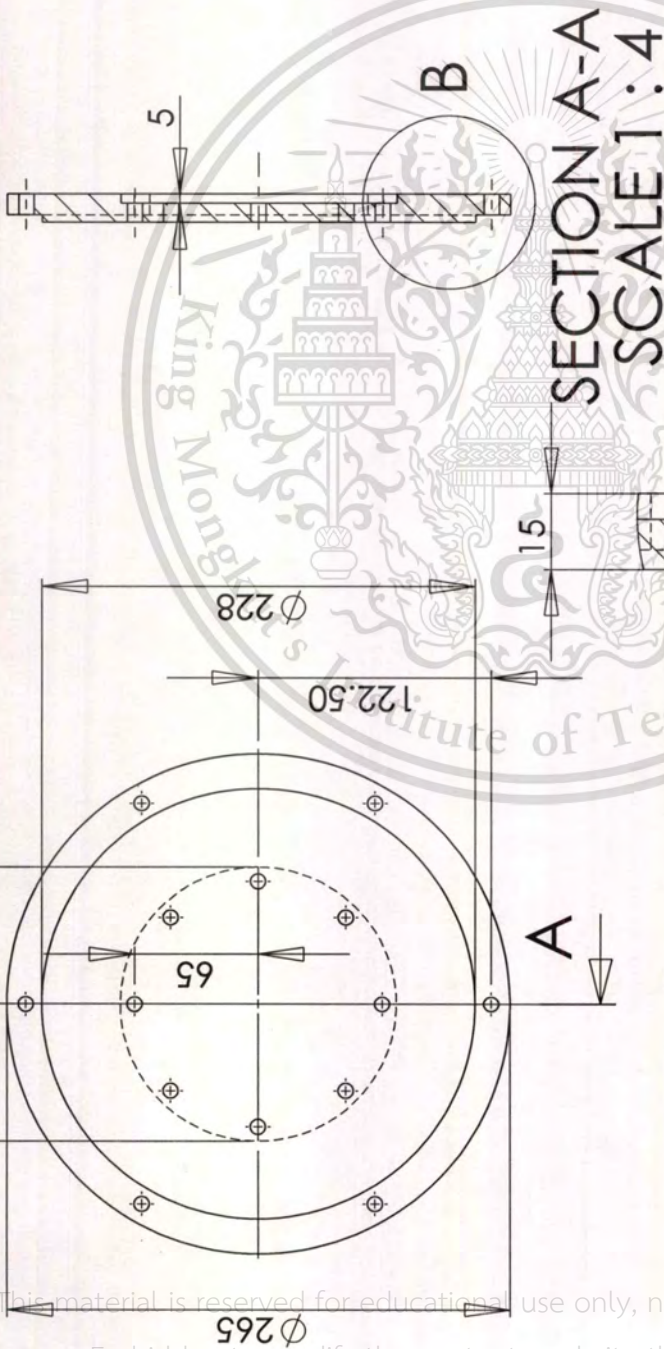
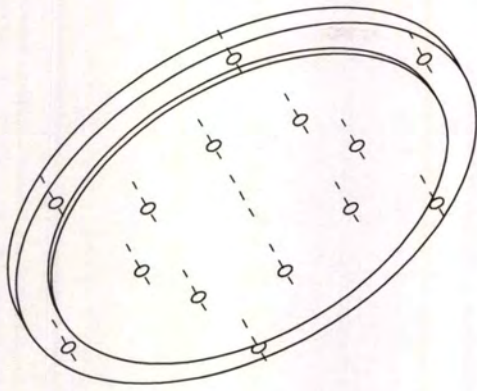
Sheet No. 11

Materal. Sheet 10mm.

Scale. 1:2

Size. 140x100

Qty. 2



SECTION A-A
SCALE 1 : 4

DETAIL B
SCALE 2 : 3

Fly Wheel Plate

Part No. 9

Dimension. mm.

Description

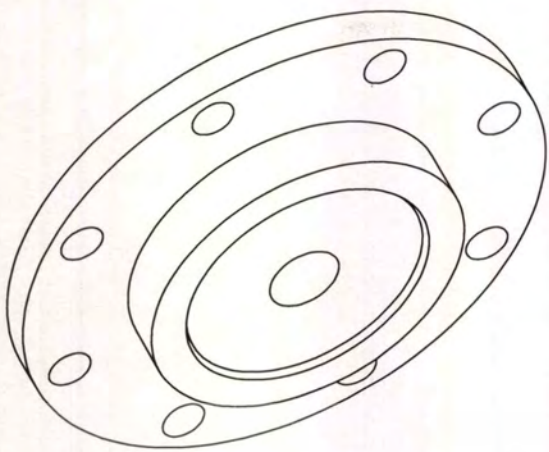
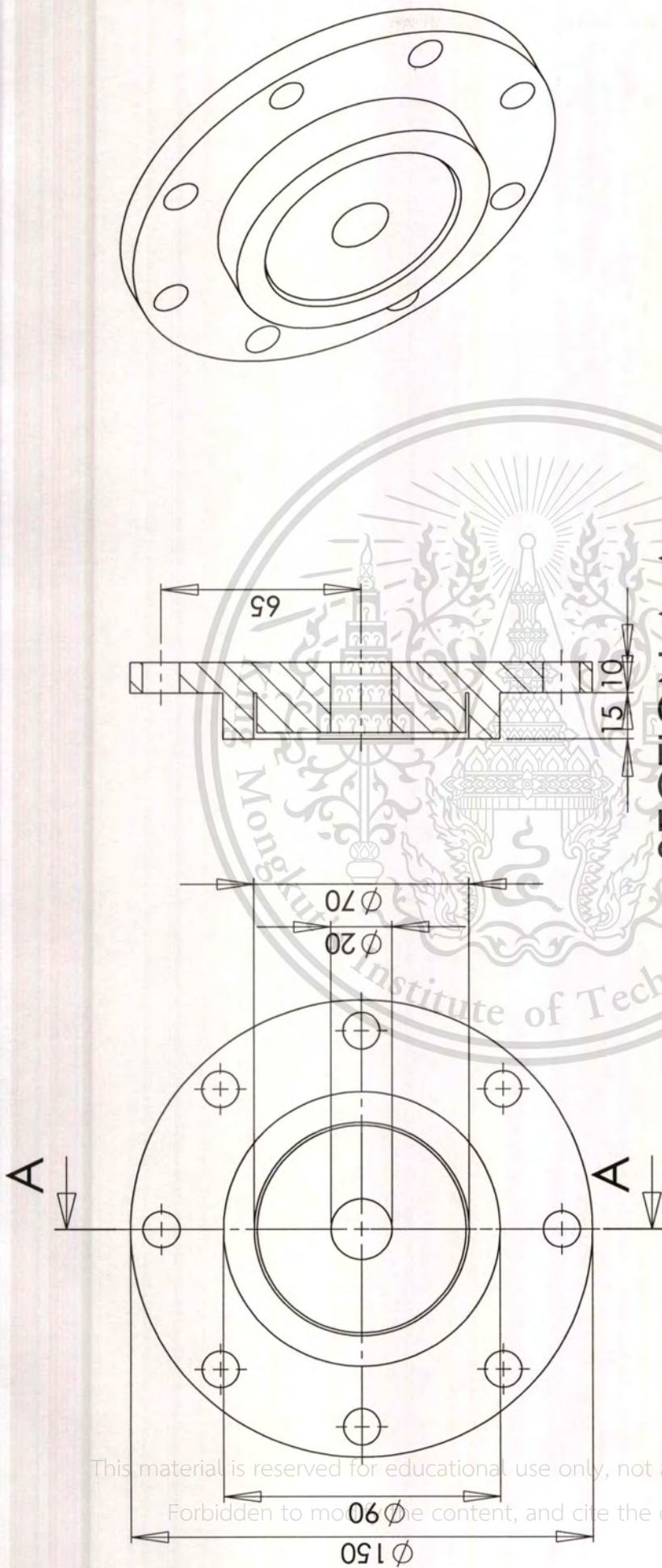
Sheet No. 12

Material. Steel

Scale. 1:4

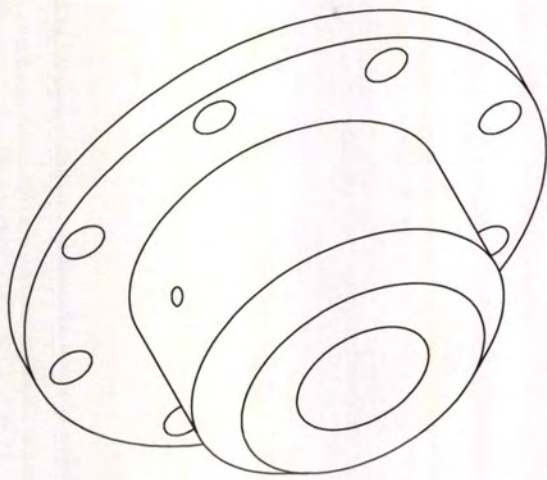
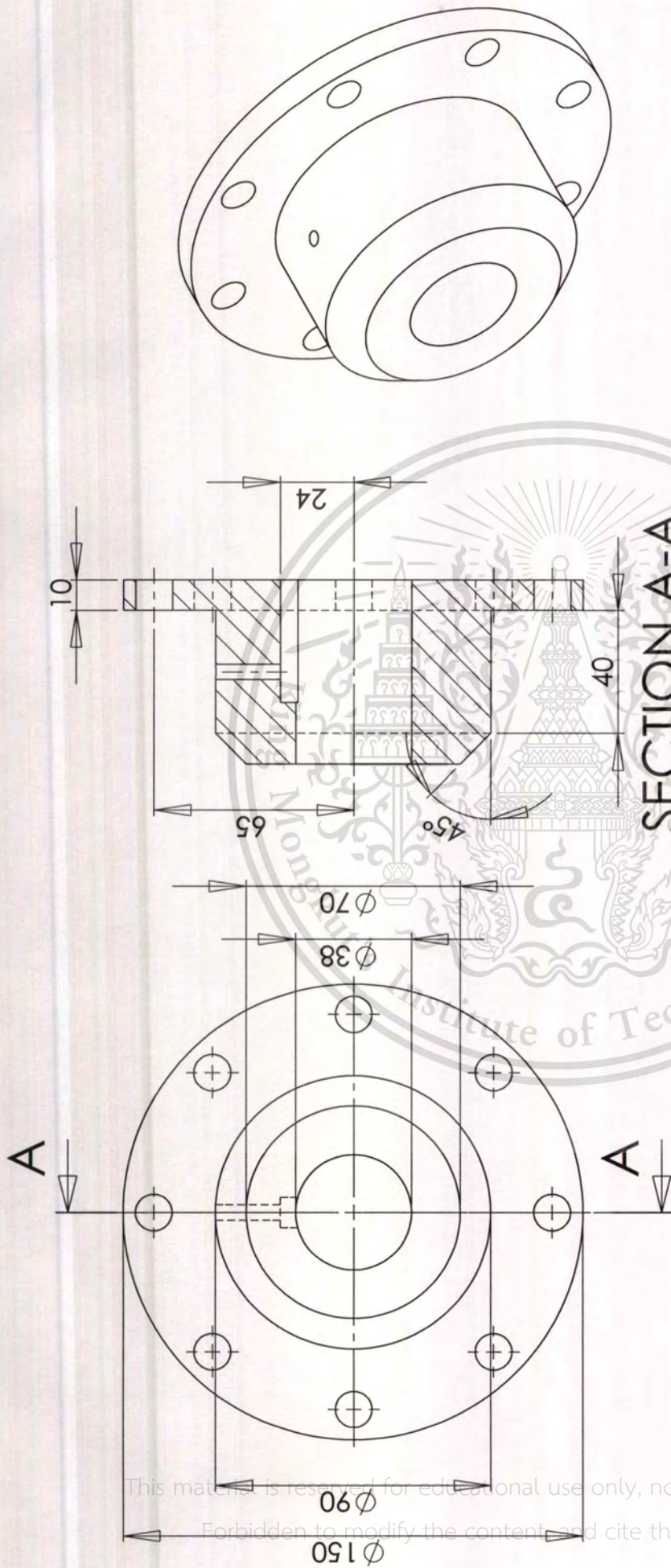
Size. 265x15

Qty. 1

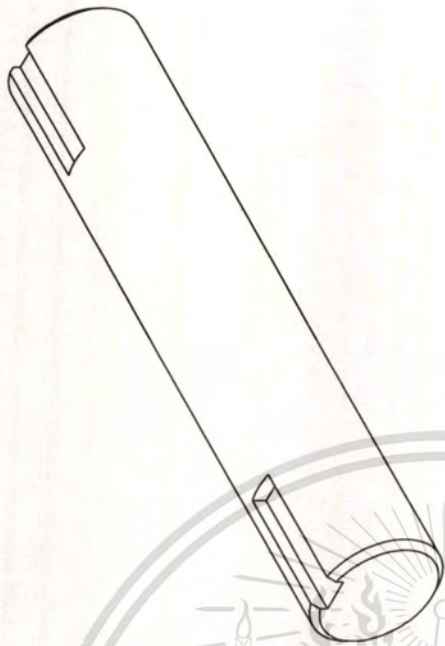
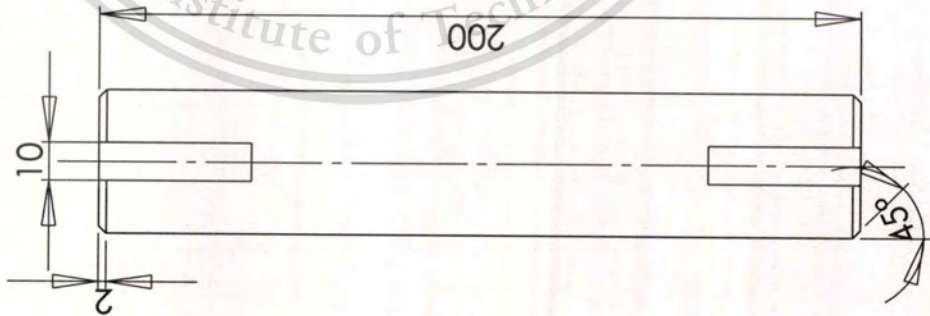
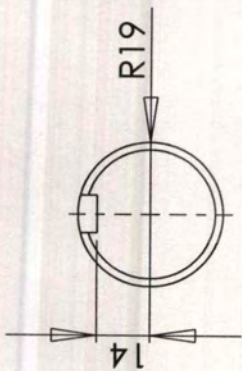


Drive Shaft Plate	
Part No.10	Dimension. mm.
Description	Sheet No.13
Material. Steel	Scale. 1:2
Size. 150x25	Qty. 2

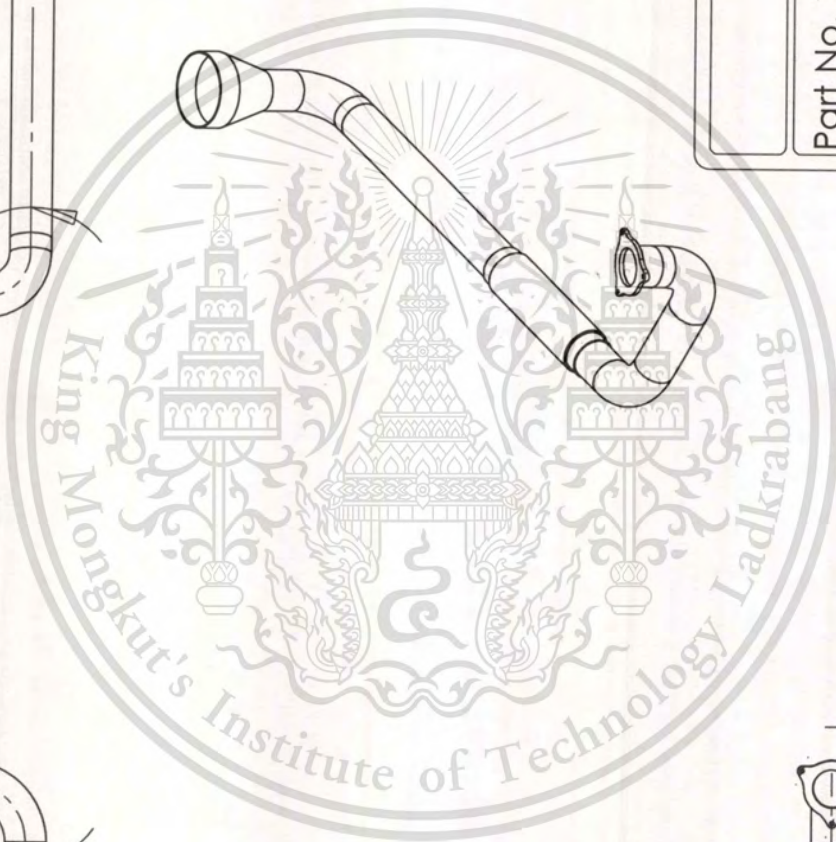
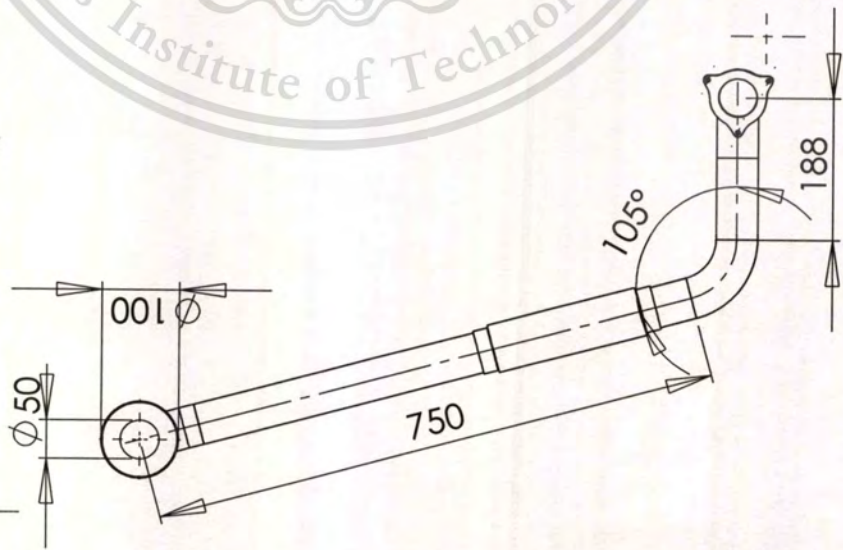
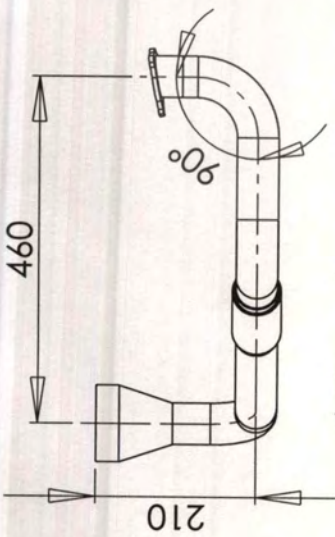
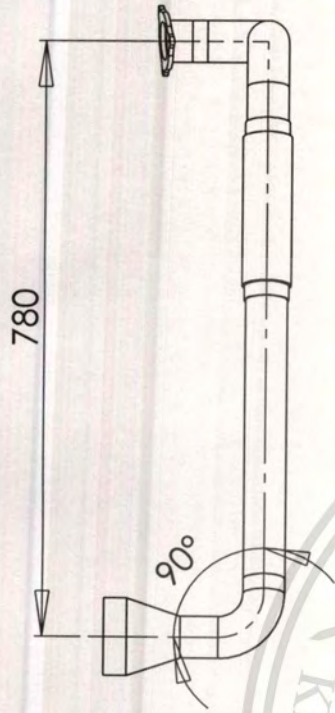
This material is reserved for educational use only, not allowed for commercial use.
 Forbidden to modify the content, and cite the document when use.



Eddy Current Plate	
Part No. 11	Dimension. mm.
Discription	Sheet No. 14
Material. Steel	Scale. 1:2
Size. 265X60	Qty. 2



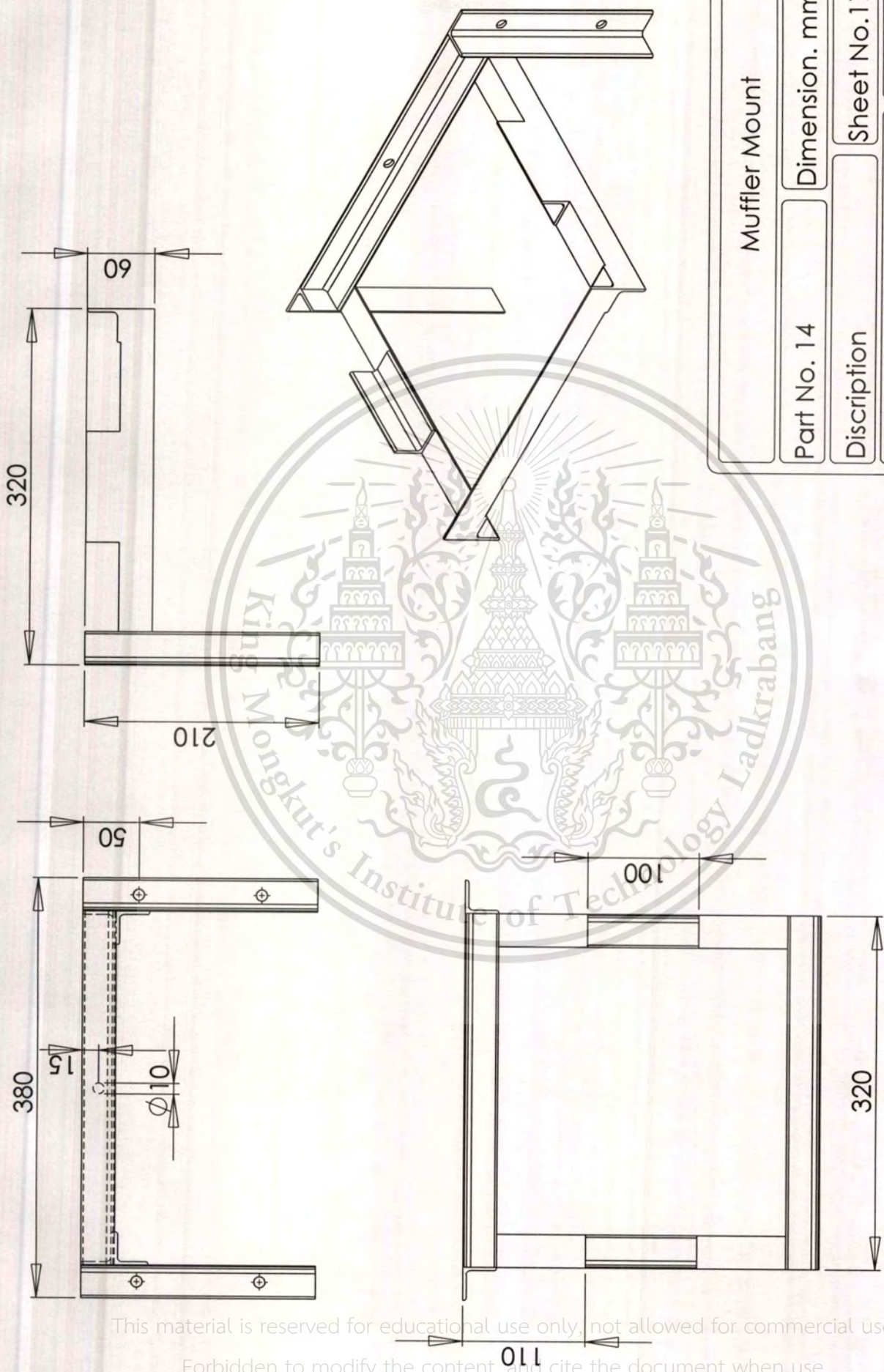
Shaft	
Part No. 12	Dimension. mm.
Description	Sheet No. 15
Material. Steel	Scale. 1:2
Size. 200x16	Qty. 2



Down Pipe	
Part No. 13	Dimension. mm.
Discription	Sheet No. 16
Materral. Stainless Steel	Scale. 1:10
Size.	Qty. 1

This material is reserved for educational use only, not allowed for commercial use.

Forbidden to modify the content, and cite the document when use.



Muffler Mount

Part No. 14

Dimension. mm.

Description

Sheet No.17

Material. Equal Angle 30x30

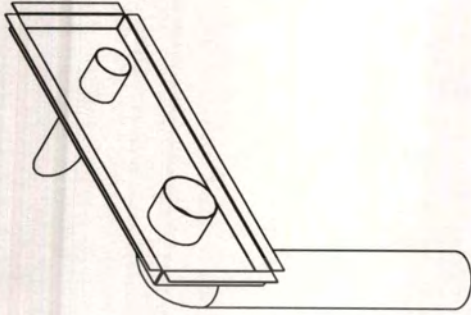
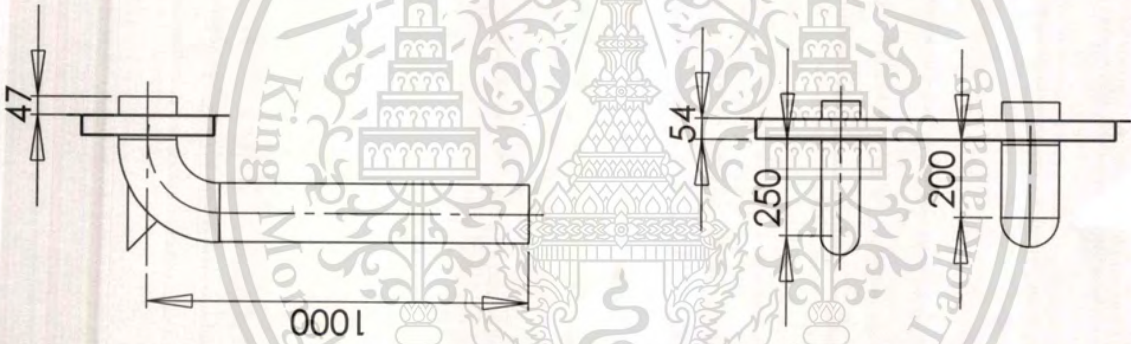
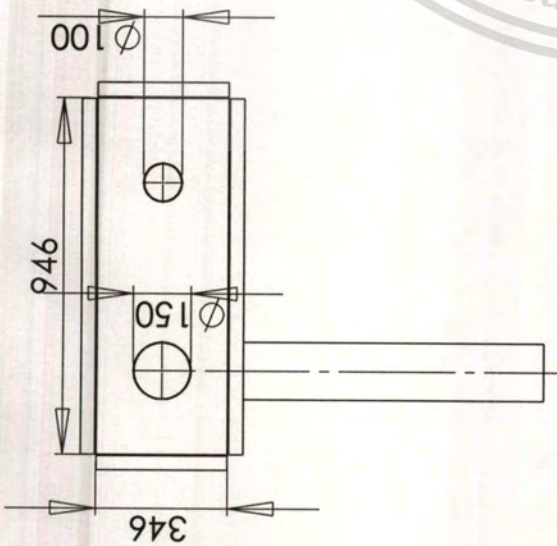
Scale. 1:5

Size.

Qty. 1

This material is reserved for educational use only, not allowed for commercial use.

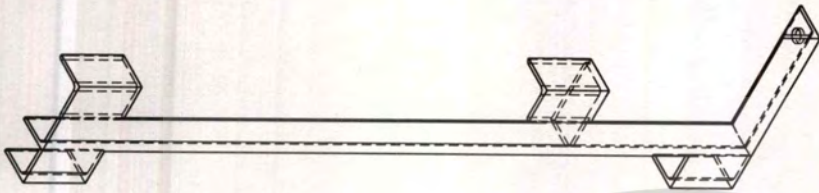
Forbidden to modify the content, and cite the document when use.



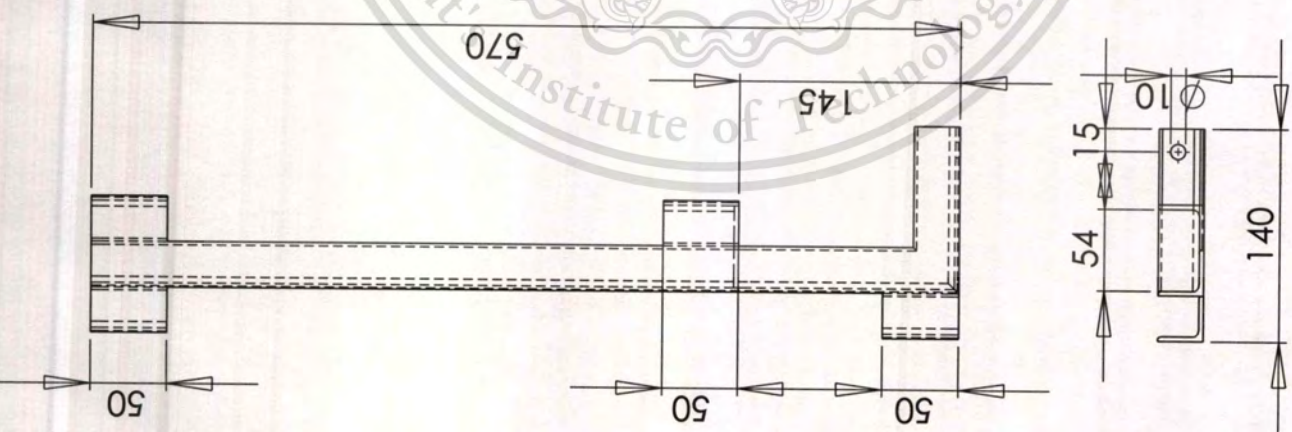
Pane	
Part No. 15	Dimension. mm.
Discription	Sheet No. 18
Materal. Stanless Steel,Zing	
Scale. 1:20	
Size.	Qty. 1

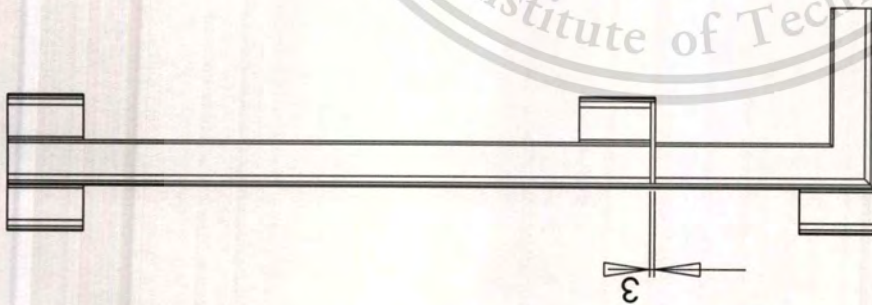
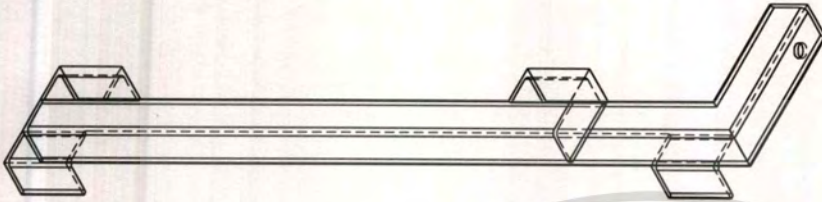
This material is reserved for educational use only, not allowed for commercial use.

Forbidden to modify the content, and cite the document when use.



Radiator mount L	
Part No. 16	Dimension. mm.
Discription	Sheet No. 19
Material. Equal Angle 30x30	Scale. 1:5
Size.	Qty. 1





radiator mount R

Part No. 17

Dimension. mm.

Discription

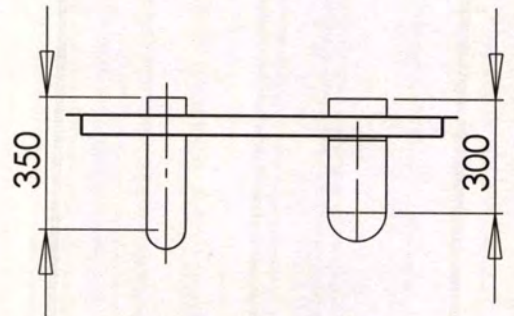
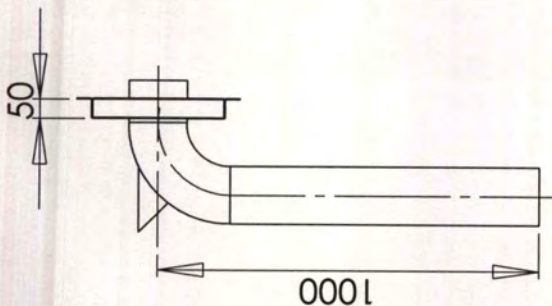
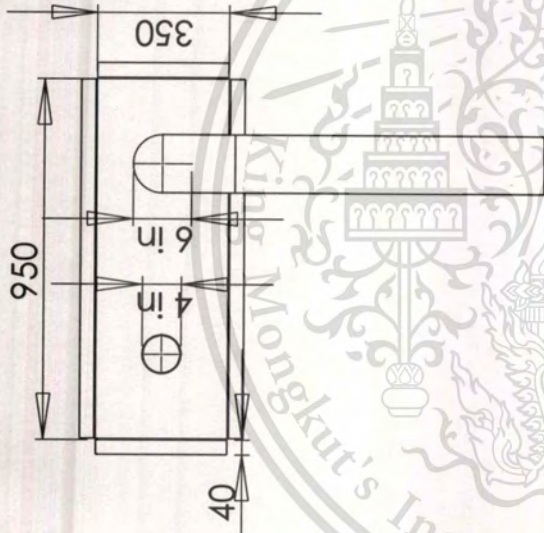
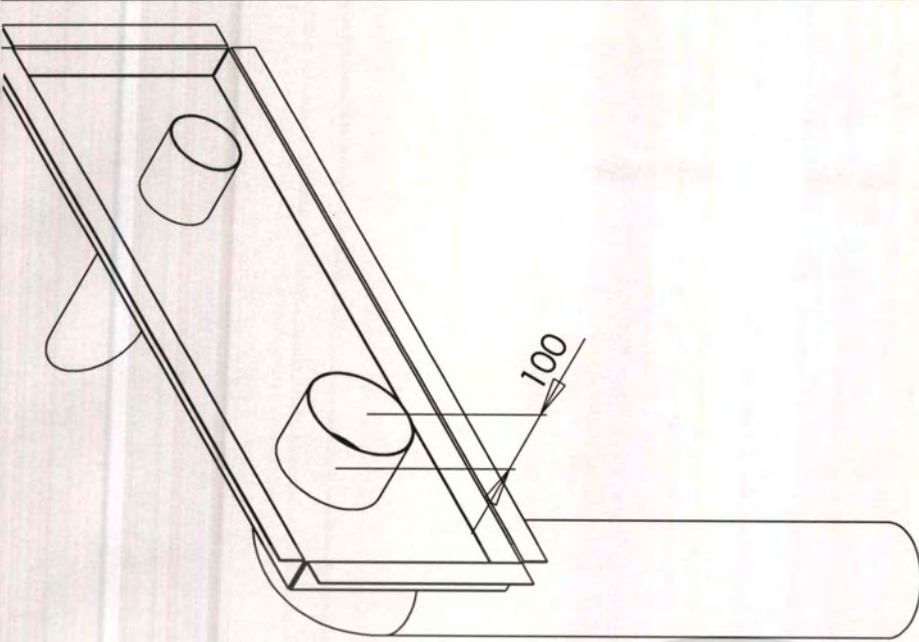
Sheet No. 20

Material.Equal Angle 30x30

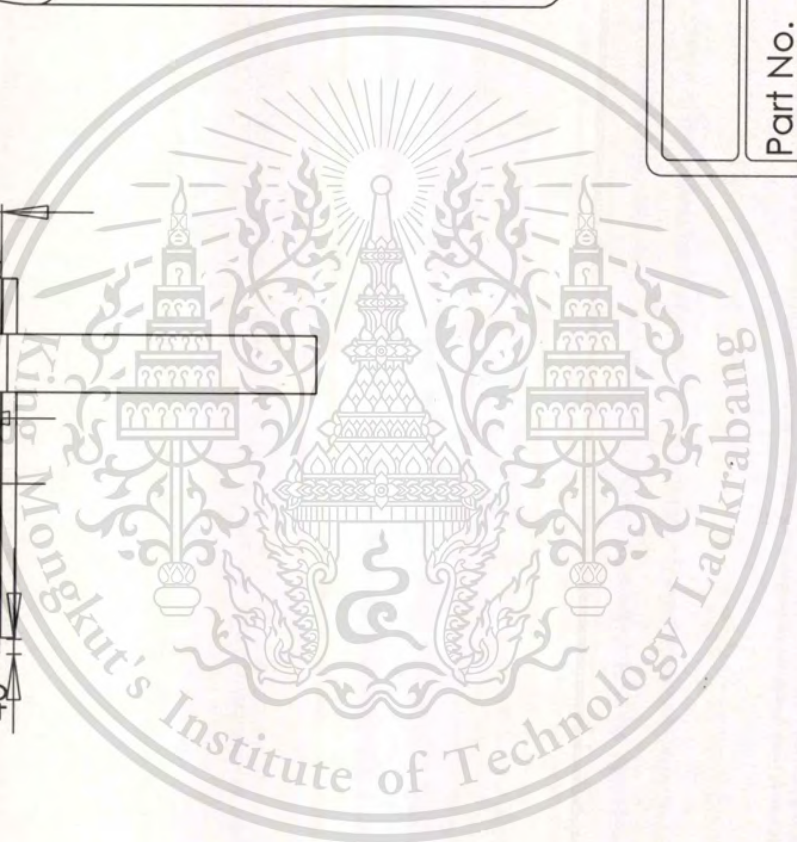
Scale. 1:5

Size. Similar RM L Sheet 19

Qty. 1

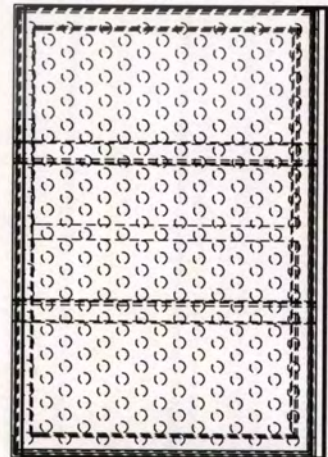
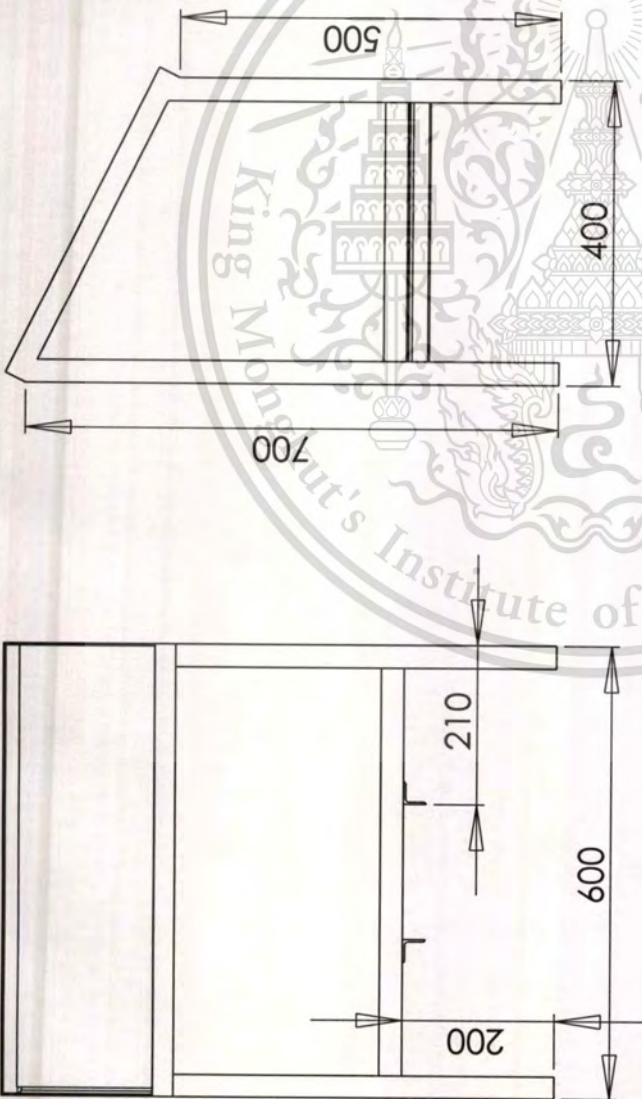
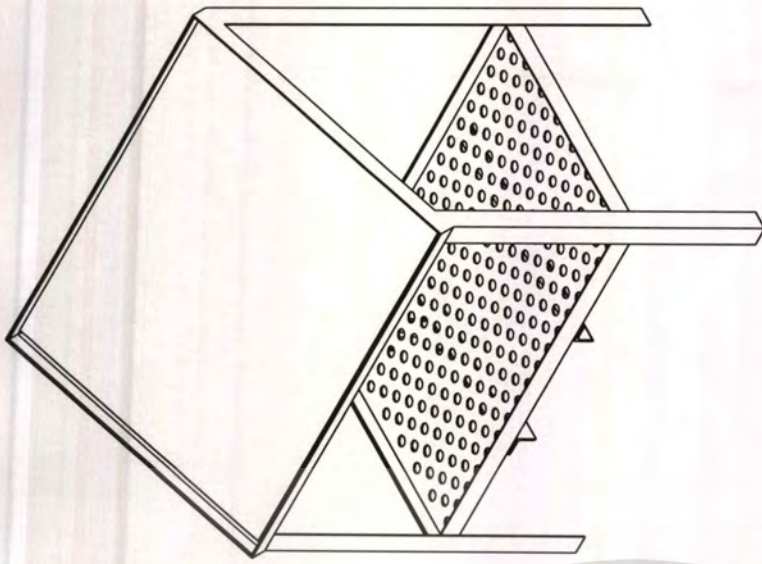


Air Duct	
Part No.	Dimension. mm.
Discription	Sheet No. 21
Materal.	Scale. 1:20
Size.	Qty. 1



This material is reserved for educational use only, not allowed for commercial use.

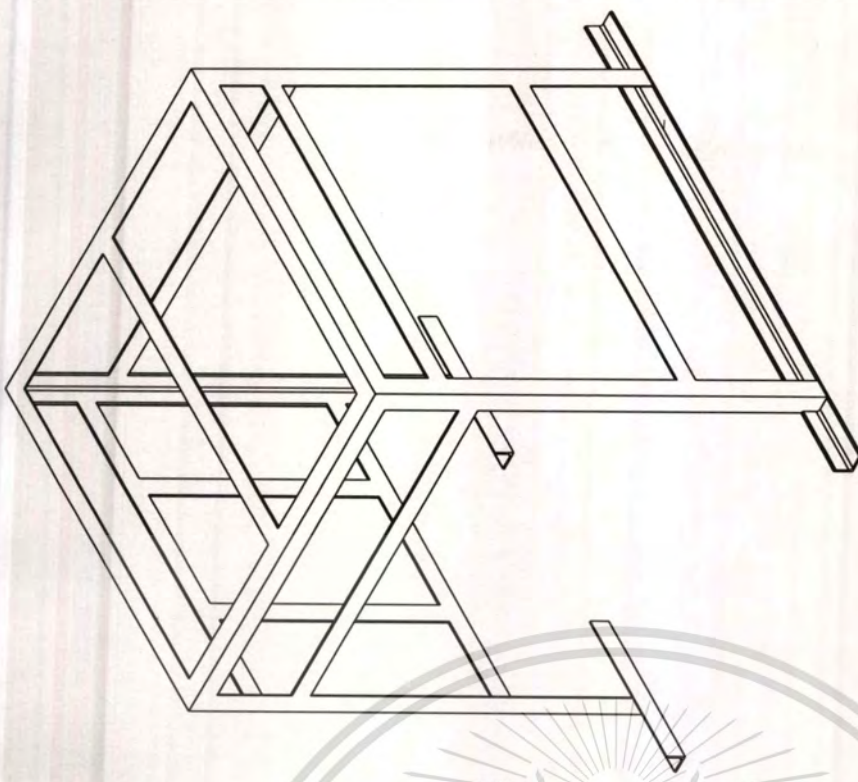
Forbidden to modify the content, and cite the document when use.



control panel	
Part No.	Dimension. mm.
Discription	Sheet No 22
Material. Equal Angle 30x30	
Scale. 1:10	
Size. 400x600x700	Qty. 1

This material is reserved for educational use only, not allowed for commercial use.

Forbidden to modify the content, and cite the document when use.



Dynamometer Cover

Part No.

Dimension. mm.

Description

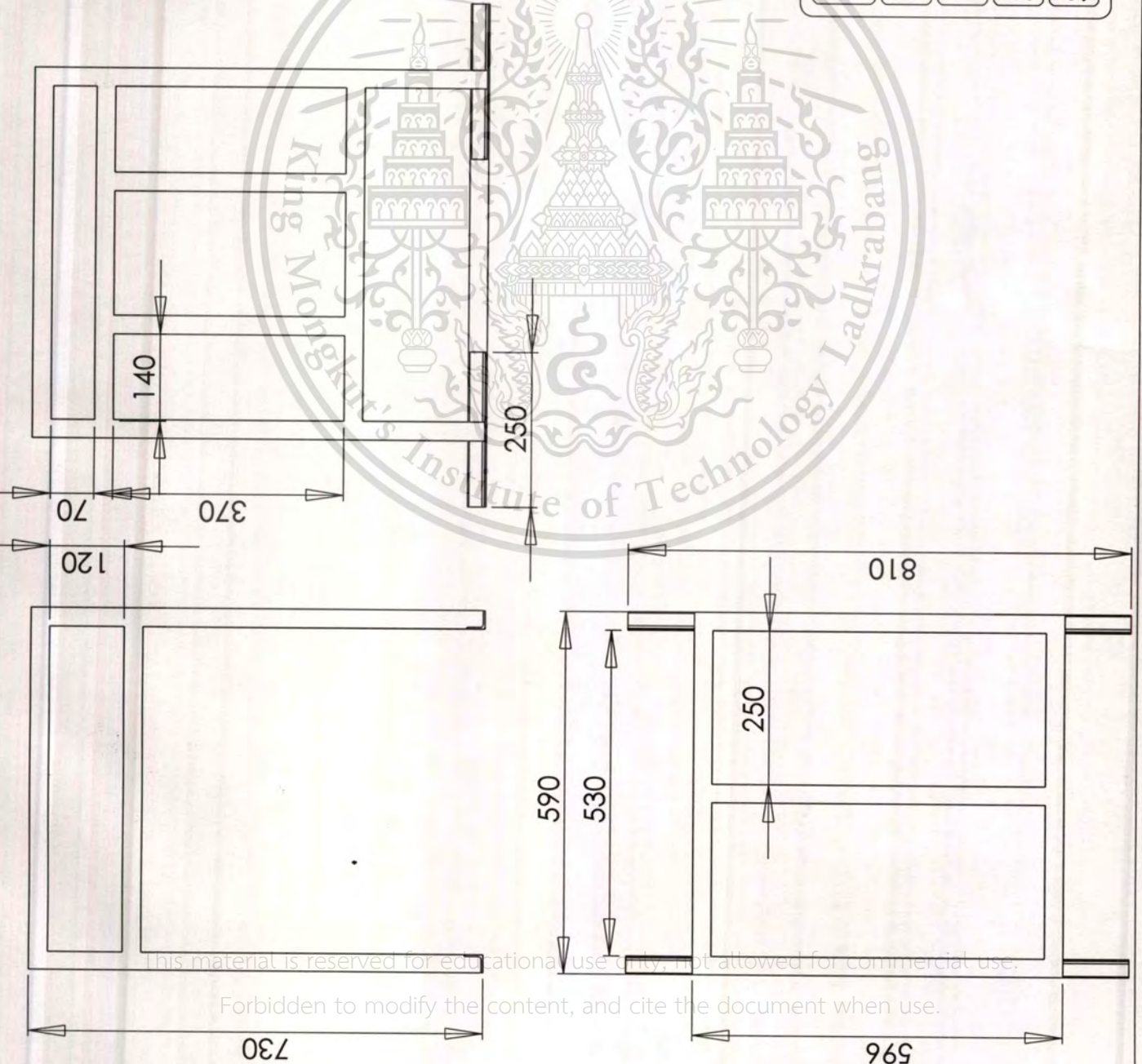
Sheet No. 23

Material. Angle 30x30x30

Scale. 1:10

Size. 590x810x730

Qty. 1



This material is reserved for educational use only, not allowed for commercial use.

Forbidden to modify the content, and cite the document when use.

730

590

590

530

250

810

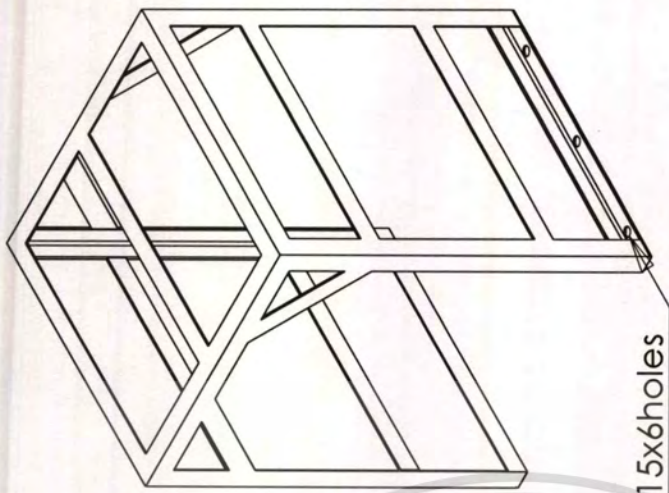
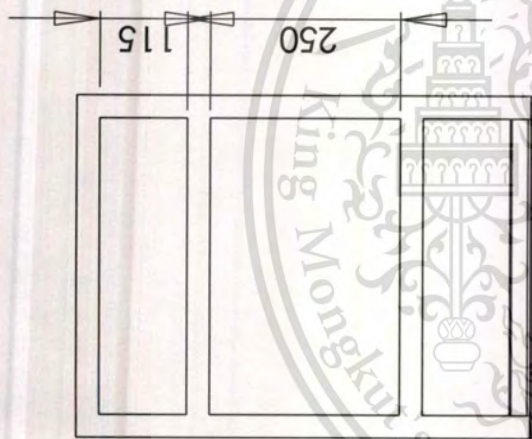
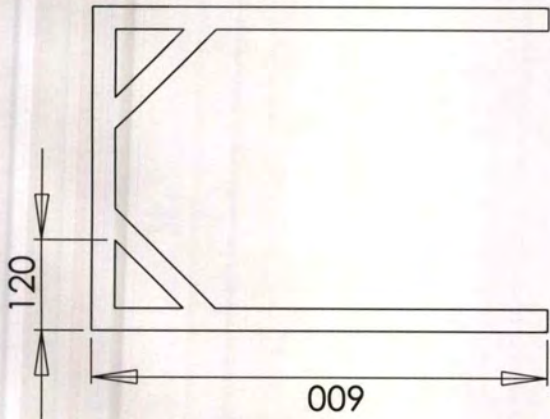
140

70

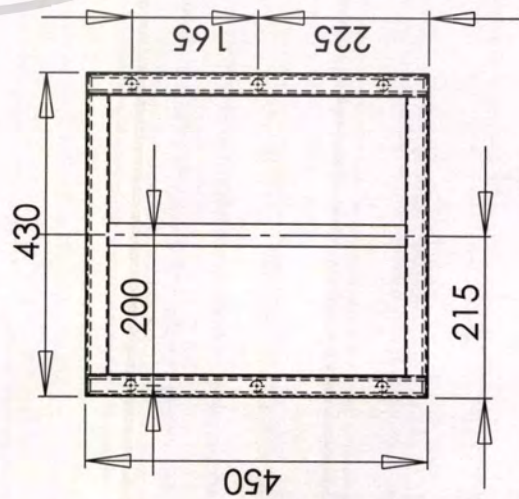
370

250

120



TRUE ϕ 15x6holes



Shaft Cover

Part No.

Dimension. mm.

Discription

Sheet No. 24

Material. Angle 30x30x3

Scale. 1:10

Size. 430x450x600

Qty. 1

This material is reserved for educational use only, not allowed for commercial use.

Forbidden to modify the content, and cite the document when use.

BIOGRAPHY

Name Mr. Nattawut Nakkaew

Date of Birth October 10, 1985

Place of Birth Bangkok, Thailand

Education 2006 B. Eng. in Mechanical Engineering, Sripatum University

Scholarship 2007-2009 Full scholarship for study in the master degree from National Science and Technology Development Agency

Knowledge Taxonomy

- Computer aided design and computer aided manufacture
- Refrigeration and air-condition system
- Commercial and industrial chiller (air and water cooled)
- Heavy duty diesel engine management

Experiences

2004 The winner of SPU 3D Model Contest Competition

2005 Trainee of NECTEC automotive testing laboratory

2006-Present NECTEC automotive testing laboratory assistant.

The collaborative projects are;

- Heavy duty diesel engine dynamometer test stand
- Spark ignition engine dynamometer test stand